Deep learning techniques for power allocation problems in cognitive relay-aided networks.

Yacine Benatia

Doctoral Thesis

Doctoral School : EM2PSI (n° 405)

Domain : STIC

Specialty : Telecommunications

Establishment : CY Cergy Paris University

Research Lab : ETIS - UMR 8051

Presented and defended by:

Yacine Ben Atia

Thesis Topic :

Deep learning techniques for power allocation problems in cognitive relay-aided networks

Thesis defended on 07/12/2023

Jury members:

Director	E. VERONICA BELMEGA	Professor, Université Gustave Eiffel, France
Co-advisor	ANNE SAVARD	Associate Prof. HDR, IMT Nord Europe, France
Co-advisor	ROMAIN NEGREL	Associate Prof., Université Gustave Eiffel, France
Reviewer	PHILIPPE MARY	Professeur des Universités, INSA Rennes, France
Reviewer	YEZEKAEL HAYEL	Professeur des Universités, Université d'Avignon, France
Examiner	ANTHONY FLEURY	Professor, IMT Nord Europe, France
Examiner	GHAYA REKAYA-BEN OTHMAN	Professor, Telecom Paris, France
Examiner	INBAR FIJALKOW	Professeure des Universités, ENSEA, France

Acknowledgements

The work you are about to read is the result of numerous meetings and exchanges. The research evolution would not have been as positive and constructive without all the opportunities provided by many people whom I would like to thank here.

My first thanks go to my advisors and mentors, Professor Elena Veronica BELMEGA, Associate Professor Anne SAVARD, and Associate Professor Romain NEGREL, to whom I express my deep gratitude for proposing the topic and agreeing to supervise me and, thanks to their trust, allowing me to complete this work. Your unwavering support, invaluable advice, and constant encouragement played a decisive role in the development of my research and helped me reach this stage of my PhD thesis. Your dedication to excellence in the academic world is a guiding light for my future career.

I would like to thank all the members of the jury who honored me by dedicating their time and traveling to contribute to reviewing and assisting in the successful completion of this modest effort.

I am immensely grateful to Full Professor Mehdi BENNIS at the Centre for Wireless Communications at the University of Oulu, Finland, for welcoming me to the intelligent connectivity and networks/systems group during my PhD thesis mobility, in conditions more than conducive to fruitful research. Thank you, Professor, for your assistance, and especially for your availability and attention to my work. I'd also like to extend my thanks to all the PhD students and post-docs at the University of Oulu.

Thanks also to all the members and researchers at the IMT Nord Europe, Digital System laboratory, ENSEA, ETIS laboratory and ESIEE, LIGM laboratory, who, directly or indirectly, contributed to the progress of this work.

I have a debt of gratitude to my laboratory colleagues, especially Hajar EL HASSANI, Rui MIN, Mohamed MADANI, Miled ALAM, Josselin LEFEVRE, Nicolas MICHEL, Mohamed Amine KHELASSI, Leonardo de MELO JOÃO, and all the researchers. Your camaraderie, stimulating work environment, and pleasant moments have comforted me during the often stressful phases of my thesis.

Thank you to all my Professors who contributed to my education throughout my journey. I would also like to express my gratitude to Associate Professor Vincent ITIER for giving me the opportunity to teach alongside him during my PhD thesis.

My thanks also go to my close family and friends for their affection and support during the most challenging moments of my life, especially my parents and my brothers, who believed in me, motivated me, and provided unwavering support throughout my studies. Their love and encouragement have been my driving force. They have always been there in all moments, both good and difficult; their constant support and generosity have been fundamental, and their integrity and the pursuit of their own projects have always been a model for me.

I also want to thank the entire department staff, including Annick BERTINOTTI, Astrid MONTELIMARD, Lalia SY, Christine CONREUR, Florence CHECH, Sandrine FOURNIER, and Laurent PROTOIS, for the assistance and support they provided during my PhD thesis.

Finally, I extend my sincere thanks to all the people I had the opportunity to work with or had the honor to meet before and during my PhD thesis.

Abstract

Future generations of wireless networks face great expectations in terms of network capacity, system throughput, user density, all on a tight energy budget. In order to reach such ambitious objectives, several emerging technologies, such as : cognitive radio, cooperative communications, full-duplexing, and AI, etc. have been proposed, each of them focusing on a specific improvement.

The objective of this PhD thesis is to jointly exploit these emerging technologies, in order to investigate a constrained and non-convex Shannon rate maximization problem in a relay-aided cognitive radio network. This network consists of a primary and a secondary user–destination pair and a secondary full-duplex relay performing compress-and-forward (CF) or decode-and-forward (DF). The primary communication is protected by a quality of service (QoS) constraint expressed in terms of tolerated Shannon rate degradation. More precisely, we tackle the non-convex power allocation problems under both perfect and imperfect channel state information (CSI) and for CF and DF relaying. In the perfect CSI case, we derive a closed-form solution for CF relaying. However, for DF relaying, no closed-form solution seems feasible due to more complex achievable rate expressions and non-convex constraints. To address this challenge, we propose an unsupervised deep learning-based power allocation policy exploiting a fully connected architecture jointly with a custom cognitive radio-tailored loss function that the deep neural network (DNN) learns to minimize. This custom loss function relies on the relaxation of the QoS within the objective function by introducing an hyperparameter to trade-off between a rate-driven and a QoS-driven optimization problem. As such, only the channel gains are provided as the input of our proposed DNN.

When only an imperfect CSI is available at the transmitter side, we propose to build on our proposed DNN by rendering it robust to channel gains estimation errors. Since our closed- form solution under CF relies on the perfect CSI assumption, we propose to use our DNN approach to optimize the power allocation policy under CF and imperfect CSI as well.

To cope with imperfect CSI, we turn to a self-supervised approach, where in the training phase, error- free channel estimations are provided to the loss function, and only channel gains impaired by estimation errors are provided at the input of the DNN. The robustness of the proposed solution was validated through numerical simulations.

Once our robust DNN-based solution validated, we seek for more general DNN-based policies, namely choosing among the best relaying scheme among CF and DF, as well as generalizing over the network system parameters, such as the individual power budgets and the level of tolerated primary degradation. Regarding the relaying scheme selection problem, we again exploit a fully connected DNN with the cross-entropy loss function, especially well-suited for classification problems. The latter exploits the power predicted by our previous proposed DNN under both CF and DF. Regarding the generalization over the system parameters, we first generalize separately over each parameter and then we propose a DNN able to generalize jointly over both the power budget and level of tolerated primary rate degradation.

Keywords :*Artificial intelligence, Deep learning, Full-duplex relaying, Cognitive radio, Imperfect CSI.*

Résumé

Les futures générations de réseaux sans fil sont confrontées à de grands défis en termes de capacité du réseau, de débit du système, de densité d'utilisateurs, le tout avec un budget énergétique serré. Afin d'atteindre ces objectifs ambitieux, plusieurs technologies émergentes, telles que la radio cognitive, les communications coopératives, le full duplex, l'intelligence artificielle, etc. ont été proposées, chacune d'entre elles se concentrant sur une amélioration spécifique.

L'objectif de cette thèse de doctorat est d'exploiter conjointement ces technologies émergentes afin de maximiser le débit de Shannon sous contraintes et non convexe dans un réseau de radio cognitive assisté par des nœuds relais. Ce réseau se compose d'une paire utilisateur-destination primaire et secondaire et d'un relais secondaire full-duplex effectuant la Compresser-et-Transférer (CF) ou Décoder-et-Transférer (DF). La communication primaire est protégée par une contrainte de qualité de service (QoS) exprimée en termes de dégradation tolérée du débit de Shannon.

Plus précisément, nous abordons les problèmes d'allocation de puissance non convexes dans le cas d'information sur l'état du canal (CSI) parfaite et imparfaite et pour CF et DF. Dans le cas d'une information parfaite sur l'état du canal, nous obtenons une solution analytique pour CF. Cependant, pour DF, en raison de débits atteignables plus complexes et des contraintes non convexes, aucune solution analytique ne semble possible. Pour relever ce défi, nous proposons une politique d'allocation de puissance non supervisée basée sur l'apprentissage profond qui exploite une architecture entièrement connectée conjointement avec une fonction de coût adaptée à la radio cognitive que le réseau de neurones profond (DNN) apprend à minimiser. Cette fonction de coût adaptée repose sur la relaxation de la contrainte de QoS dans la fonction objectif en introduisant un hyperparamètre permettant le compromis entre une optimisation axée sur le débit et une optimisation axée sur la QoS. Ainsi, seuls les gains du canal sont fournis en entrée de notre DNN.

Lorsque seule une CSI imparfaite est disponible à l'émetteur, nous proposons d'exploiter notre DNN en le rendant robuste aux erreurs d'estimation des gains du canal. Étant donné que notre solution analytique pour le relais CF repose sur une CSI parfaite, nous proposons également d'utiliser notre DNN pour optimiser la politique d'allocation de puissance pour CF en présence de CSI imparfaite. Pour faire face à la CSI imparfaite, nous adoptons une approche auto-supervisée où, dans la phase d'apprentissage, des estimations de canaux sans erreur sont fournis à la fonction de coût, et seuls les gains de canaux altérés par des erreurs d'estimation sont fournis à l'entrée du DNN. La robustesse de la solution proposée a été validée par des simulations numériques.

Une fois notre solution robuste basée sur le DNN validée, nous recherchons des politiques plus générales exploitant des DNN, à savoir le choix du meilleur schéma de relayage parmi CF et DF, ainsi que la généralisation sur les paramètres du système de réseau, tels que les budgets de puissance individuels et le niveau de dégradation primaire toléré. En ce qui concerne le problème de sélection du schéma de relayage, nous exploitons à nouveau un DNN entièrement connecté avec la fonction de coût d'entropie croisée, particulièrement bien adaptée aux problèmes de classification. Ce dernier exploite la puissance prédite par le DNN que nous avons proposé précédemment, à la fois pour CF et DF. En ce qui concerne la généralisation sur les paramètres du système, nous généralisons d'abord séparément sur chaque paramètre, puis nous proposons un DNN capable de généraliser conjointement sur le budget de puissance et le niveau de dégradation du débit primaire toléré.

Mots clés :*Intelligence artificielle, Apprentissage profond, Relais full-duplex, Radio cognitive, CSI imparfait.*

Contents

List of Figures

List of Tables

List of Abbreviations

AF:	Amplify-and-Forward
AI:	Artificial intelligence
AWGN:	Additive White Gaussian Noise
CF:	Compress-and-Forward
CSI:	Channel State Information
DF:	Decode-and-Forward
DL:	Deep Learning
DPC:	Dirty paper coding
DNN:	Deep Neural Network
DSA:	Dynamic spectrum access
D2D:	Device-to-Device
IoT:	Internet of Things
MIMO:	Multiple-Input Multiple-Output
ML:	Machine Learning
OFDM:	Orthogonal Frequency-Division Multiplexing
PUs:	Primary users
QoS:	Quality of service
SINR:	Signal-to-Interference-plus-Noise-Ratio
SNR:	Signal-to-Noise Ratio
SUs:	Secondary users

Chapter 1

Introduction

1.1 Background and motivation

As the number of wireless devices and network users continues to grow (see Figure 1.1), the need to improve future generations of wireless networks has become increasingly important [4–6]. This is due to the growing demand for system throughput and spectrum resources, which pose significant challenges. To address these challenges, it has become necessary to leverage not one but a combination of various technologies such as: artificial intelligence (AI), cognitive radio, cooperative communications, full-duplexing, multi-antenna (MIMO) devices, mmWave, etc. [7–9]. For example, in cooperative communications, it is possible to utilize relaying scheme selection, which involves choosing the most suitable protocol between decode-and-forward (DF), compress-and-forward (CF), and amplify-and-forward (AF), based on specific requirements [10, 11]. By selecting the most appropriate relaying scheme, it is possible to enhance the system efficiency. However, the effectiveness of all these technologies is greatly influenced by resource allocation policies.

The allocation of resources, such as power, time, frequency, etc. plays a critical role in optimizing the system efficiency and spectral utilization. An optimized resource allocation policy can enhance the system performance by minimizing the interference, increasing throughput, and improving reliability. Conversely, a suboptimal allocation policy can lead to an inefficient use of resources and lower system performance. Therefore, the optimization of resource allocation policies is crucial for achieving optimal system performance in wireless communication networks.

In this PhD thesis, we aim to integrate several promising technologies, including cognitive radio, cooperative communications, full-duplexing, and AI, and investigate novel resource

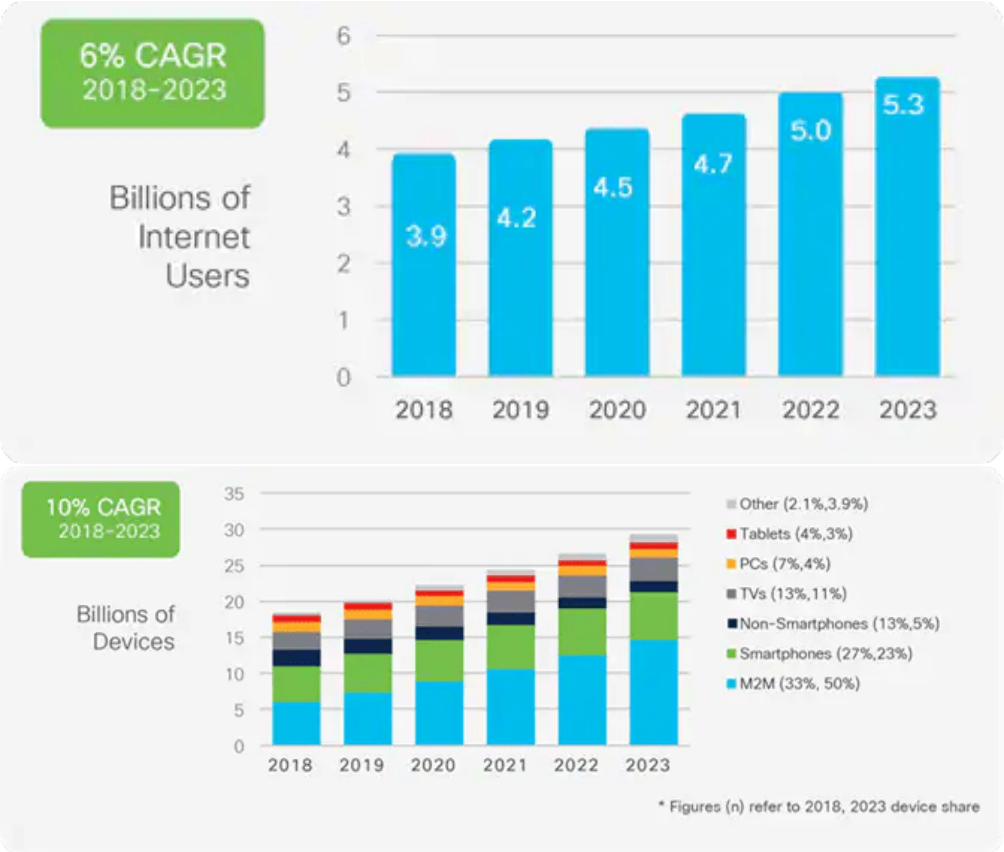

Figure 1.1: Cisco Annual Internet Report (2018–2023) White Paper, 2020 [1]

allocation policies under perfect and imperfect channel state information (CSI) that can further enhance the performance of future wireless communication systems. In addition, we also analyze and evaluate the selection of the most appropriate relay scheme to optimize the system performance.

In the following Section, we will provide a comprehensive overview of the technologies that have been utilized in this PhD thesis, outlining their key features and applications.

1.2 Main exploited technologies

To tackle the challenges arising from the growing number of connected users and devices, as well as the heterogeneity of mobile applications, a large range of technologies has been leveraged in this PhD thesis. A key technology that has been employed is *cognitive radio*, which intelligently utilizes the available spectrum by detecting and adapting to changes in the radio environment. Additionally, *cooperative communications* have been investigated to improve the network capacity by making use of signals sent by a source, which are available to

all receivers within range. Furthermore, *deep neural networks* (DNNs) have been increasingly employed in various fields, including wireless systems, to achieve more consistent and more reliable results [12–14]. The integration of these technologies has resulted in enhanced wireless communication system capabilities in terms of improved spectrum utilization, better network efficiency, as demonstrated by the promising results obtained in this PhD thesis.

Below, we discuss in further details the main technologies exploited in this PhD thesis.

1.2.1 Cognitive radio

The rapid growth of wireless technologies in the telecommunication industry has resulted in an exponential increase in spectrum demands. Hence, the allocation of wireless spectrum resources has become problematic [15–17]. Currently, wireless networks undergo a static spectrum allocation policy, where government agencies allocate wireless spectrum to license holders for large geographic regions over long time periods [18]. Unfortunately, this policy has resulted in a shortage of available spectrum in certain frequency bands due to the increasing demand for wireless communication. Additionally, a considerable portion of the assigned spectrum is used only rarely, resulting in inefficient use of this valuable resource.

To address these spectrum inefficiency issues, dynamic spectrum access (DSA) techniques have been proposed. Cognitive radio is the key technology that enables these techniques, and its primary goal is to enhance the efficient utilization of limited spectrum while ensuring that other users are not affected by interference [18, 19]. DSA enables cognitive radio systems to exploit underutilized spectrum, which can in turn increase the overall spectrum efficiency and enable new wireless applications. Moreover, cognitive radio systems can be used in a wide range of applications, such as cellular networks, wireless medical networks and emergency communication systems [8, 20, 21].

Cognitive radio systems refer to wireless communication systems that can dynamically adjust to their environment by using advanced signal processing, machine learning, and decision-making algorithms [8, 18, 22]. This approach was first introduced by Joseph Mitola III in 1998, and was published in an article by Mitola and Gerald Q. Maguire, Jr. in 1999 [23]. By dynamically sensing the radio frequency environment, cognitive radio systems can analyze the spectrum usage and select the best frequency band and communication parameters, such as power [19, 24].

In cognitive radio, users who have obtained a license to use a particular frequency band are referred to as primary users (PUs), while users who do not have a license are referred to as secondary users (SUs) or opportunistic users. Cognitive radio networks can be classified

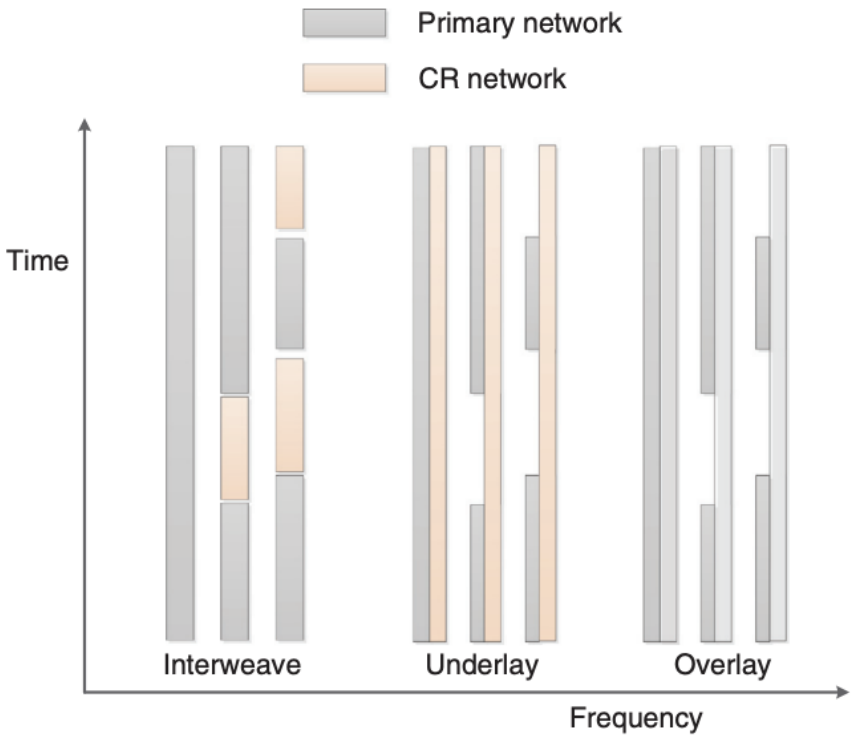

Figure 1.2: Cognitive radio modes [2].

into three paradigms illustrated in Figure 1.2: interweave networks, underlay networks, and overlay networks [25–27], which will be discussed below.

Interweave networks In the interweave DSA model, secondary users are only allowed to access the frequency band of interest if it is not currently being used by a primary user. PUs are given absolute priority over the spectrum band, and SUs must release the band if the PU wants to access it. This model is also known as opportunistic spectrum access, as SUs exploit spectrum holes in time, space, and/or frequency domains. To implement this model, SUs sense the surrounding spectrum environment, identify idle spectrum bands, and switch to the selected bands to ensure uninterrupted transmission. Reliable spectrum sensing mechanisms are essential for SUs in this model.

Underlay networks The underlay paradigm requires that primary and secondary transmissions occur concurrently only if the interference generated by secondary transmitters at primary receivers stays below a certain acceptable threshold. To meet this requirement, secondary transmitters can limit their power to stay within the interference constraints, which restricts them to short-range and low-rate communications.

Overlay networks These networks allow both PUs and SUs to transmit concurrently. Furthermore, unlike underlay DSA, which limits the SU's transmit power to constrain the interference to PU, overlay DSA aims to maintain PU performance. In overlay DSA, SUs are allowed to simultaneously transmit with PUs over the same band as long as no performance degradation is inflicted on PUs. However, unlike underlay networks, SUs devices in overlay networks must possess knowledge about the PUs transmitted data sequence (eg. messages), including encoding methods or code book. This information can be utilized in two distinct ways. Firstly, SUs receivers can use this knowledge to cancel out the PUs interference using techniques such as dirty paper coding (DPC), which involves precoding transmitted data to counteract interference effects. Secondly, SUs nodes can use this information to collaborate with the primary network by relaying PUs messages.

This PhD thesis is focused on underlay cognitive radio networks, where spectrum sensing is not considered. Indeed, we assume that primary and secondary transmissions can occur simultaneously, and we utilize power control and interference management techniques to ensure that the interference from secondary users remains below a given threshold.

In the following Subsection, we will provide an extensive discussion regarding another technology that has been utilized in this thesis, namely cooperative communication.

1.2.2 Cooperative communications

In traditional point-to-point communication systems, the communication is established between a transmitter and a receiver directly. In cooperative communications, multiple devices collaborate to transmit or receive the same message, leading to enhanced signal quality, better coverage, and higher reliability [28, 29]. For example, in a relay-based cooperative communication system (Figure 1.3), one device acts as a relay node that receives the signal from the transmitter and forwards it to the receiver.

The concept of cooperative communications relies on a basic three-terminal relay channel proposed by Van der Meulen [28,30,31]; Subsequently, it was demonstrated that a relay node can provide assistance to both the transmitter and receiver nodes in enhancing the rate region of the transmitter. Sendonaris et al. [32] later introduced the concept of cooperative communications and provided evidence to support the claim that cooperative communications enhances the achievable rate.

Cooperative communications can be used in a wide range of wireless applications, such as cellular networks [33], sensor networks [34], and satellite communication systems [35]. Moreover, this smart promising technology has become an important research topic in wireless

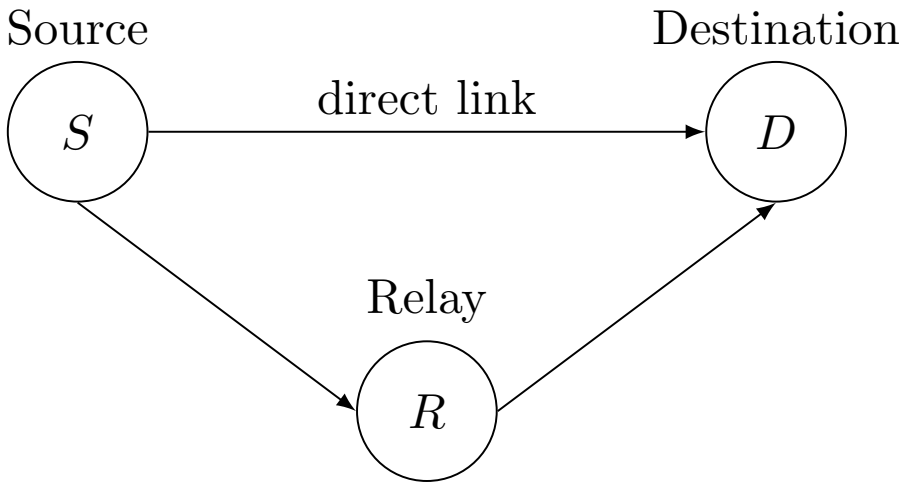

Figure 1.3: Cooperative communications system.

communication systems, and many researchers are exploring new techniques and algorithms to optimize cooperative communication systems. These efforts aim to improve the efficiency and reliability of wireless communication systems and enable new applications in areas such as smart cities, internet of things (IoT), and vehicular networks [36,37]. Three primary methods for relaying have been suggested in the literature. The first one is Amplify-and-Forward (AF), where the relay amplifies the signal it receives [31]; the second one is Decode-and-Forward (DF), where the relay receives the message from the transmitter, decodes it, re-encodes it, and then sends it to the intended destination; the third one is Compress-and-Forward (CF), where the relay sends a compressed version of its received signal [38].

In this PhD thesis, the AF relaying scheme is not considered due to its potential to amplify interference. This PhD thesis conducted several experiments to determine the optimal relaying scheme between DF and CF in terms of the secondary achievable rate and primary rate degradation based on the relay's position in a cognitive radio setup. Our findings indicate that CF outperforms DF when the relay is in proximity to the secondary destination, while DF performs better when the relay is closer to the secondary user. The comprehensive experiment details will be presented in Section 4.

In the upcoming Subsection, we will provide a brief introduction on DNNs and the different types of learning employed in this PhD thesis.

1.2.3 Deep Neural Networks

Deep learning is a subfield of machine learning that uses artificial neural networks with multiple layers to process data and extract high-level features [39] as depicted in Figure 1.4 for instance. These models are trained using large datasets and algorithms that iteratively adjust the weights and biases of the neural network to minimize errors in the output. Due to their ability to handle complex data structures, deep learning methods have achieved remarkable results in diverse fields and are considered state-of-the-art in many applications, such as image and speech recognition, natural language processing, and computer vision. Recently, they have also been implemented in the field of telecommunications due to their capability to solve complex and non-convex optimization problems [40–42]. The term *deep* refers to the multiple layers used in the neural network architecture, which enables the model to learn increasingly complex representations of the input data.

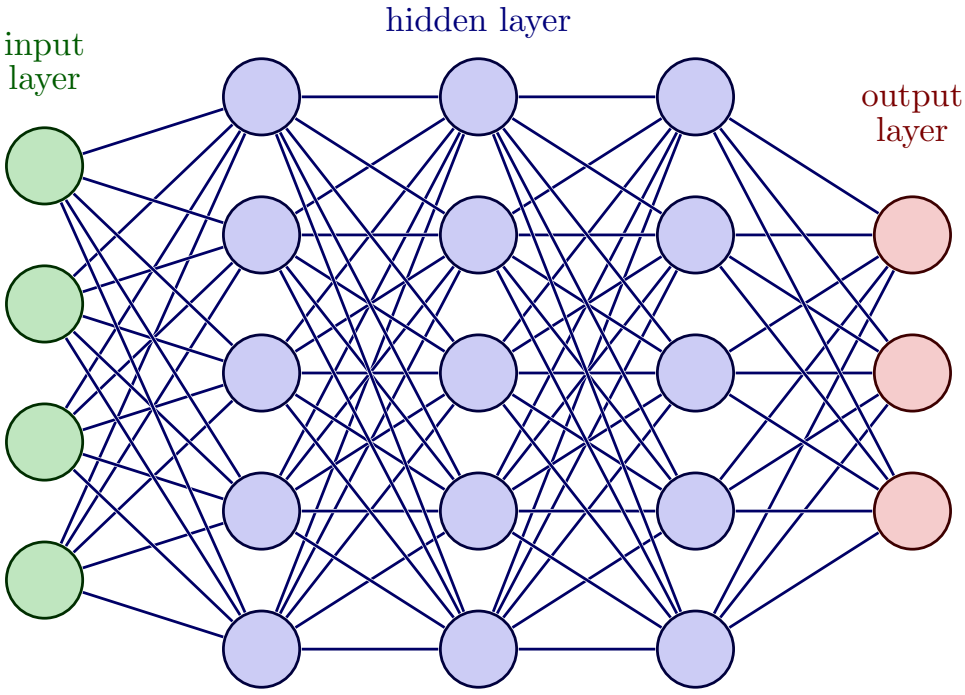

Figure 1.4: Fully connected DNN architecture [3].

There are two primary types of machine learning approaches: supervised learning and unsupervised learning [43]. These approaches differ in the way the models are trained and the type of training data that is required. Due to their different training approaches and data requirements, supervised and unsupervised learning models are usually applied to different tasks or problems, based on their individual strengths, as we will see on later. In addition

to these two approaches, there is another category known as reinforcement learning, which involves training an agent to interact with an environment and learn from the feedback received; this approach is not exploited in this PhD thesis.

Supervised learning Supervised learning is a machine learning technique that uses labeled datasets in the learning algorithms, allowing the model to "learn" from the labeled data and accurately classify new data or predict outcomes [44]. The labeled input and output data enable the model to measure its accuracy and improve its performance over time during the training phase.

Unsupervised learning Unlike supervised learning, unsupervised learning algorithms are generally designed to work with datasets that do not have ground truth labels and only consist of input data. In this case, the learning algorithm relies solely on input features to identify patterns, similarities, and differences within the data to perform the desired task. Since unsupervised learning aims to create a model without the help of labeled output data, it mainly employs clustering algorithms like K-Means [44] to form clusters or groups of similar examples.

Self-supervised learning Self-supervised learning is a form of unsupervised learning in which inputs and targets are generated from the given data without the help of external labels. In other words, training a model does not require separately labelled data because the information needed is already present in the data. For instance, self-supervised autoencoder is a type of neural network used in the field of image processing to learn effective coded representations of input data, typically for dimensionality reduction or for tasks like denoising. For instance, for the denoising task the autoencoder is trained to reconstruct a denoised image from a noisy input. The benefit of this method is that denoising does not require a separate labelled dataset; instead, the original data can be exploited to create noisy versions of it to train the autoencoder. This is a typical instance of self-supervised learning in which the training information is provided by the data itself [45].

Supervised vs. Unsupervised learning The key distinction between supervised and unsupervised learning lies in the utilization of labelled versus unlabelled training data. Supervised learning depends on labelled input and output data samples to teach the model the relationship between the two. The model is fine-tuned until it can accurately predict outcomes for unseen data. However, creating labelled training data is typically resource-

intensive. Unsupervised learning, on the other hand, learns from raw unlabelled data to identify inherent patterns and relationships within the dataset.

Unsupervised vs. self-supervised learning Self-supervised learning can be viewed as a specific case of unsupervised learning since there is no manual labeling involved. However, self-supervised learning generates its labels automatically from the data, whereas generic unsupervised learning does not use labels and aims to find hidden patterns or structures in the data.

To an in depth reading about deep learning methods, we refers the interested readers to [43–49] and references within.

The following Section will provide a review of the state-of-the-art techniques used for addressing power allocation problems in relay-aided cognitive radio networks considered in this PhD thesis.

1.3 State of the art of resource allocation techniques in relay-aided cognitive radio networks

Efficient management and allocation of resources, including transmit power, are crucial for achieving high performance in wireless communication systems. As wireless communications become more popular, the number of users is increasing, resulting in a higher density of users. This highlights the growing importance of properly allocating wireless resources. Consequently, researchers have extensively studied resource allocation, particularly transmit power control [50–53], in various wireless communication systems such as device-to-device [51,54,55] communication, vehicular communication [56–58] and cellular communication [52, 59, 60].

1.3.1 Traditional methods

Extensive research has been conducted on resource allocation problems in wireless networks; it is literally impossible to be exhaustive on this literature. Below we only discuss some of the most relevant papers.

The state of the art on resource allocation includes various works that can be classified based on the network types (multiple-input multiple-output (MIMO), orthogonal frequency-division multiplexing (OFDM), device-to-device (D2D), etc), their time variability (static, fading, arbitrarily varying), the objectives to be optimized (maximization of rate or energy

efficiency), etc. Additionally, these works may consider perfect or imperfect channel state information, and may employ different types of algorithms.

Regarding the various types of algorithm used, the existing works include: closed-form solutions [61–64]; exhaustive search [65,66]; iterative algorithms: iterative water-filling [67–71], iterative weighted MMSE [72,73], adaptative online learning algorithms [74–79]; heuristic algorithms: classical water-filling [80], genetic algorithms [81], particle swarm optimization [82].

We now focus on the most relevant works related to resource allocation policies in cognitive radio networks and relay-aided cognitive radio networks, i.e., the focus of this PhD thesis.

Several studies have investigated power allocation in cognitive networks without cooperative modes. For example, exhaustive search techniques are used to optimize the capacity of SUs in OFDM based cognitive radio systems [66]. Moreover, iterative waterfilling is proposed in [71] to maximize the sum-rate in multi-user networks, specifically in cognitive radio networks that use OFDM. Furthermore, the authors of [82] employed the particle swarm optimization technique to maximize signal-to-interference-plus-noise ratio utility, while ensuring the quality of service (QoS) for both primary and secondary users in a cognitive radio networks.

There have also been many research studies on relay-aided cognitive radio networks [83–86]. For instance, the authors of [83] investigate the optimal power allocation policies for the opportunistic user and the relay under an overall power constraint and a primary QoS constraint protecting the primary users. They provide a closed-form solution for the optimal power allocation policy in the case of CF relaying. In the context of DF the optimization problem poses a greater challenge due to its non-convex nature. However, the authors successfully demonstrate that finding the 3-dimensional optimal solution can be reduced to a 2-dimensional search. The authors of [84] proposed an alternative optimization algorithm for a rate maximization problem in the presence of AF relay. Specifically, they investigate these problems in two settings: half-duplex mode and when the direct link is neglected. Another related study, similar to [84], can be found in [85]. In that work, the authors propose an optimal approach utilizing dual methods for addressing rate maximization problems in AF relay scenarios.

Furthermore, the authors in [86] focus on studying the resource allocation (specifically, subcarrier and power allocation) in a relayed cellular cognitive radio network based on orthogonal frequency division multiple access and employing DF relaying. To optimize the power allocation process, iterative waterfilling technique is employed. Finally, the authors

of [87] present two approaches, an iterative algorithm and a genetic algorithm, with the aim to maximize the sum rate of unlicensed users while respecting a tolerated interference threshold in scenarios with both perfect and imperfect CSI.

Moving on to other techniques, relay selection and relaying scheme selection are important considerations and aspects of cooperative wireless communication systems to improve the performance and efficiency of such networks.

Various approaches can be found in the literature for relay selection and relaying scheme selection. Relay selection is a widely employed strategy in which the most suitable relay node is selected from a pool of multiple candidates based on criteria such as achievable rate or spectral efficiency, etc. Several studies, such as [88–91], have investigated this approach. For instance, the authors of [90] considered cognitive networks with multiple DF relays and investigated the selection of the best relay using a strategy that maximizes the effective capacity. The authors of [91] considered a cognitive underlay radio network with multiple half-duplex DF relays. The selection approach for the best relay is the one that maximizes the achievable rate for the secondary transmission while guaranteeing the QoS of the primary network.

In contrast to relay selection, relaying scheme selection involves choosing the most suitable relaying scheme out of several options, with the aim of achieving the best possible performance, in terms of metrics such as achievable rate, spectral efficiency, outage, and other relevant factors. For instance, studies such as [10] and [11] considered both AF and DF relaying schemes, with the selection criteria based on maximizing the signal to noise ratio in [10], while [11] utilized an outage-based and symbol error rate-based approach.

Overall, the resource allocation problems in relay-aided cognitive radio networks are generally complex and non-convex ones that require innovative tools and methods going beyond traditional ones. The use of such methods, for instance based on deep learning techniques, which will be presented in the following Subsection, can help to overcome the challenges associated with resource allocation in relay-aided cognitive radio networks and improve the performance of these networks [92–94].

1.3.2 DNN-based methods

Machine learning techniques have been used to address a range of resource allocation problems [95–100], including optimizing the allocation of spectrum, power, and computing resources in wireless networks.

These techniques have been extensively used in multi-user networks to maximize the

achievable sum rate [95], improve the spectral efficiency [59,96,97,99], or enhance the energy efficiency of the network [98, 100]. Moreover, the authors of [101], introduced a DNN to optimize the sum rate of a non-orthogonal multiple access D2D network aided by a relay.

In cognitive radio networks DNN-based resource allocation policies have been proposed to maximize the spectral efficiency while meeting power budget and QoS requirements and ensuring the protection of primary users. These DNN-based resource allocation policies have been proposed in several studies, including [92,102–106], to improve the overall performance of the cognitive radio networks under study. By utilizing the advanced capabilities of DNNs, these policies have the potential to adapt to dynamic network conditions and improve spectrum utilization, resulting in improved efficiency and performance. Other works focus on minimizing power consumption while meeting a pre-determined signal-to-noise interference ratio for both primary and secondary users [104]. The authors in [105] have suggested a deep learning methodology for resource allocation problems in cognitive radio networks with the goal of maximizing both spectrum and energy efficiency. Finally, in [106], a deep reinforcement learning approach is implemented to address a distributed resource allocation problem in cognitive radio networks. Despite the potential of DNN-based resource allocation policies to adapt to dynamic network conditions and improve spectrum utilization, their effectiveness can be limited by the lack of perfect CSI. As a result, several studies have explored the use of DNNs to address this issue and improve the robustness of resource allocation processes in cognitive radio networks [97, 107].

In order to address the issue of robustness to imperfect CSI, the authors in [107], proposed an autoencoder based on DNNs to improve channel estimation quality in the presence of CSI imperfections. This was then utilized as input to a second DNN, which aimed to maximize the achievable sum-rate of cognitive radio networks. Similarly, in [97], a power allocation policy was proposed for underlay D2D communications that maximizes the average spectral efficiency of the D2D user while maintaining the QoS of the cellular user equipment to an allowable level, even under imperfect CSI. To handle this issue, DNN techniques were employed to make the power allocation policy robust to channel estimation errors.

Regarding relay selection, previous studies have focused on the use of deep learning techniques, as demonstrated in [89, 108, 109]. However, to the best of our knowledge, there is currently no research that specifically investigates the application of DNNs for relaying scheme selection.

Our work stands out from the existing literature by focusing on the utilization of DNN techniques to develop optimal power allocation strategies for networks exploiting jointly co-

operative communication and cognitive radio. We address both CF and DF relaying schemes, in the presence of imperfect CSI, which, to the best of our knowledge, has not been previously proposed.

Additionally, we explore the selection of the most suitable relaying scheme using DNN-based techniques. To the best of our knowledge, this is the first study to consider DNN-based methods for relay scheme selection. So far, only traditional approaches have been proposed in this context. Furthermore, we introduce a novel DNN-based approach that enhances the generalizability of the DNN across various system parameters. This approach, to the best of our knowledge, has not been previously proposed in existing literature.

1.4 Manuscript contributions and organization

The main focus of this PhD manuscript revolves around the following topics:

- Resource allocation techniques for cognitive radio assuming perfect CSI;
- Deep learning based resource allocation techniques assuming imperfect CSI;
- Relaying scheme selection and generalized DNN solutions;

Chapter 2 of this PhD thesis is dedicated to investigating resource allocation techniques for cognitive relay-aided networks, assuming perfect CSI. First, we present the system model under study and formulate the non-convex optimization problem, with the goal of maximizing the achievable secondary rate under a primary QoS constraint, when the relay and secondary transmitter are also subject to maximum power budgets under both CF and DF relaying scheme. We demonstrate also that closed-form solutions are feasible for CF relaying. This is not the case for DF however. Hence, we introduce an unsupervised deep learning approach that can efficiently address the constrained and non-convex power allocation problem under DF relaying. Finally, we present simulation results that demonstrate the performance of the DNN solution compared to the exhaustive search algorithm in terms of secondary user data rate maximization and primary user QoS protection. The results confirm the potential of the proposed approach to overcome the limitations of traditional optimization techniques and provide practical solutions for power allocation in cognitive relay-aided networks.

Chapter 3 of this PhD thesis delves into the investigation of the resource allocation problem in the scenario where the channel static estimations are not perfect. Firstly, we introduce the channel errors estimation model. Secondly, we present our novel unsupervised DNN-based

solution for both CF and DF relaying schemes. Through numerous simulation experiments, we demonstrate the superiority of our proposed approach by comparing it against exhaustive search. The results illustrate the potential of our solution in achieving optimal resource allocation, even under the presence of imperfect channels.

Chapter 4, first addresses the problem of relaying scheme selection in cognitive radio networks. As both CF and DF relaying schemes have their advantages and limitations, we propose two distinct approaches to choose between them. The first approach is a method that relies on protecting the most the primary transmission, while the second one is a DNN-based solution that can efficiently handle the relaying scheme selection problem in a more optimized way. Second, while the previous Chapters (2 and 3) assumed fixed values for the system parameters, the maximum allowed primary rate degradation and power budget within the secondary network, in this Chapter, we propose a new DNN-based approach that can generalize the optimal power allocation policy when either the maximum allowed primary rate degradation or power budget in the secondary network are not predefined but can vary within a given range.

In conclusion, Chapter 5 provides a comprehensive summary of the contributions of this PhD thesis and discusses several open issues and perspectives for future investigation.

1.5 List of publications and invited talks

The research carried out in this PhD thesis has resulted in the following publications:

International journals

[J1prep] **Y. Benatia**, A. Savard, R. Negrel and E. V. Belmega, "Robust DNNs for power allocation problems in cognitive relay networks," in preparation for submission to IEEE Transactions on Machine Learning in Communications and Networking, June, 2023.

International conferences

[C2] **Y. Benatia**, A. Savard, R. Negrel and E. V. Belmega, "Unsupervised deep learning to solve power allocation problems in cognitive relay networks," IEEE ICC Workshop on

Data Driven Intelligence for Networks and Systems (DDINS), p. 1-6, Seoul, South Korea, May 16-20, 2022.

[C1] **Y. Benatia**, R. Negrel, A. Savard and E. V. Belmega, "Robustness to imperfect CSI of power allocation policies in cognitive relay networks," IEEE 23rd International Workshop on Signal Processing Advances in Wireless Communication (SPAWC), July 4-6, Oulu, Finland, 2022.

French national conferences

[CF1] R. Negrel, **Y. Benatia**, A. Savard and E. V. Belmega, "Sélection de relais robuste aux canaux imparfaits pour la radio cognitive coopérative exploitant des réseaux profond", presented in GRETSI, Grenoble, France, Apr. 2023.

Invited talks

[S4] Robustness to imperfect CSI of power allocation policies in cognitive relay networks, ETIS PhD student day, 25/05/2023 (Poster).

[S3] Robustness to imperfect CSI of power allocation policies in cognitive relay networks, University of Oulu, Finland, 16/06/2022.

[S2] Unsupervised deep learning to solve power allocation problems in cognitive relay networks, ETIS PhD student day, 10/03/2022 (Virtual).

[S1] Cooperation, optimization and artificial intelligence for future communications, ETIS PhD student day, 01/04/2021 (Virtual).

Chapter 2

Resource allocation techniques for cognitive radio assuming perfect CSI

2.1 Introduction

This Chapter focuses on studying resource allocation techniques for cognitive relay-aided networks, assuming perfect CSI.

First, we present the system model and formulate the non-convex power optimization problem under study. The cognitive relay-aided network under study consists of a primary and a secondary user–destination pair and a secondary full-duplex relay performing CF and DF. The primary communication is protected by a QoS constraint in terms of tolerated Shannon rate degradation. Because of the non-linear and complex relay operations, the resulting power allocation problems in such relay-aided cognitive networks are non-convex and can be solved in closed-form only in special cases, such as: negligible interference links [110], negligible opportunistic direct links [111]. Outside these very specific cases, such power allocation problems become difficult to tackle and even intractable using traditional techniques.

Second, we find the closed-form solution for CF relaying. Additionally, we present an unsupervised deep learning approach that can efficiently address the power allocation problem under DF relaying, for which a closed-form solution does not seem possible.

Finally, we evaluate the performance of our DNN solution through a series of experiments. The outcomes of this Chapter have been published in two conference papers [112, 113]. More specifically, [112] presents the closed-form solution to the optimization problem under consideration for CF relaying. On the other hand, [113] proposes a DNN-based solution to address the power allocation problem under DF relaying.

In the following Section, we describe the system model under study and formulate the power allocation optimization problem.

2.2 System model and problem formulation

In this Section, we define the system model under study and formulate the non-convex power allocation optimization problem, maximizing the constrained and non-convex Shannon rate problem under primary QoS constraints and power budgets in a relay-aided cognitive radio network.

2.2.1 System model

The system under study, depicted in Figure 2.1, is composed of a primary user or transmitter U_P and its destination D_P; a secondary full-duplex relay; and a secondary user or transmitter U_S and its destination D_S, similarly to [83,110–113]. The received signals at the relay, primary and secondary destinations write as

$$Y_R = h_{PR}X_P + h_{SR}X_S + Z_R \tag{2.1}$$

$$Y_i = h_{Ri}X_R + h_{ii}X_i + h_{ji}X_j + Z_j, \tag{2.2}$$

where $i \in \{P, S\}$, $j \in \{P, S\}\backslash i$; X_P, X_S and X_R, of average power P_P, P_S and P_R respectively, denote the message send by the primary user, the secondary user and the relay respectively; Z_R and Z_i denote the additive white gaussian noise (AWGN) at the relay and at destination D_i of variance N_R and N_i respectively. Without loss of generality, we assume that all noise processes are of unit variance $N_R = N_S = N_P = 1$ or equivalently we consider channel gains normalized by the receiver noise variance, defined as $g_{ij} = \frac{h_{ij}^2}{N_j}$. Furthermore, we assume that the channel gains follow a common fading and path-loss model given as $g_{ij} \sim \frac{\mathcal{N}(0,\sigma_g^2)}{\sqrt{1+d_{ij}^{\gamma}}}$, where d_{ij} denotes the distance between the nodes i and j and γ is the path loss factor [114]. We let $\mathbf{g} \triangleq (g_{ij}, \forall i, \forall j)$ denote the vector collecting all channel gains in the network.

Furthermore, we consider a full-duplex relay which is assumed to cancel out any self-interference [83, 110–113]. Both messages sent from the secondary network are treated as additional noise at the primary destination; and the primary message is treated as additional noise for all secondary receivers (relay and destination D_S). Hence, we can consider equivalent correlated Gaussian noises at the relay and secondary destination of variance $\widetilde{N}_R = g_{PR}P_P + 1$ and $\widetilde{N}_S = g_{PS}P_P + 1$ respectively; where the correlation coefficient equals $\rho_Z = \frac{\sqrt{g_{PR}g_{PS}}P_P}{\sqrt{\widetilde{N}_R\widetilde{N}_S}}$.

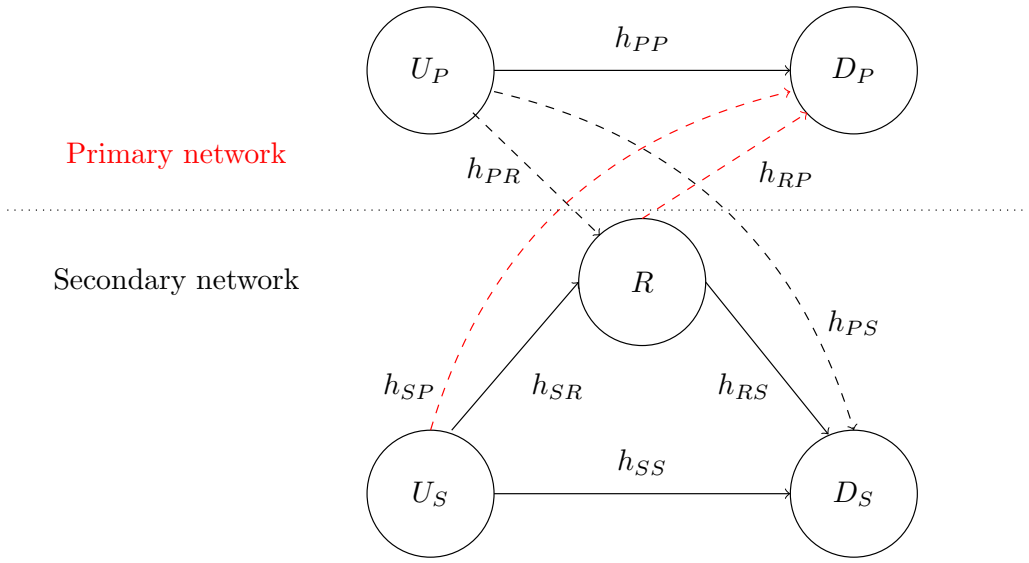

Figure 2.1: The cognitive relay-aided network under study.

Also, the messages sent by the secondary user and the relay are treated as additional noise at the primary destination; and the primary message is treated as additional noise throughout the secondary network. Let $R_i, i \in \{P, S\}$ denote the achievable rate of the primary and secondary user respectively; and $\overline{R_P}$ denote the primary achievable rate in the absence of the secondary transmission:

$$\overline{R_P} = \frac{1}{2}\log_2(1 + g_{PP}P_P).$$

The primary network allows the opportunistic communication provided that the following minimum QoS constraint is met in terms of achievable primary rate [83, 110, 113]:

$$R_P \geq (1-\tau)\overline{R_P},\ \tau \in [0,1]. \tag{2.3}$$

Notations To simplify the presentation, the following notations will be used:

$A = \frac{g_{PP}P_P}{(1+g_{PP}P_P)^{1-\tau}-1} - 1$, $x^+ = \max\{0, x\}$ and $C(x) = \frac{1}{2}\log_2(1+x)$ denotes the capacity of the point-to-point AWGN channel. Let K_1, K_2 denote

$$K_1 = g_{SR}\widetilde{N}_S + g_{SS}\widetilde{N}_R - 2\rho_Z\sqrt{g_{SR}g_{SS}\widetilde{N}_S\widetilde{N}_R},\quad K_2 = (1-\rho_Z^2)\widetilde{N}_R\widetilde{N}_S.$$

In the following Subsection, we formulate the power allocation problem under CF and DF relaying.

2.2.2 Problem formulation

Our main objective is to maximize the opportunistic achievable rate R_S, when both the relay and secondary user are constrained by a maximum power expressed as $\overline{P_R}$ and $\overline{P_S}$ respectively. To sum up, the resulting generic form of the optimization problem under study for both CF and DF writes as

$$\begin{aligned}(\mathbf{OP}) \quad & \max_{P_R,P_S} R_S(P_S,P_R) \\ & \text{s.t. } R_P \geq (1-\tau)\overline{R_P}, && \text{(QoS)} \\ & \quad 0 \leq P_S \leq \overline{P_S}, \;\; 0 \leq P_R \leq \overline{P_R}, && \text{(TP)}\end{aligned}$$

where the secondary and primary achievable rates R_S and R_P depend on the specific relaying scheme. The constraint (QoS) is the primary QoS constraint used to protect the primary transmission, constraints (TP) correspond to the individual power constraint of the secondary user and relay.

Next, we focus on the optimization problems specific to CF and DF relaying by substituting the achievable rate regions obtained in [83] into the original optimization problem (OP).

Compress-and-Forward (CF): Under CF, exploiting the achievable rate region of [83] leads to the following optimization problem

$$\begin{aligned}(\mathbf{OCF}) \quad & \max_{P_R,P_S} R_S(\mathbf{h},P_S,P_R) \\ & \text{s.t. } Q(\mathbf{h},P_S,P_R) \leq A, && \text{(QoS)} \\ & \quad 0 \leq P_S \leq \overline{P_S}, \;\; 0 \leq P_R \leq \overline{P_R}, && \text{(TP)}\end{aligned}$$

$$\text{with, } R_S(\mathbf{h},P_S,P_R) = C\left(\frac{K_1 g_{RS} P_S P_R + g_{SS} P_S (K_1 P_S + K_2)}{K_2 g_{RS} P_R + \widetilde{N_S}(K_1 P_S + K_2)}\right)$$
$$Q(\mathbf{h},P_S,P_R) = g_{SP} P_S + g_{RP} P_R.$$

Although non-convex, this optimization problem can be solved in closed-form under perfect CSI, as shown in the following.

Decode-and-Forward (DF): Under DF, exploiting the achievable rate region of [83] leads to the following optimization problem

$$
\begin{aligned}
(\mathbf{ODF}) \quad & \max_{P_R,P_S,\alpha} R_S(\mathbf{h},\alpha,P_S,P_R) \\
& \text{s.t. } Q(\mathbf{h},\alpha,P_S,P_R) \leq A, && (\text{QoS}') \\
& \quad 0 \leq P_S \leq \overline{P_S}, \;\; 0 \leq P_R \leq \overline{P_R}, && (\text{TP}) \\
& \quad 0 \leq \alpha \leq 1, \text{ with} && (\text{ADF})
\end{aligned}
$$

$$
\begin{aligned}
R_S(\mathbf{h},\alpha,P_S,P_R) &= C(\min\{f_R(\mathbf{h},\alpha,P_S,P_R), f_S(\mathbf{h},\alpha,P_S,P_R)\}) \\
Q(\mathbf{h},\alpha,P_S,P_R) &= g_{SP}P_S + g_{RP}P_R + 2\alpha\sqrt{g_{SP}g_{RP}P_SP_R}, \\
f_R(\mathbf{h},\alpha,P_S,P_R) &= \frac{g_{SR}(1-\alpha^2)P_S}{\widetilde{N}_R}, \\
f_S(\mathbf{h},\alpha,P_S,P_R) &= \frac{g_{SS}P_S + g_{RS}P_R + 2\alpha\sqrt{g_{RS}g_{SS}P_SP_R}}{\widetilde{N}_S},
\end{aligned}
$$

where the additional variable $\alpha \in [0,1]$ trades-off between sending a new codeword and repeating the previous one under the information-theoretic superposition coding scheme [83]. Despite its non-convex nature, this optimization problem can be effectively addressed using DNN techniques under perfect CSI, as shown in Section 2.4.

In the following Section, we present the closed-form solutions for the power allocation problem under study related to CF relaying.

2.3 Closed-form solution for CF

For CF relaying, in spite of (**OCF**) not being a convex problem, we provide below its closed-form analytical solution. To simplify its derivation, we will use the following notations:

$$
\begin{aligned}
C_1 &= K_1 g_{RP}(g_{SS}g_{RP} - g_{RS}g_{SP}) \\
C_2 &= K_1 g_{RS}g_{SP}A - 2K_1 g_{SS}A g_{RP} - g_{SS}g_{RP}g_{SP}K_2 \\
C_3 &= g_{SS}A(K_1 A + g_{SP}K_2) \\
C_4 &= K_2 g_{RS}g_{SP}^2 - \widetilde{N}_S K_1 g_{RP}g_{SP} \\
C_5 &= \widetilde{N}_S g_{SP}(K_1 A + K_2 g_{SP})
\end{aligned}
$$

The objective function of the optimization problem (**OCF**) can be shown to be monotonically increasing unilaterally as a function of P_S for fixed P_R, and as a function of P_R for fixed P_S. This implies that the optimal power allocation lies on the Pareto boundary of

the feasible set. Now, regarding the specific shape of the feasible set defining the solution of (**OCF**), five cases can arise as depicted in Figure 2.2, depending on the relative position of the QoS curve and the total power box-type constraints:

[H1] if $\frac{A}{g_{RP}} < \overline{P_R}$ and $\frac{A}{g_{SP}} < \overline{P_S}$, (aside from positivity) only the QoS constraint restricts the feasible set;

[H2] if $\frac{A}{g_{RP}} < \overline{P_R}$ and $\frac{A}{g_{SP}} > \overline{P_S}$, the QoS constraint intersects the secondary user power constraint;

[H3] if $\frac{A}{g_{RP}} > \overline{P_R}$ and $\frac{A}{g_{SP}} < \overline{P_S}$, the QoS constraint intersects the relay's power constraint;

[H4] if $\frac{A}{g_{RP}} > \overline{P_R}$ and $\frac{A}{g_{SP}} > \overline{P_S}$ and $g_{SP}\overline{P_S} + g_{RP}\overline{P_R} < A$, the QoS constraint intersects both total power constraints;

[H5] if $\frac{A}{g_{RP}} > \overline{P_R}$ and $\frac{A}{g_{SP}} > \overline{P_S}$ and $g_{SP}\overline{P_S} + g_{RP}\overline{P_R} \geq A$, only the total power constraints define the feasible set.

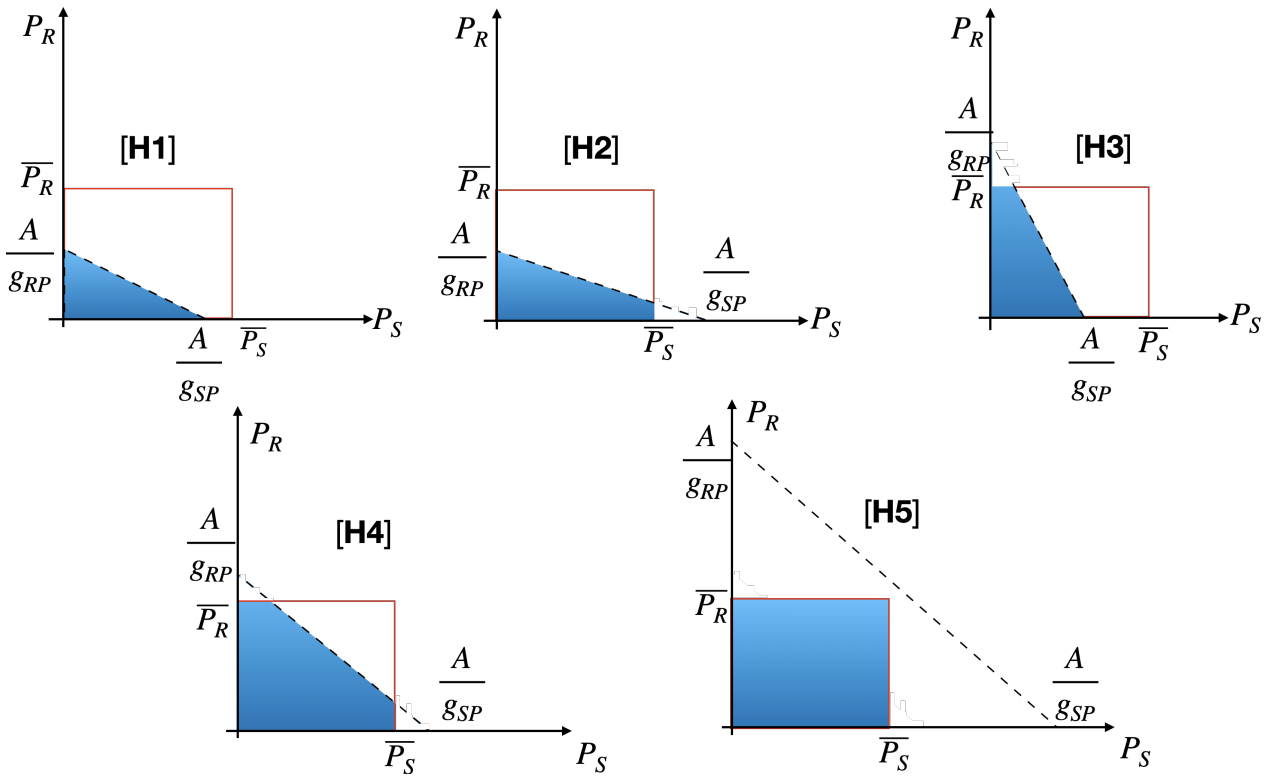

Figure 2.2: Feasible set of (**OCF**).

A close analysis of these five cases and, since the optimal solution lies on the Pareto boundary of the feasible set, leads us to the following result.

Theorem 1 *When the relay employs CF over the cooperative cognitive radio network, the solution to* (**OCF**) *can be found analytically in closed form. Indeed, when* ***[H5]*** *is met, the QoS constraint is not restrictive and the solution is simply* $P_R^* = \overline{P_R}, P_S^* = \overline{P_S}$. *In all other cases,* ***[H1]***–***[H4]****, the solution to* (**OCF**) *lies on the QoS constraint such that* $P_R^* = x^*$, $P_S^* = \frac{A - g_{RP}\, x^*}{g_{SP}}$, *where* x^* *is the closed-form solution to the following single-value optimization problem*

$$(\mathbf{OCF_x}) \quad \max_{x} \quad f(x) \triangleq \frac{C_1 x^2 + C_2 x + C_3}{C_4 x + C_5}, \\ s.t. \;\; x \in [x_\ell;\; x_u]. \tag{2.4}$$

The values of x_ℓ *and* x_u *defining the box-type constraints depend on the system parameters and the specific case.*

The complete proof is given in Appendix A and follows from the study of the equation $f'(x) = 0$, i.e., finding the critical points of $f(x)$.

It is important to note that there is a difference between the problem formulation presented in Section 2.2.2 and those in [83] and [110]. The difference lies in the constraints imposed on the transmit powers and the treatment of interference links. In [83], the problem involves the sum of the relay and secondary powers as a constraint, which must be less than a certain total budget. In contrast, in our case, we consider individual power constraints for the relay and secondary transmitter. This means that our feasible set is distinct from that in [83] and hence the solutions are also different. Furthermore, we do not make the assumption that interfering links between licensed and opportunistic users are negligible. This contrasts with the problem studied in [110], where the interfering links are considered negligible.

In the following Section, we present the proposed DNN-based solution to solve the power allocation problem under study related to DF relaying. We provide a comprehensive description of the custom loss function employed and elaborate on the architecture of the DNN used in our approach.

2.4 DNN-based solution for DF relaying

Regarding CF relaying, the presence of the ratio in the objective function of (**OCF**) leads to its non-convexity. Despite the non-convex nature of (**OCF**) we could still solve it analytically. One advantage compared to (**ODF**) is that the constraints in (**OCF**) are affine. Additionally, CF relaying involves only P_R and P_S as optimizing variables. At last, due to the monotonicity

proprieties of the objective function in (**OCF**), we could show that the solution lies on the Pareto region of the feasible set which is a simple polyhedre.

A close analysis of the problem (**ODF**) reveals a non-concave objective function coupled by a non-convex QoS constraint (QoS$'$), which is due to the non-linear operations performed by the relay.

When compared to (**OCF**), the optimization problem (**ODF**) consists of an additional optimizing variable α. Furthermore, the term involving a square root: $\alpha\sqrt{P_S P_R}$ that is present both in the objective function via f_S and in the QoS constraint, renders the (**ODF**) problem not only non convex, but significantly more difficult compared to (**OCF**). Therefore, finding a closed-form solution for (**ODF**) seems highly difficult and unlikely.

Instead, to solve (**ODF**) we propose an unsupervised approach based on deep neural networks (DNN). The reason behind the unsupervised learning is that, a supervised approach would require computing a labeled training dataset containing the solutions to the non-convex problem (**ODF**) for a large number of sampled system parameters. This would be too computationally heavy (via exhaustive search) and, henceforth, we opt for an unsupervised approach relying on a training dataset composed of only samples of the inputs (i.e., system parameters) of our DNN and exploiting a specifically tailored communication loss to perform the training.

2.4.1 Custom loss function

A key component of our proposed approach is the loss function that the network will be trained to minimize. Solving constrained optimization problems with DNNs is highly non-trivial, unless the constraints are of box-type such as (TP, ADF). This is not the case of the QoS constraint (QoS$'$) which is a difficult non-convex constraint. Nevertheless, as opposed to the power constraints (TP), the primary QoS constraint is not a physical (hard) constraint but rather a requirement, which can be relaxed and included as a penalty in the objective function below

$$\mathcal{L} = \sum_{\ell=1}^{N} \left(-R_S(\mathbf{g}_\ell, \alpha, P_S, P_R) + \lambda [Q(\mathbf{g}_\ell, \alpha, P_S, P_R) - A]^+ \right), \tag{2.5}$$

with $[x]^+ = \max\{0, x\}$ and N denoting the total number of channel realizations $\mathbf{g}_\ell$, $\ell \in \{1, \ldots, N\}$ in the training dataset.

The hyperparameter λ denotes the unit price in bits/Watt of the primary QoS violation. A small value of λ will result in maximizing the achievable opportunistic rate without taking into account the primary QoS constraint; whereas large values of λ will strictly satisfy the primary

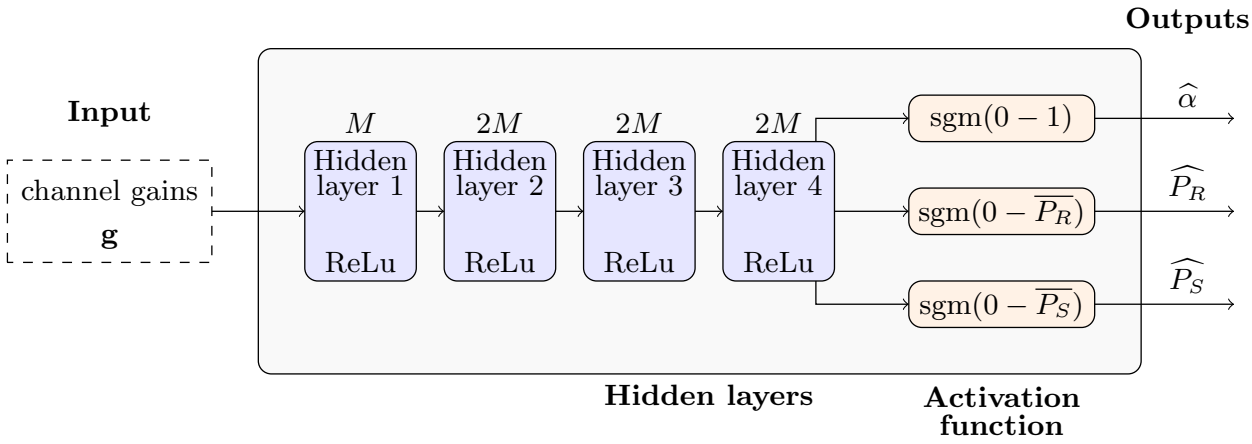

Figure 2.3: Our proposed DNN architecture.

QoS constraint but at the cost of opportunistic rate. This tradeoff between opportunistic rate and primary QoS will be further investigated via numerical results.

The concept of employing custom loss functions has already been explored in various research studies, including [59, 103, 115–117].

2.4.2 Proposed DNN architecture

Our proposed DNN architecture to solve (**ODF**) is composed of four fully connected hidden layers and is depicted in Figure 2.3. The input consists of the channel gains vector $\mathbf{g}$ which is used to predict the outputs: $(\hat{\alpha}, \hat{P}_R, \hat{P}_S)$, i.e., the solution of (**ODF**). The fully connected architecture is justified because of its generality and given that there is no *a priori* structural or temporal information within the input vector $\mathbf{g}$ to be exploited via more specific architectures such as convolutional or recurrent networks.

The four hidden layers are composed of $M - 2M - 2M - 2M$ neurons with $M = 128$ and are followed by a rectified linear unit (ReLU) activation function due to its low computational complexity. This specific architecture has been chosen based on extensive empirical experiments, as we discuss in the numerical Section.

The final layer is followed by sigmoid activation functions: a standard one $\text{sgm}_\alpha(x) = 1/(1+\text{e}^{-x})$ to map the predicted α into its feasible set $[0, 1]$, and two modified ones $\text{sgm}_{P_i}(x) = \overline{P_i}/(1 + \text{e}^{-x})$, $i \in \{S, R\}$, to map the predicted powers P_R and P_S into $[0, \overline{P_R}]$ and $[0, \overline{P_S}]$ respectively. This final layer ensures that the hard constraints (TP), (ADF) are met.

In the following Section, we provide a comprehensive overview of our numerical results. This Section encompasses a summary of various experiments conducted to evaluate the ef-

fectiveness of our DNN-based solution.

2.5 Numerical results

Below, we discuss our numerical setup and DNN training procedure as well as the performance evaluation of our approach. Complete details and source codes of our experiments are available online at https://github.com/yacine074/.

Experimental setup: We consider a square cell of dimension 10×10 m in which the relay is positioned in the center whereas both primary and secondary user positions are uniformly distributed in the cell, unless specified otherwise. As described in Section 2.2, the channel gains follow a common fading and path loss model given as, $h_{ij} \sim \frac{\mathcal{N}(0,\sigma_g^2)}{\sqrt{1+d_{ij}^{\gamma}}}$, where d_{ij} is distance between nodes i and j. The path loss factor is set to $\gamma = 3$ and the channel gain standard deviation $\sigma_g = 7$. We assume that $P_P = \overline{P_R} = \overline{P_S} = 10$ W and set the threshold $\tau = 0.25$ for the maximum primary rate degradation. This means that the opportunistic network is allowed to communicate over the licensed bands provided that the primary achievable rate is not degraded below a fraction $(1 - \tau)$ of its achievable rate in the absence of the secondary network.

Dataset: To the best of our knowledge, the majority of related works exploiting DNNs use simulated data [102,105,115,116], given the lack of real data that is available and open access. Thus, to train and test our proposed DNN architecture, we use a dataset composed of: i) a training set containing 10^6 channel realizations $\mathbf{g}_\ell$, out of which 20 % is used for validation, i.e., to evaluate the generalization capability of our proposed DNN during training; ii) a test set containing 2×10^5 channel realisations $\mathbf{g}_\ell$, as well as the optimal resource allocation policy (α^*, P_R^*, P_S^*) obtained by brute force (or exhaustive search) to evaluate the optimality gap of our predicted solution.

DNN training: In our numerical simulations, we use the ADAM optimizer [118] to iteratively update the weights of our DNN. The batch size is set to 4096, the learning rate to 10^{-4}; these values allows the DNN weights optimization to converge within 1000 epochs.

Benchmarks and performance metrics: We define here the relevant performance metrics used for the evaluation purpose. First, we define the relative gap between the predicted

achievable rate via our DNN and the achievable rate obtained by brute force, our ideal benchmark, as follows:

$$\mathrm{G} = \frac{\frac{1}{N}\sum_{\ell=1}^{N} \hat{R}_{S,\ell} - R^*_{S,\ell}}{\frac{1}{N}\sum_{\ell=1}^{N} R^*_{S,\ell}} \tag{2.6}$$

where $\hat{R}_{S,\ell} = R_s(\mathbf{g}_\ell, \hat{\alpha}, \hat{P}_S, \hat{P}_R)$ denotes the secondary achievable Shannon rate obtained based on our DNN prediction for the ℓ-th sample in the dataset and $R^*_{S,\ell}$ denotes the optimal rate for the ℓ-th sample in the dataset obtained via brute force or exhaustive search. We choose brute force as benchmark thanks to its implementation simplicity and because it approximates the optimal solution with an adjustable precision. In our approach, we use a uniform grid with a step size of $\frac{1}{10}$ for each problem dimension (α, P_R, P_S).

Intuitively, if the value of G is zero, then the secondary achievable rate obtained from our DNN model $\hat{R}_{S,\ell}$ is equal to $R^*_{S,\ell}$ obtained by the brute force. If G is positive, our DNN solution outperforms the brute force, which can happen since the brute force must always meet the primary QoS constraints, which is not necessarily true for the DNN method. Conversely, if G is negative, the brute force performs better than our DNN, in terms of achievable secondary rate.

Second, the degradation of the primary achievable rate caused by the opportunistic interference is defined as:

$$\Delta_\ell = 1 - \hat{R}_{P,\ell}/\overline{R}_{P,\ell}, \tag{2.7}$$

where $\hat{R}_{P,\ell} = R_P(\mathbf{g}_\ell, \hat{\alpha}, \hat{P}_S, \hat{P}_R)$ denotes the achievable primary rate of our predicted policy, and $\overline{R}_{P,\ell}$ is the obtained achievable primary rate without the secondary interference. If Δ_ℓ is equal to one, it implies that $\hat{R}_{P,\ell}$ is zero, indicating that the secondary communication crucially degrades the primary communication. Conversely, if Δ_ℓ is equal to zero, it means that $\hat{R}_{P,\ell}$ is equal to $\overline{R}_{P,\ell}$, signifying that the secondary communication has no detrimental impact on the primary communication. In the figures presented in the numerical simulation section, where we analyze the degradation of the primary network, the term "Average" corresponds to the mean value of the primary rate degradation (Δ_ℓ).

Based on this metric, we can also define the maximum primary rate degradation (Max = $\max(\Delta_\ell)$), and the empirical outage as the proportion of samples in the dataset (or channel settings) for which the target primary QoS constraint is not met:

$$\text{Outage} = \frac{1}{N}\sum_{\ell=1}^{N} \mathbb{I}\left[\Delta_\ell > \tau\right], \tag{2.8}$$

where ℓ, denote the ℓ-th sample in the test set, and N is the total number of samples in our test set. The summation is performed over each sample in the test set. Moreover, for every

sample in the test set, we calculate Δ_ℓ, which represents the degradation in the primary rate. Then, we sum the samples where Δ_ℓ exceeds the predetermined threshold τ, and divide this sum by the total number of samples in our test set N.

A high value of the empirical outage (close or equal to one) indicates a poor performance of the system, reflecting significant interference coming from secondary users. This interference leads to a larger number of instances where the primary rate fails to meet the required level, as indicated by the empirical outage. Furthermore, this interference contributes to a larger number of Δ_ℓ values surpassing the maintained threshold τ.

At last, we introduce the average primary rate degradation metric Δ_{out} to measure the level of degradation in the primary rate when the system is in an outage state, i.e., when the interference from the secondary network exceeds the predefined threshold τ. It represents the average impact on the primary rate specifically during these outage scenarios.

It is important to note that Δ_{out} is consistently greater than the predefined threshold τ. Consequently, the objective is to minimize the difference between Δ_{out} and τ, aiming for a Δ_{out} that is as close as possible to τ.

$$\Delta_{\text{out}} = \frac{\sum_{\ell=1}^{N}(\mathbb{I}\left[\Delta_\ell > \tau\right] \times \Delta_\ell)}{\sum_{\ell=1}^{N} \mathbb{I}\left[\Delta_\ell > \tau\right]}, \tag{2.9}$$

where $\mathbb{I}\left[x\right]$ equals 1 when x is true and 0 otherwise.

Δ_{out} represents the average of Δ_ℓ values that exceed the maximum allowed primary degradation threshold τ.

As previously explained for the Outage, the summation definition in Δ_{out} is performed over each sample in the test set, and ℓ, is the ℓ-th sample in the test set, and N is the total number of samples in our test set.

DNN architecture choice: To choose the architecture in Figure 2.3, we have performed extensive numerical simulations. In Figure 2.4, we report the most significant results. On the left, we analyze the impact of the number of layers and compare four different architectures composed of one up to four hidden layers as follows: M, $M-2M$, $M-2M-2M$, and $M-2M-2M-2M$, with $M = 128$. We see that there is a significant gain in secondary rate when increasing the number of layers from 1 to 3; moving to 4 layers helps to decrease the outage. Including a fifth layer in the DNN architecture will result in an increased computational time without any gain in secondary rate. Hence, a 4-layer architecture is a good compromise between performance and computational cost. Now, on the right, we compare three different such four-layer DNNs, by varying the number of neurons per layer $M \in \{64, 128, 256\}$. We

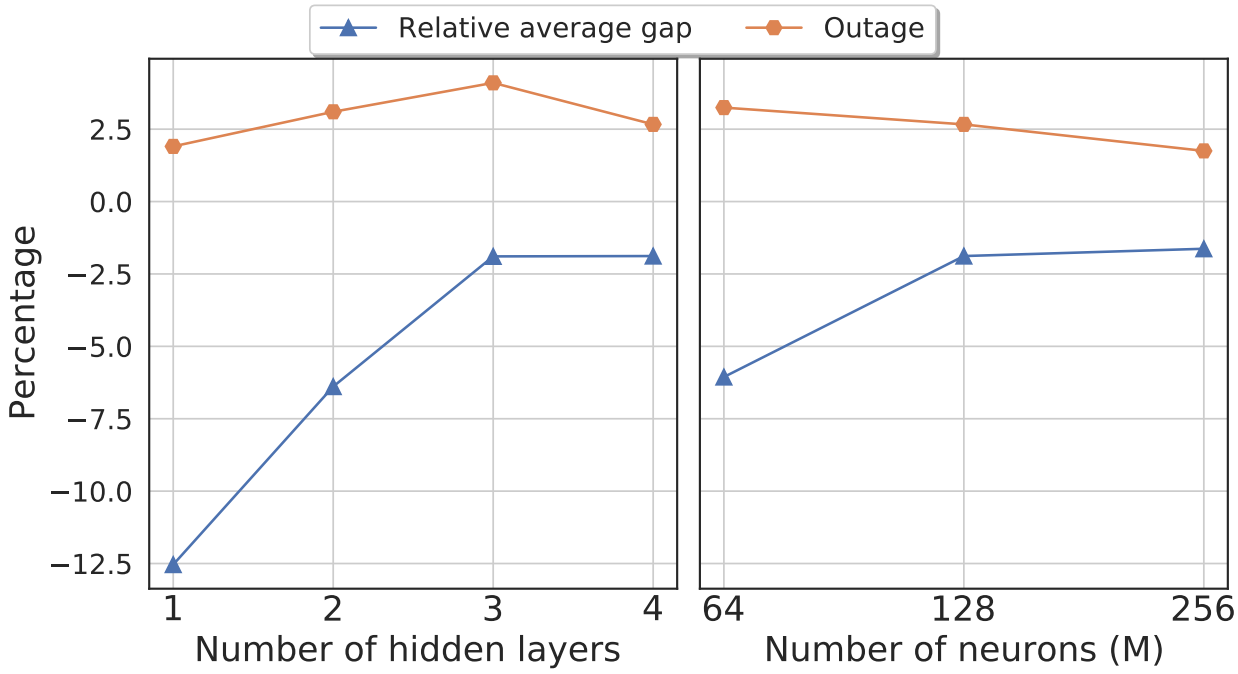

Figure 2.4: Impact of the number of layers and number of neurons on the prediction performance.

see that increasing M from 64 to 128 neurons leads to a significant gain in secondary rate; increasing further the number of neurons does not seem justified given the incurred computational cost. For these reasons, we choose $M = 128$ coupled with the 4-layer architecture in Figure 2.3 henceforth.

Performance on train and validation sets (No overfitting): In Figure 2.5, we plot the evolution of our custom loss function $\mathcal{L}$ over the number of epochs within the training and validation sets for $\lambda \in \{10^{0.5}, 10^{2}\}$. First, notice that the DNN training converges within 1000 epochs. The superposed performance obtained within the training and validation sets highlights the high generalization capability of our proposed DNN. In addition, no overfitting effects can be noticed, since the loss function does not increase within the validation set. Finally, the convergence of optimizing the weights of the DNN is much faster for relatively small values of λ. Indeed, when λ is small, the custom loss is mainly rate-driven and not much emphasis is put on the primary QoS constraint; this leads to a much easier optimization problem to solve without (QoS$'$). At the opposite, for larger values of λ, the custom loss puts an emphasis on satisfying (QoS$'$), which leads to a more difficult problem. Of course, this parameter needs to be tuned whenever the system parameters change significantly.

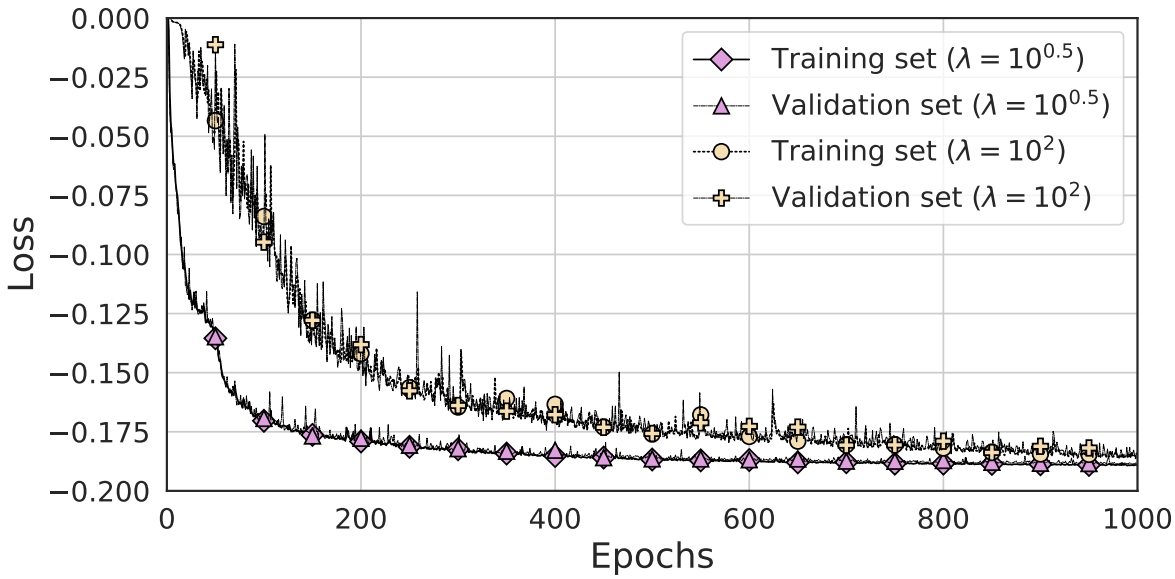

Figure 2.5: Evolution of the loss function evolution over the training epochs over the training and validation sets (no overfitting effects).

Prediction performance on the test set: Henceforth, we evaluate the performance of our predicted solution $(\hat{\alpha}, \hat{P}_R, \hat{P}_S)$ obtained with new samples (i.e., test data) unseen during the training or validation phases.

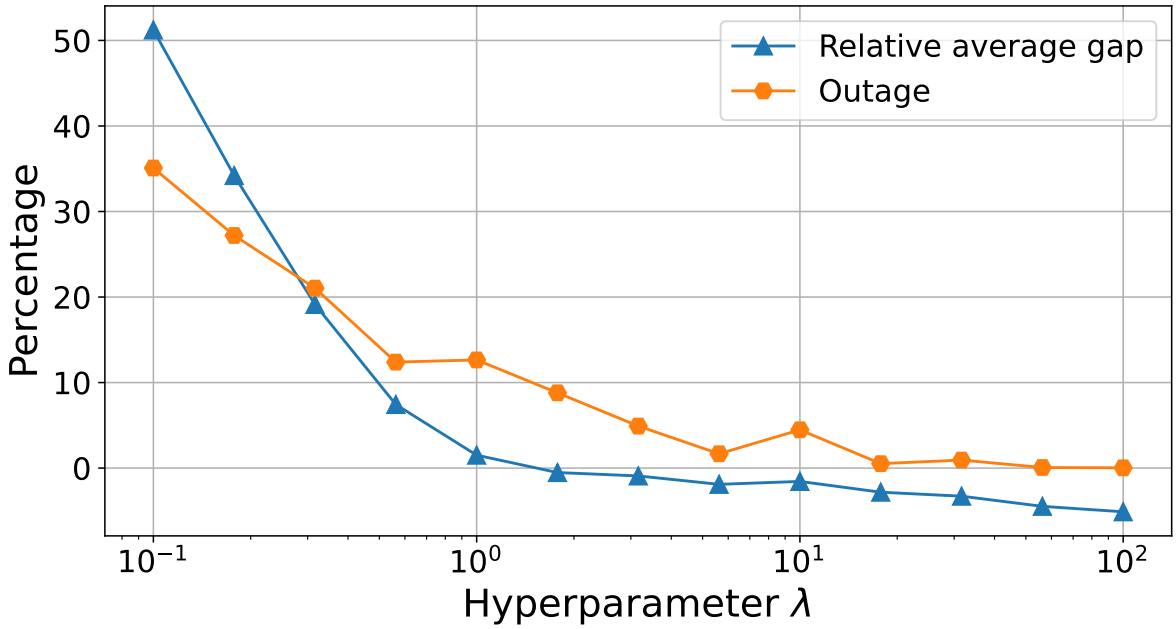

Figure 2.6: Relative average gap G and outage as functions of the hyperparameter λ over the test set.

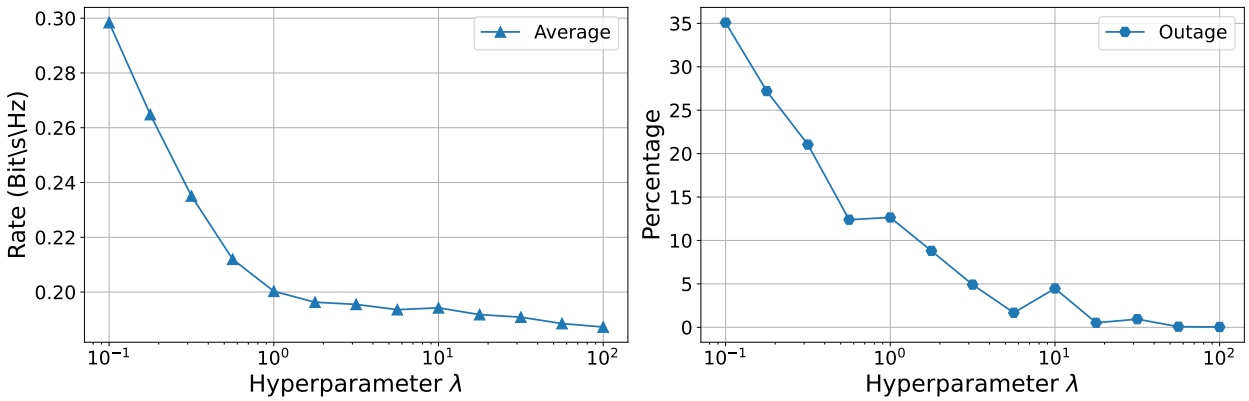

Figure 2.7: Average secondary rate R_S and outage as functions of the hyperparameter λ over the test set.

Choice of the hyperparameter λ: In Figure 2.6, the relative gap in equation (2.6) and the outage in (2.8) are depicted as functions of λ. For small values of λ (rate-driven custom loss), the relative gap G is positive, which means that the secondary rates obtained via the DNN are larger than the optimal ones via brute force. The reason is that the primary QoS constraints are not necessarily met by our DNN solutions, as illustrated by the high outage levels. At the opposite, for large values of λ (primary QoS-driven custom loss), the outage goes to zero as expected at a cost in terms of secondary rates. Indeed, our predicted secondary rates are smaller than the optimal ones (negative relative gain G), but this gap is kept below 10%.

This observation is also supported by Figure 2.7, where the average of the secondary rate and outage are plotted as functions of the hyperparameter λ. The main objective in Figure 2.7 is to identify an optimal value of λ, without the need to compute the relative gap as done in Figure 2.6, which requires the brute force method. The figure clearly illustrates that a low value of λ leads to a higher secondary rate but an increased outage. Conversely, a high value of λ results in a lower secondary rate but with a reduced number of outage. An optimal choice of λ maximizes the secondary rate and satisfies the QoS of the primary network as much as possible. Therefore, the value $\lambda = 10^{0.5}$ achieves a good tradeoff between the achievable secondary rate and the primary QoS degradation in our setting and will be used in the test phase below.

In Figure 2.8, we investigate closer the impact of λ on the primary rate degradation within the test set. For this, we plot the average and maximum values of the primary rate degradation as well as the average degradation when in outage Δ_{out} in (2.9) in Figure 2.8a. Also, in Figure 2.8b, we illustrate the histogram of the primary rate degradation (Δ) for

$\lambda \in \{10^{0.5}, 10^{2}\}$. Notice that the average primary rate degradation falls quickly below the threshold $\tau = 25$ %. For small values of λ, the worst case primary degradation can reach up to 90 %. Nevertheless, such extreme degradation is obtained only for a small number of out-layer data points. This is indicated by the curve Δ_{out} hitting the 25 % threshold reasonably fast as well as by the histogram of the degradation in Figure 2.8b.

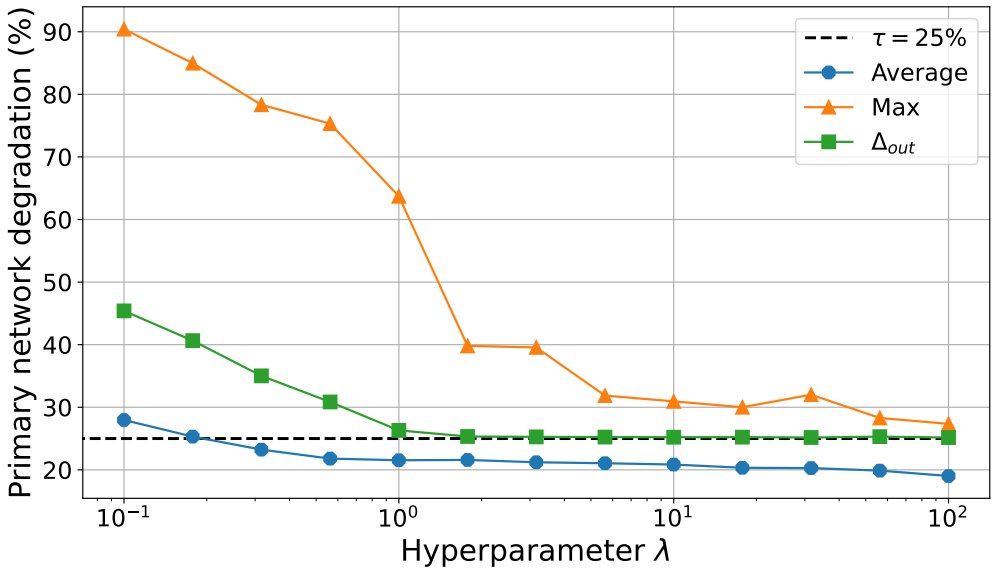

(a) Average and maximum primary rate degradation and average degradation when in outage (Δ_{out}) as functions of λ over the test set.

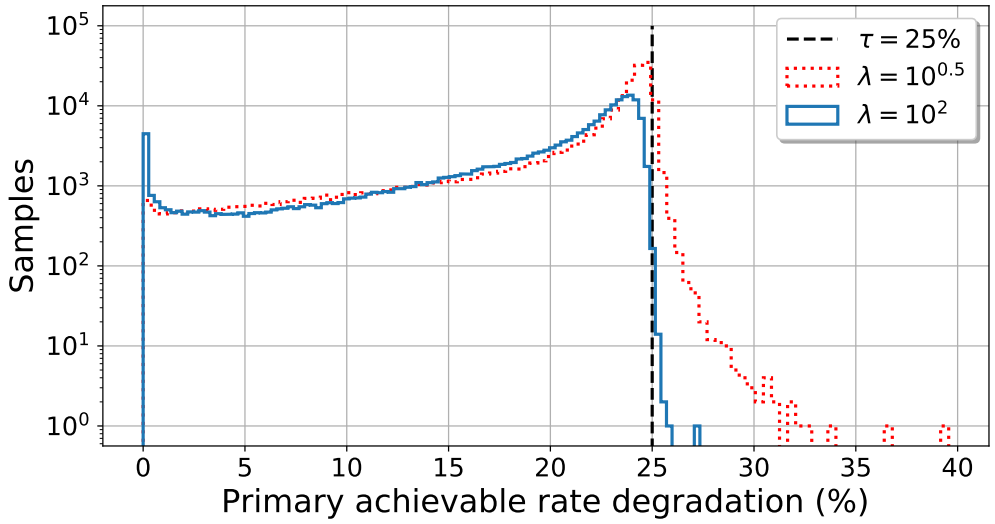

(b) Histogram of the primary rate degradation over the test set.

Figure 2.8: Impact of the hyperparameter λ.

To sum up, the hyperparameter λ highlights the tradeoff between achievable secondary rate and primary QoS degradation and has to be carefully tuned depending on the target application and primary network tolerance. As already mentioned above, we choose $\lambda = 10^{0.5}$ due to its good compromise between the achievable secondary rate and the primary QoS degradation.

Impact of the relay position: We now wish to investigate the effect of the relay position relative to the other system nodes. For this, we consider three different scenarios with fixed positions for the primary and secondary user/destination pairs.

- 1st scenario: symmetric positions,
  $U_S(5, 2.5)$, $D_S(7.5, 5)$, $U_P(2.5, 5)$, $D_P(5, 7.5)$, as depicted in the top plots of Figure 2.9.
- 2nd scenario: asymmetric positions,
  $U_S(3.2, 3)$, $D_S(6.5, 1)$, $U_P(2, 7)$, $D_P(6.5, 8.5)$, as shown in the middle plots of Figure 2.9. We note that the direct links are stronger than the interfering ones, in this case.
- 3rd scenario: asymmetric and crossed positions among primary and secondary network,
  $U_S(3.2, 3)$, $D_S(6.5, 8.5)$, $U_P(2, 7)$, $D_P(6.5, 1)$, as depicted in the bottom plots of Figure 2.9. We note that the interfering links are stronger than the direct links, in this case.

All simulation results are averaged over 10^4 channel realizations with $\lambda = 10^{0.5}$, as this value achieves a good tradeoff between the achievable secondary rate and the primary QoS degradation. In all scenarios, the relay position (x_R, y_R) varies within the entire cell. For this, we generate 256×256 positions for the relay, hence the grid step is $\frac{10}{256}$ m in each 2D axis. In Figure 2.9a, Figure 2.9b, and Figure 2.9c, we illustrate the average primary rate degradation, the average predicted relay power $\hat{P}_R$ and the average secondary rate $\hat{R}_S$, respectively as functions of the relay position (x_R, y_R).

In Figure 2.9a, we see that for all scenarios, the average degradation in the primary rate always falls below the fixed threshold of $\tau = 25$ % irrespective from the relay position. When the relay is very close to the primary nodes, the degradation drops below 20 %, since very little power is allocated to the relay as shown in Figure 2.9b to meet the QoS constraints. We remark that the worst degradation for DF occurs when the relay is close to the secondary transmitter (see Figure 2.9a). This is also the case in which the relay is allocated more power (see Figure 2.9b) and the secondary rate is maximized (see Figure 2.9c). Our observations are consistent with information theoretic results; since the relay has to first decode the

transmitted message before forwarding it, the relay is best located near the information source.

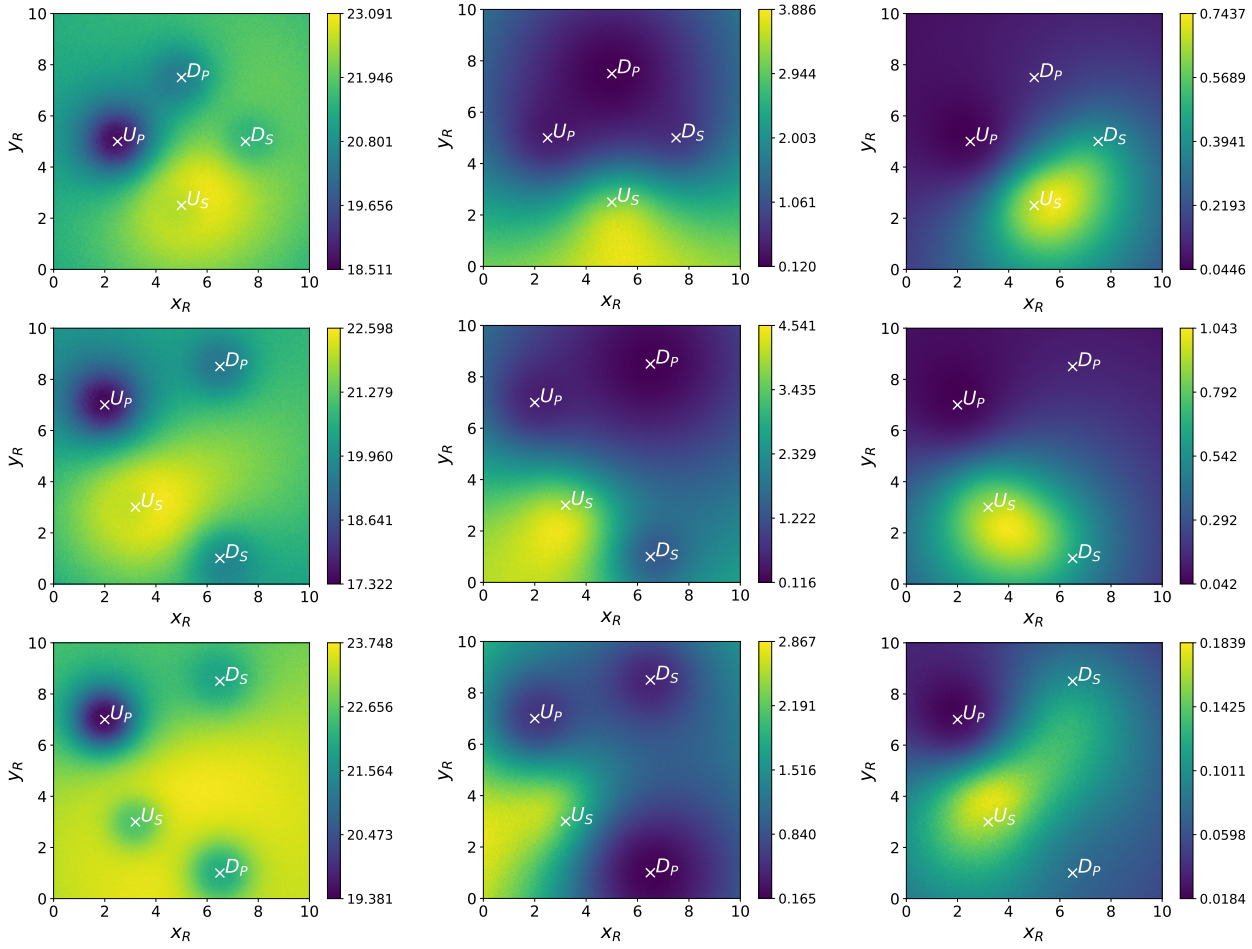

(a) Average primary rate degradation (%). (b) Average predicted relay power (W). (c) Average secondary rate (bpcu).

Figure 2.9: Impact of the relay position (x_R, y_R) for DF relaying. Top plots: symmetric users' positions; middle: non-symmetric users' positions; bottom: crossed users' positions.

The first two scenarios are somewhat similar. However, the third scenario is significantly different. In the third scenario, the average primary rate degradation is slightly higher compared to the other scenarios. Additionally, the average predicted relay power is lower, indicating that the relay is utilized less frequently. Moreover, the average secondary rate is also lower in this scenario. This observation can be explained by the fact that in the third scenario, the positions are crossed among primary and secondary network and the secondary transmitter is located close to the primary receiver. As a result, the interfering links are stronger, hence cause more damage to the primary user, compared to the direct links.

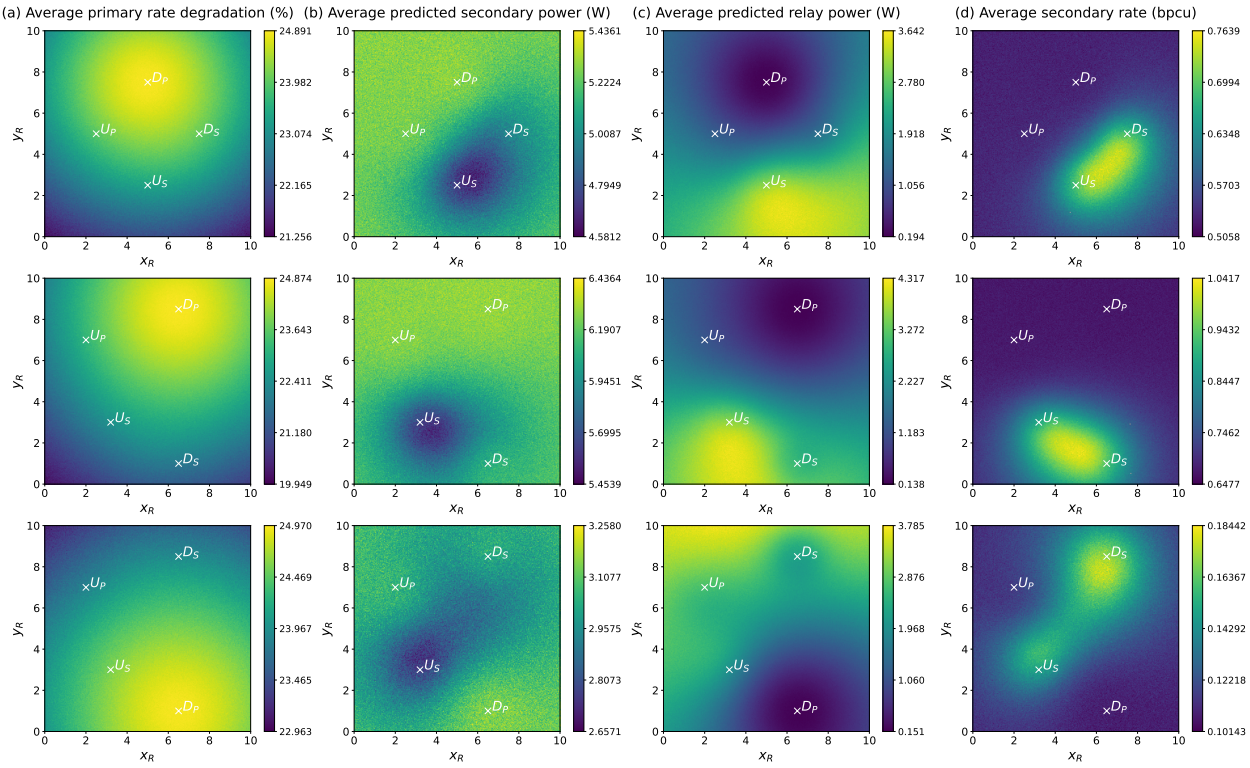

Figure 2.10: Impact of the relay position (x_R, y_R) for CF relaying. Top plots: symmetric users' positions; middle: non-symmetric users' positions; bottom: crossed users' positions.

In Figure 2.10, we illustrate the impact of the relay position on the system performance under CF relaying, using our proposed closed-form solution. For this, we examine the same three scenarios as for DF described above. All results are averaged across 10^4 channel realizations. Figure 2.10a, Figure 2.10b, Figure 2.10c and Figure 2.10d represent the average primary rate degradation, the average predicted secondary power P_S^*, the average relay power P_R^*, and the average secondary rate R_S^*, respectively. These metrics are showcased as functions of the relay position (x_R, y_R).

We note that the average primary rate degradation consistently remains below the predefined threshold of $\tau = 25\%$, irrespective from the relay position and the scenario, as under DF relaying. When the relay is positioned in close proximity to the primary destination, the primary rate degradation is in the range 23% to 25%. This result is primarily attributed to the high interference coming from the secondary communication, and the larger power allocation to the secondary transmitter, as presented in Figure 2.10b. Furthermore, we can see that in Figure 2.10c, more power is allocated to the relay when it lies between the secondary transmitter and destination. Finally, we can see that the highest secondary achievable rates are obtained when the relay is placed in between the secondary transmitter and receiver, in particular when the relay is closer to the destination (see Figure 2.10d); results consistent

with information theoretic insights as for DF relaying.

In the next Section, we provide a summary of the current Chapter and outline the objectives of Chapter 3.

2.6 Summary

In this Chapter, we present the cognitive relay-aided system under study and formulate a non-convex power allocation problem at the secondary user. We derive the optimization problem under both CF and DF relaying schemes, when perfect and global CSI is available at the transmitters. The objective of the optimization problem under study is to maximize the achievable secondary rate while satisfying a primary QoS constraint and a transmit power budget.

The optimization problem is non-convex when considering CF and DF relaying schemes because of the non-linear relaying operations. While a closed-form solution can be derived under perfect CSI for CF, the same is not feasible for DF because of the more complex expressions (including square root terms) of the non-convex objective function coupled with a non-convex QoS constraint (as opposed to an affine one for CF) involving an additional variable α under DF. To overcome this challenge and solve the problem, we propose an unsupervised DNN-based method using a fully connected architecture. The method incorporates a cognitive radio tailored loss function, which includes a hyperparameter that requires careful tuning. This custom loss function effectively incorporates both the secondary rate and the primary QoS constraint.

We conduct a series of experiments to fine-tune and evaluate our DNN-based solution. The results demonstrate that our DNN performs effectively, yielding an outage level of approximately 5%. Moreover, the secondary rate predicted by our DNN closely matches with the results obtained by the brute force method. These findings show the high generalization capability of our DNN solution on unseen data. Furthermore, our study highlights the tradeoff between the secondary rate and meeting the primary QoS constraint.

Additionally, we conduct experiments to investigate the impact of the relay position under both CF and DF by exploiting respectively our closed-form solution or our DNN-based method. Our results reveal that DF relaying performs well when the relay is located in close proximity to the secondary transmitter. Regarding CF relaying scheme, we also study the impact of the relay position using our closed-form solution; whereas CF relaying performs well when the relay is close to the secondary destination. This information provides valuable

insights into optimizing the relay position for an efficient performance.

In summary, our experiments demonstrate the effectiveness of our DNN-based solution in achieving a low outage level and while maximizing the secondary rate. We highlight the generalization capability of our DNN, the tradeoff between the secondary rate and primary QoS constraint, and the favorable performance of DF relaying when the relay is positioned near the secondary transmitter, which is consistent to the information theoritic results.

In the next Chapter, we investigate the problem by relaxing the knowledge of perfect CSI. Under imperfect CSI, at the transmitters, we show the particular relevance and robustness of our DNN-based approach compared to the traditional solutions requiring perfect CSI which perform poorly when the channel estimations are not perfect.

Chapter 3

Deep learning based resource allocation techniques assuming imperfect CSI

3.1 Introduction

This Chapter is dedicated to study the same power allocation problems as in the previous Chapter, but where we now assume that the transmitters have only access to imperfect CSI (denoted as CSIT), whereas the receivers have still access to perfect CSI (denoted as CSIR). In the following and to simplify the reading, whenever we mention imperfect CSI, we actually mean imperfect CSIT. To the best of our knowledge, DNN-based techniques have not been used to address resource allocation problems in cooperative cognitive networks with imperfect CSI. This suggests an opportunity for exploring the potential of DNNs in improving the performance and efficiency of such networks through optimized resource allocation.

We begin this Chapter by introducing the model of estimation errors affecting the channel gains. Secondly, since our obtained closed-form solution under CF presented in the previous Chapter relies on perfect CSI, it is not well-suited for imperfect CSI. In order to address this limitation, we propose a self-supervised DNN-based alternative solution with a robust training strategy that leverages the unsupervised DNN we proposed for DF under perfect CSI and described in the previous Chapter. We conduct a series of numerical experiments to find the optimal value of the hyperparameter λ, which trades off between rate driven or QoS driven optimization, for CF relaying under imperfect CSI. We then introduce a robust training strategy specifically designed to tackle the challenges of imperfect CSI. Finally, we

conduct numerical simulation experiments to evaluate the performance of our approach. The outcomes of this Chapter have been published in the conference paper [112].

In the following Section, we introduce the channel errors estimation model used in this study.

3.2 Imperfect CSI model

Whereas in the previous Chapter we assumed that all nodes, i.e. receivers and transmitters, can access perfect CSI, we here propose to relax the later. Indeed, within the cognitive radio framework, the assumption of perfect CSIT regarding links related to the primary network is not very realistic. Nonetheless, we still assume that the receivers have access to perfect CSIR, as usually assumed in the relevant resource allocation literature involving information theoretic performance measure [119–122], in order to compute the data rates to be optimized. In the remaining of this Chapter, imperfect CSIT is modeled as an additive Gaussian noise, as considered in [107, 123]. Hence, $\widehat{h}_{ij} = h_{ij} + \varepsilon_{ij}, \varepsilon_{ij} \sim \mathcal{N}(0, \sigma_{ij}^2)$, $\forall (i,j) \in \{(P,P),(S,P),(R,P),(P,R),$ and $(P,S)\}$ and the normalized estimated channel gains are given as $\widehat{g}_{ij} = (\widehat{h}_{ij})^2/N_j$. In the above, the estimation error variance is assumed to be of the form $\sigma_{ij}^2 = \mathrm{Var}[h_{ij}]/\mathrm{SNR}$, where $\mathrm{Var}[h_{ij}]$ denotes the variance of the true channels h_{ij} and $\mathrm{SNR} \in [-10, 20]$ dB represents the signal-to-noise ratio (SNR) of the estimator. The normalized channel gains within the secondary network are on the other hand perfectly known at both the transmitter and receiver and given as $\widehat{g}_{ij} = (\widehat{h}_{ij})^2/N_j = h_{ij}^2/N_j$, $\forall (i,j) \in \{(S,S),(S,R),$ and $(R,S)\}$. We henceforth let $\widehat{\mathbf{h}}$ denote the vector collecting all the estimated channel links.

The closed-form solution designed to solve the power allocation problem for CF relaying, relies on perfect CSI and is not hence suitable under imperfect CSI. Indeed, our formulation does not take into account explicitly the imperfect channel gain estimations, which would require a complete reformulation of the optimization problem and, hence, a different solution methodology. To overcome this, we propose a self-supervised DNN-based solution. In the following Section, we present our self-supervised DNN-based solution under CF and DF relaying to solve the power allocation problem under imperfect CSI.

3.3 Robust training to imperfect CSI

In the following, we present the proposed self-supervised DNN architecture and the used loss function, along with the training strategy employed to address the power allocation problem under imperfect CSI and under both CF and DF relaying.

Self-supervised DNN: In the previous Chapter, during the training phase, the DNN relied solely on perfect CSI both as its inputs and in the loss function. In the test phase, we also had access to the perfect CSI. Therefore, there was no additional information introduced in either the training or test phases. Consequently, the proposed DNN can be classified as a generic unsupervised DNN [124]. In contrast, in this Chapter, during the training phase error-free channel estimations are provided to the loss function, while channel gains impaired by estimation errors are provided as input of the DNN, similarly to a self-supervised denoising autoencoder [45, 125]. Hence, in the training phase both perfect and imperfect CSI are exploited. In the test phase, we only have access to imperfect CSI. This approach is thus characterized as a self-supervised DNN similarly to [117]. More precisely, self-supervised learning is a specific case of unsupervised learning where the model generates its own supervision signal from the input data. In our case, the perfect channel gains used in the loss function act as a form of self-supervision, allowing the model to learn and optimize for the task of predicting optimal allocated powers without the need for external ground truth labels.

DNN architecture and custom loss: Based on the numerous numerical simulations conducted described in Section 2.5 of the previous Chapter, we choose to use the same DNN architecture, namely 4 fully connected hidden layers, to solve the power allocation problem under imperfect CSI. Our objective is to utilize this DNN architecture with a novel training strategy to effectively address the challenges that arise from imperfect CSI. In addition, we decide to reuse the previously developed custom loss function, which forms the fundamental component of our self-supervised DNN-based solution for both CF and DF relaying schemes.

Under imperfect CSI, another performance metric to be considered is the outage probability defined as:

$$P_{out} = \Pr\left[R_S(\mathbf{h}, \alpha, P_S, P_R) < r\right],$$

where r denotes the fixed transmit rate and the probability is taken with respect to the randomness in the system channels $\mathbf{h}$. In our study, we propose a simplified approach compared to minimizing the outage probability, where the training dataset contains perfect CSI, and our DNN aims at maximizing the instantaneous rates, a term similar to that used in the

context of minimizing outage probability:

$$\mathcal{L}(\mathbf{h}_\ell, \hat{\mathbf{h}}_\ell) = \sum_{\ell=1}^{N} \left(-R_S(\mathbf{h}_\ell, \hat{\alpha}(\hat{\mathbf{h}}_\ell), \hat{P}_S(\hat{\mathbf{h}}_\ell), \hat{P}_R(\hat{\mathbf{h}}_\ell)) + \lambda \left[(1-\tau)\overline{R_{P_\ell}}(\mathbf{h}_\ell) - R_{P_\ell}(\hat{P}_S(\hat{\mathbf{h}}_\ell), \hat{P}_R(\hat{\mathbf{h}}_\ell)) \right]^+ \right).$$

Therefore, we can conjecture that our approach should also perform well in terms of outage probability.

To effectively address the power allocation problem under imperfect CSI, it is necessary to adapt the DNN training method to incorporate the effects of imperfect CSI. In the following, we present a detailed analysis, focusing on the necessary modifications that must be made to the DNN training process to accommodate the presence of imperfect CSI.

DNN training: For the training phase, we assume that we have access to a dataset containing perfect or high quality channel samples $\{\mathbf{h}_\ell\}_\ell$ obtained offline, but that in the running or test phase we only have access to erroneous channel estimations. We propose a new different training process to improve the robustness of our predictions to imperfect CSI. To this aim, we build a different training dataset containing pairs of perfect and imperfect channel estimations: $(\widehat{\mathbf{h}}_\ell, \mathbf{h}_\ell)_\ell$, obtained simply by adding Gaussian noise to the initial samples. The perfect channels $\mathbf{h}_\ell$ are exploited in the loss function $\mathcal{L}$ in equation (2.5), whereas the imperfect ones $\widehat{\mathbf{h}}_\ell$ are used as inputs to the self-supervised DNN. To avoid overfitting effects, we adopt an early-stopping method for both CF and DF, with a patience parameter of 20 epochs, which is selected after conducting several experiments.

In the following Section, we present our numerical results, which summarize the various experiments conducted to investigate the optimal hyperparamter λ for CF, and evaluate our self-supervised DNN-based solution for CF and DF under imperfect CSI.

3.4 Numerical results

Dataset: The simulation setup is the same as in our previous Chapter and described in details at https://github.com/yacine074/Robustness_SPAWC22, where all source codes can be found.

Benchmarks and performance metrics: Our comparison benchmarks are: the brute force or exhaustive search for DF (due to its' implementation simplicity), and our closed-form solution for CF (due to its' minimal computational cost).

First, we define the *relative gap* between the predicted instantaneous rate with imperfect CSI and the rate obtained by the benchmark with perfect CSI, as follows:

$$\mathrm{G} = \frac{\frac{1}{N}\sum_{\ell=1}^{N} \hat{R}_{S,\ell} - R^{*}_{S,\ell}}{\frac{1}{N}\sum_{\ell=1}^{N} R^{*}_{S,\ell}} \tag{3.1}$$

where $\hat{R}_{S,\ell}$ denotes the secondary rate achieved by either our unsupervised or self-supervised DNNs, or the benchmark when the corresponding power allocation policy relies on imperfect CSI and $R^{*}_{S,\ell}$ denotes the ideal optimal rate via the benchmark obtained with perfect CSI, both for the ℓ-th sample in the dataset.

In this Chapter, we exploit the same performance metrics to evaluate the QoS of the primary network, as described in the previous Chapter, namely Δ_{ℓ}, which represents the primary rate degradation of the ℓ-entry of the dataset, the Outage and Δ_{out} (see Section 2.5), denoting the average primary rate degradation when in outage. The only difference regarding to the previous Chapter is that we here consider the primary rate obtained under imperfect CSI in all these metrics computation.

In the following, we conduct a series of experiments to determine the optimal λ value that balances between maximizing the secondary rate and satisfying the primary QoS under DF when perfect CSI is available, for the CF relaying under imperfect CSI.

Choice of the hyperparameter λ for CF relaying under imperfect CSI: In Section 2.5, we performed multiple simulations to identify the λ hyperparameter.

In order to address the CF relay scheme, it is necessary to perform similar simulations but this time using imperfect CSI when we have access to a very good estimator (SNR = 20 dB). The objective is to determine the value of λ that satisfies the QoS and achieves large rates for CF relaying.

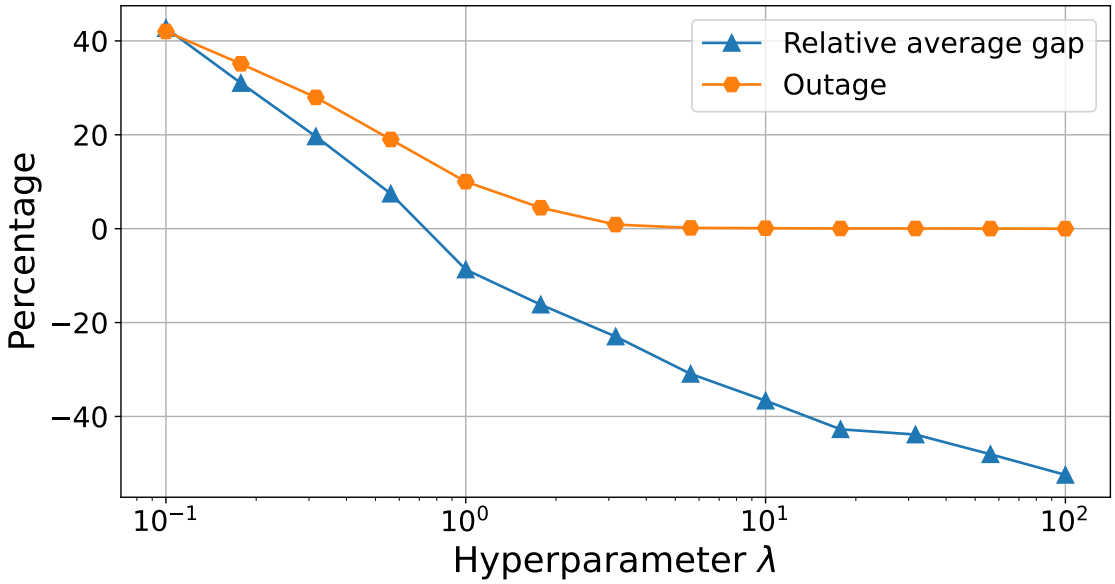

Figure 3.1: Relative average gap G and outage as functions of the hyperparameter λ over the test set (CF Relaying).

Figure 3.1 illustrates the relationship between λ and the relative gap of equation (3.1) as well as the outage. We observe that for small λ values (rate-driven custom loss), the relative gap G is positive. This indicates that the secondary rates obtained through the self-supervised DNN are larger than the optimal rates obtained via brute force. The reason behind this discrepancy is that our self-supervised DNN solutions may not necessarily meet the primary QoS constraints, leading to higher outage levels, and higher secondary rates.

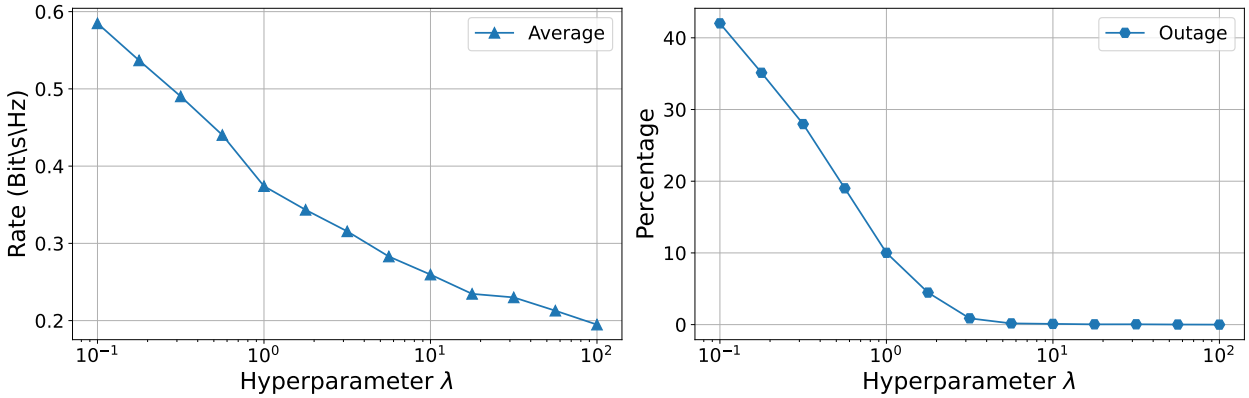

Figure 3.2: Average secondary rate R_S and outage as functions of the hyperparameter λ over the test set (CF relaying).

Conversely, for large λ values (primary QoS-driven custom loss), the outage approaches

zero as expected. However, this comes at the expense of secondary rates (negative relative gain G). This observation is further supported by the results presented in Figure 3.2.

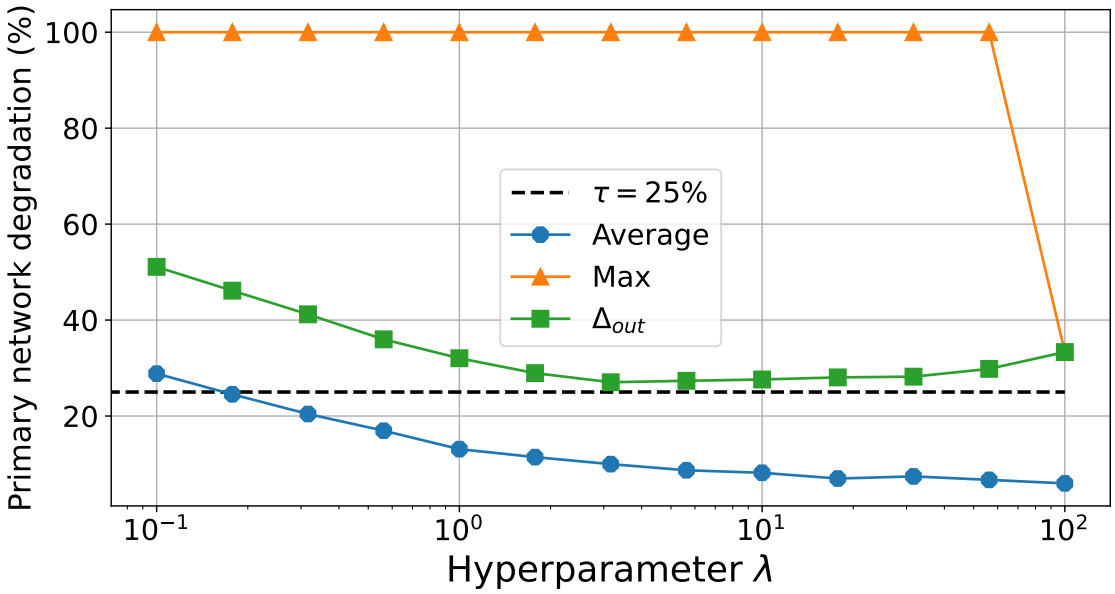

Figure 3.3: Average and maximum primary rate degradation and average degradation when in outage (Δ_{out}) as functions of λ over the test set (CF relaying).

In Figure 3.3, similarly to the analysis conducted in Section 2.5, we investigate further the impact of λ on the primary rate degradation within the test set. For this, we plot the average and maximum values of the primary rate degradation as well as the average degradation when in outage Δ_{out} given in (2.9) in Figure 3.3. When considering small values of λ, the primary degradation can reach a maximum of 100%. However, it is important to note that such severe degradation is observed only for a limited number of data points in the out-layer. This is evident from the curve of Δ_{out}, which is close to 25% threshold imposed by our chosen value of $\tau = 25\%$.

Robustness analysis over the test set: We now evaluate the performance over new data samples that have not been seen during the training phase and that are imperfect, i.e., $\{\widehat{\mathbf{h}}_\ell\}_\ell$. In Figure 3.4, we plot: the relative secondary rate gap G (top sub-figures), empirical outage (middle) and average primary rate degradation Δ_{out} (bottom) as functions of the quality of the channel estimator SNR $\in [-10, 20]$ dB and for both DF (left sub-figures) and CF (right) relaying schemes. In each sub-figure we evaluate and compare the robustness to imperfect CSI of the power allocation policy obtained by the benchmark (i.e., brute force for DF, our closed-form solution for CF), by our unsupervised DNN trained with perfect CSI

only, and by our self-supervised DNN trained with both perfect and imperfect CSI, i.e., our robust training method described above. When searching for the λ value in the presence of imperfect CSI, it is important to note that the value of λ may differ from that obtained when using perfect CSI (in Section 2.5). This observation can be inferred from Figure 2.6 and Figure 3.4, which depict the relative gap G under DF relaying. Indeed, with the same value of $\lambda = 10^{0.5}$, the relative gap G under perfect CSI equals 0% whereas it drops to -38% under imperfect CSI, meaning that the brute force achieves higher rates than the self-supervised DNN. However, despite this discrepancy, we choose $\lambda = 10^{0.5}$ for the following simulations, since it ensures better satisfaction of the primary QoS, also under imperfect CSI.

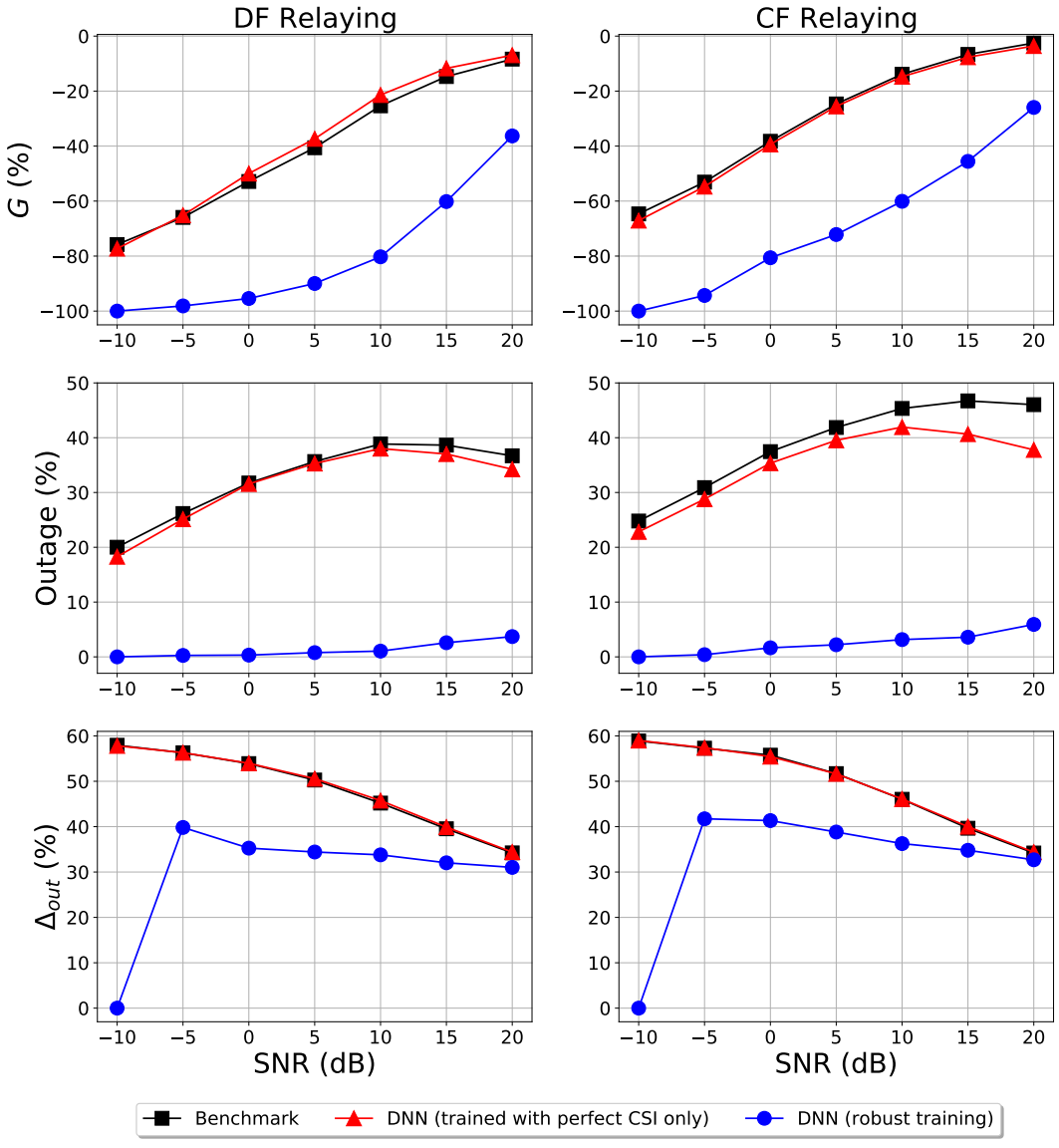

Figure 3.4: Impact of imperfect CSI on our proposed solutions (via deep learning and in closed form for CF) for DF and CF relaying over the test set.

Notice that the performance of the unsupervised DNN trained with perfect CSI matches almost perfectly that of the benchmark in all plots. This shows the high generalization capability of our unsupervised DNN approach, which was tuned (its architecture and choice of λ) for DF relaying, and also exploited for CF relaying with almost no change in the architecture beside removing the output corresponding to α, coming from the use of superposition coding under DF, and by tuning the hyperparameter λ in a similar way as for DF. Nevertheless, in the case of unsupervised DNN without robust training, having access to imperfect CSI reduces the secondary rate and, most critically, highly damages the primary communication: the primary QoS is violated in $20-40$ % of cases (Outage) and the average degradation when in outage (Δ_{out}) is of $35-60$ %. Finally, the outage of the self-supervised DNN approach trained in a robust manner is much improved and stays below 5%. At the same time, the average degradation Δ_{out} is also reduced (in between $0-40\%$). All this comes at the cost of secondary rate, which is acceptable in cognitive radio settings where the primary communication must be protected.

Impact of the position of the relay for CF and DF relaying under imperfect CSI: We start by investigating DF relaying and focus on the second scenario, which involves an asymmetric positions configuration as described in Section 2.5.

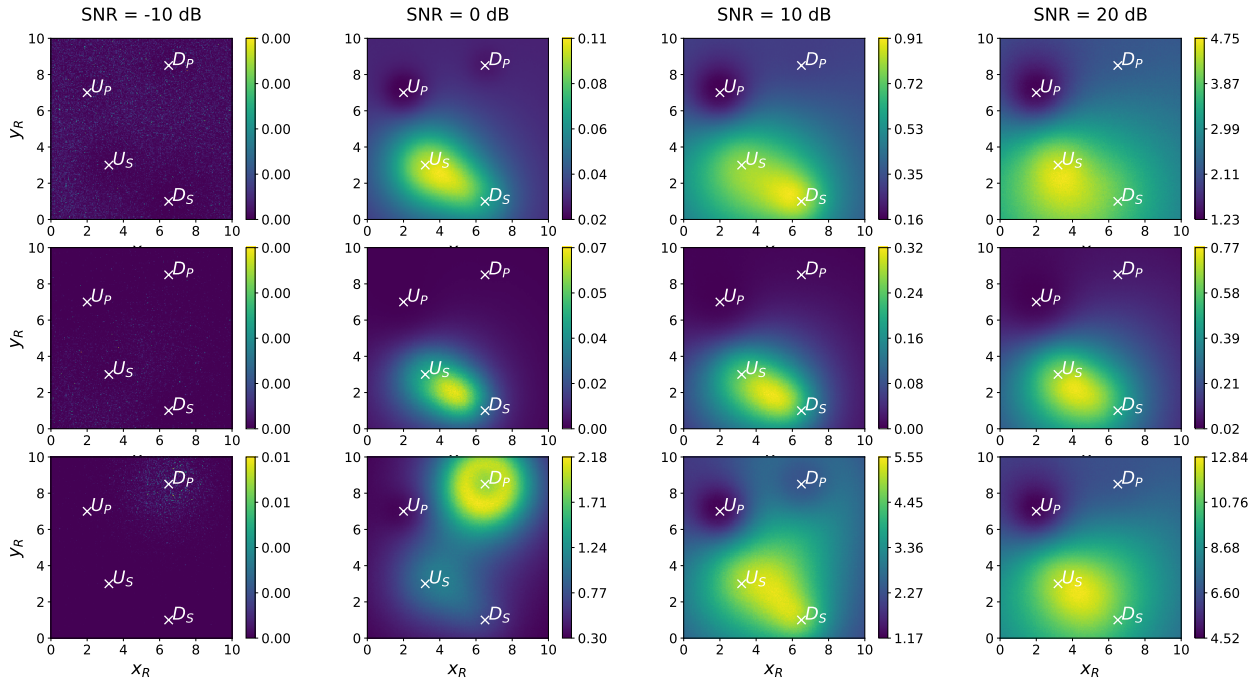

Figure 3.5: Impact of the relay position for DF relaying (second scenario). Top plots: average total power (W); middle: average secondary rate (bpcu); bottom: average primary rate degradation (%).

Figure 3.5 depicts the average power transmitted by the secondary network, the average secondary rate as well as the average primary rate degradation for four different channel estimation SNRs under DF relaying. Each simulation result has been averaged over 10^4 random channel realizations, not included in the test set. The channel gains for these simulations are generated in the same manner as described in Section 2.2.1. Under poor channel estimation, SNR $\in \{-10, 0\}$ dB, the secondary network barely transmits at all, leading to almost no primary rate degradation and almost zero secondary rate. As the quality of the CSI increases, i.e. SNR $\in \{10, 20\}$ dB, one can note that DF performs well in terms of secondary rate when the relay is close to the secondary user, as for the standard relay channel. Furthermore, in all cases, one can see that the average primary rate degradation stays below the fixed threshold value of $\tau = 25\%$.

At last, when SNR $= 0$ dB, we can observe that although the power of the secondary communication is very small when the relay is in close proximity of the primary receiver, such a configuration has a marginally degrading impact to the primary communication. This is equivalent to the case of SNR $= 10$ dB, where the primary degradation is about 2% when the relay is close to the primary receiver. To understand this counter-intuitive behavior, we study in the top plots of Figure 3.6 the maximum primary rate degradation as a function of the relay position for SNR $= 0$ dB and SNR $= 10$ dB, and we can note the presence of a noise, corresponding to outliers where the primary rate degradation reaches 100%, when computing this maximum. In order to mitigate the influence of this added noise, we apply a median filter [126]. Interestingly, we observe that as we increase the radius of the disk-shaped mask used for filtering, the noise progressively decreases, as shown in the bottom plots of Figure 3.6 (maximum of primary degradation with median filter when disk is equal to 3), and that the maximum of degradation is around the primary receiver.

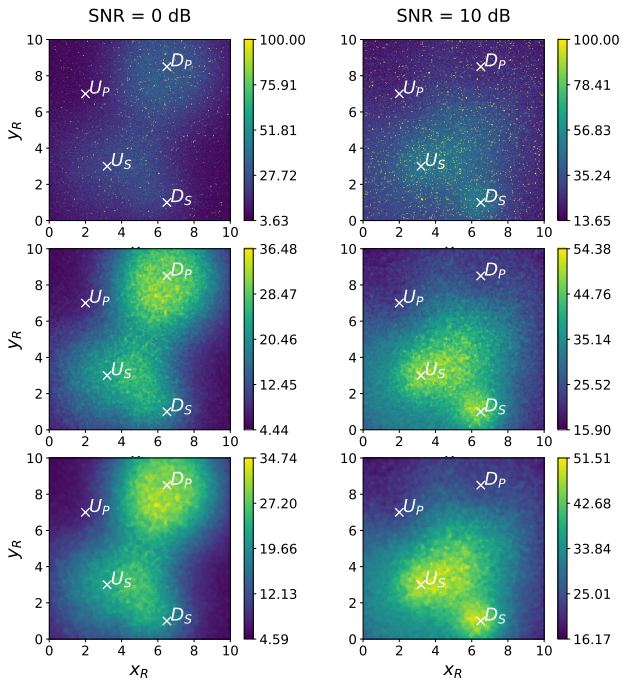

Figure 3.6: Impact of the relay position for DF relaying (maximum of primary degradation (%)): Top plots: maximum of primary degradation without median filter; middle: maximum of primary degradation with median filter (disk = 2); bottom: maximum of primary degradation with median filter (disk = 3).

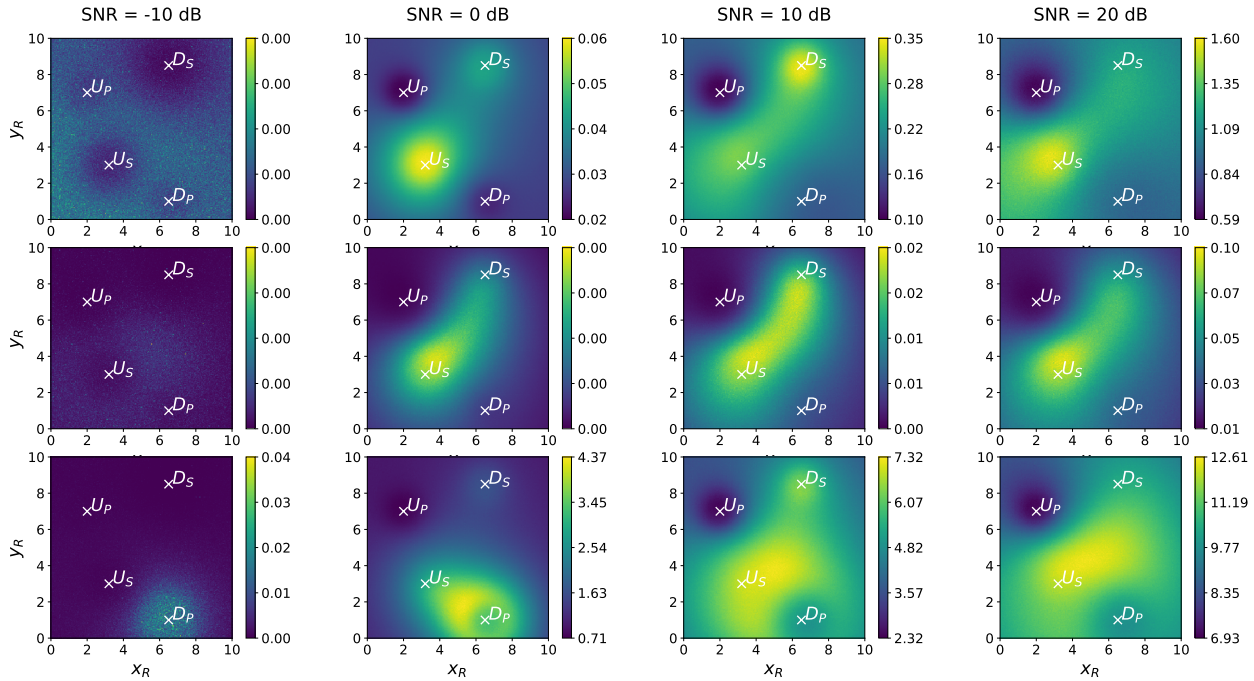

Figure 3.7: Impact of the relay position for DF relaying (third scenario). Top plots: average total power (W); middle: average secondary rate (bpcu); bottom: average primary rate degradation (%).

Finally, we investigate in Figure 3.7 the impact of the relay positions for DF relaying under imperfect CSI in the third scenario with the asymmetric and crossed positions among primary and secondary network. We observe that even with the change in users positions, the earlier conclusions remain unaffected. Specifically, DF yields better results when the relay is near the secondary user.

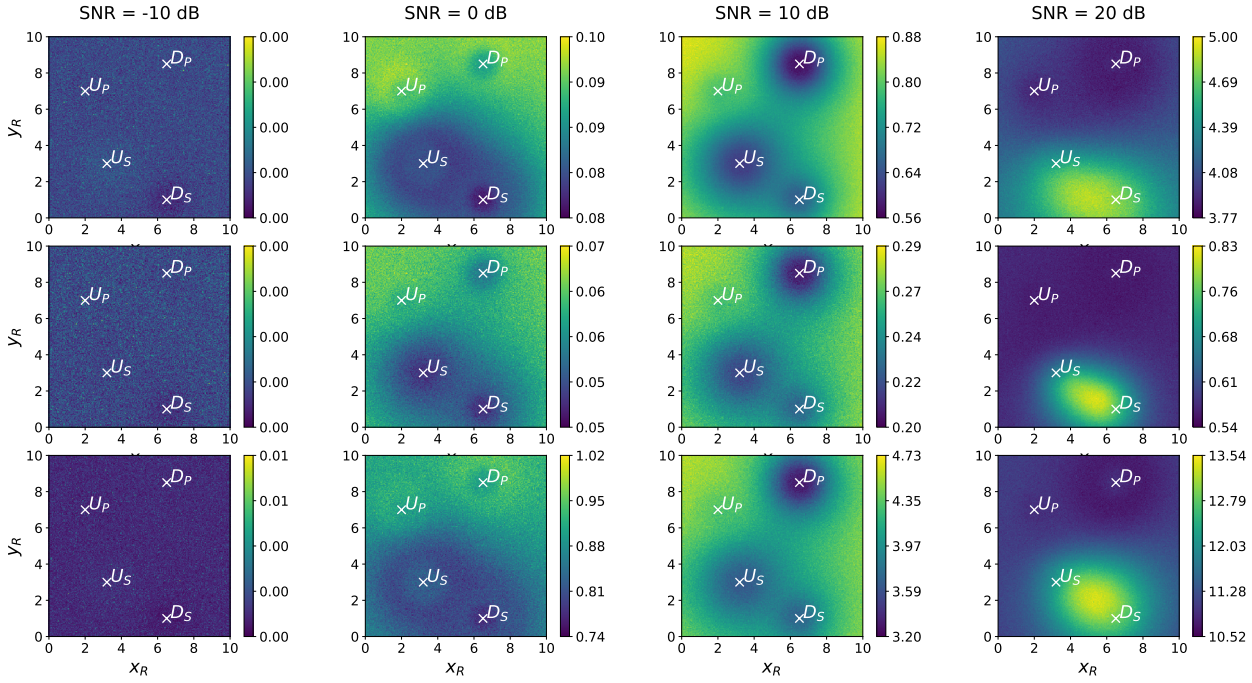

Figure 3.8: Impact of the relay position for CF relaying (second scenario). Top plots: average of secondary network power (W); middle: average secondary rate (bpcu); bottom: average primary rate degradation (%).

Regarding CF relaying, we conduct similar numerical experiments. Our investigation focuses on the scenario with the asymmetric positions described in the previous Chapter. The results showing the average power transmitted by the secondary network, the average secondary rate, and the average primary rate degradation for four different channel estimation SNRs are presented in Figure 3.8. Similar to DF, in the case of poor channel estimation SNR $\in \{-10, 0\}$ dB, the secondary network exhibits minimal transmission, resulting in no primary rate degradation and nearly zero secondary rate. As the quality of the CSI improves (SNR $= 20$ dB), we can observe that CF performs best when the relay is close to the secondary destination. Furthermore, in all cases, the average degradation of the primary rate remains below the predetermined threshold value of $\tau = 25\%$. These observations hold true across all the simulations, each of which averages results over 10^4 channel realizations, as for DF relaying.

In Figure 3.8, it can be inferred that when SNR $\in \{-10, 0, 10\}$ dB, indicating a significant amount of estimation error, the utilization of the relay decreases. To investigate these cases, further exploration of the self-supervised DNN performance and the hyperparameter λ are necessary in order to improve the relay's effectiveness under such conditions. We opt to explore the impact of the hyperparameter λ variation to see whether a lower λ value results in increased utilization of the relay.

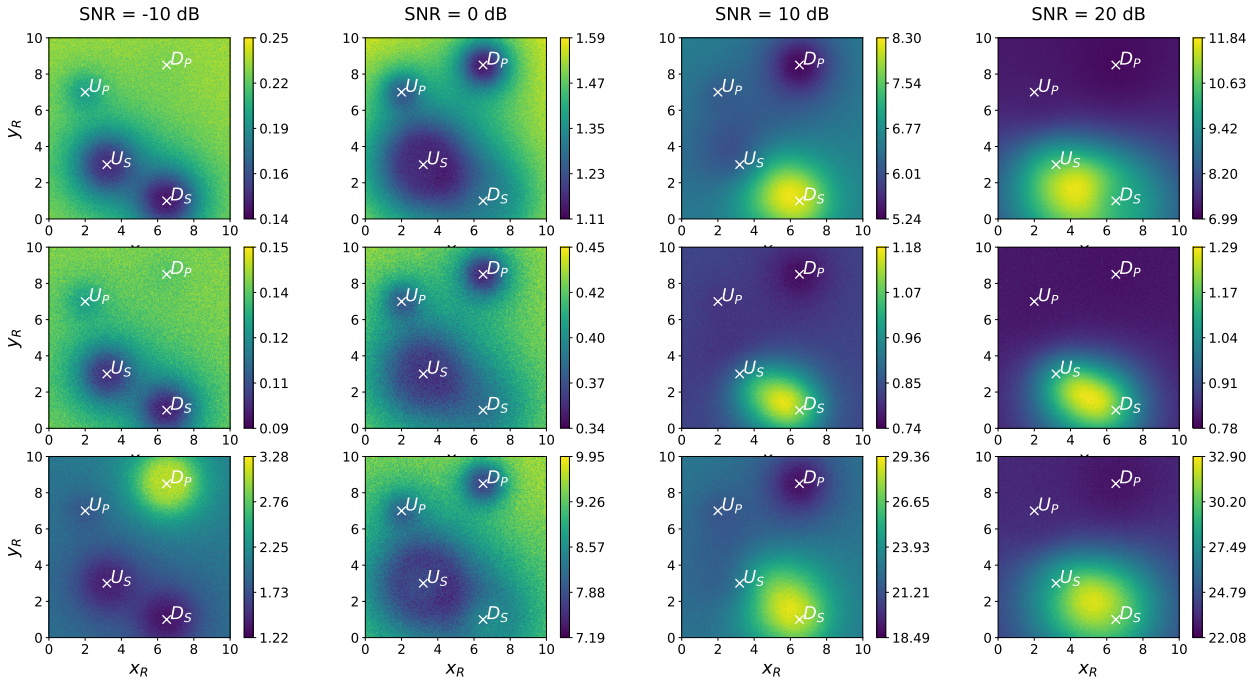

Figure 3.9: Impact of the relay position for CF relaying ($\lambda = 10^{-0.5}$). Top plots: average total power (W); middle: average secondary rate (bpcu); bottom: average primary rate degradation (%).

When we modify λ from $10^{0.5}$ to $10^{-0.5}$, as shown in Figure 3.9, its impact becomes evident. We observe that as the value of λ decreases, the relay utilization increases, leading consequently to an improved secondary rate, as expected. However, it is noteworthy that this enhancement in throughput comes at the expense of significant degradation in the primary communication, reaching up to 32%. This degradation exceeded our predefined threshold of 25%, indicating a notable decrease in the primary communication's overall quality.

Similarly to DF relaying, we extend our investigation to see the effect of relay positions for CF under imperfect CSI, specifically focusing on the third scenario with the asymmetric and crossed positions among primary and secondary network as illustrated in Figure 3.10. Despite the variations in user positions, we see that CF performs well even when using asymmetric and crossed positions between the primary and secondary networks, especially when the relay

is close to the secondary destination.

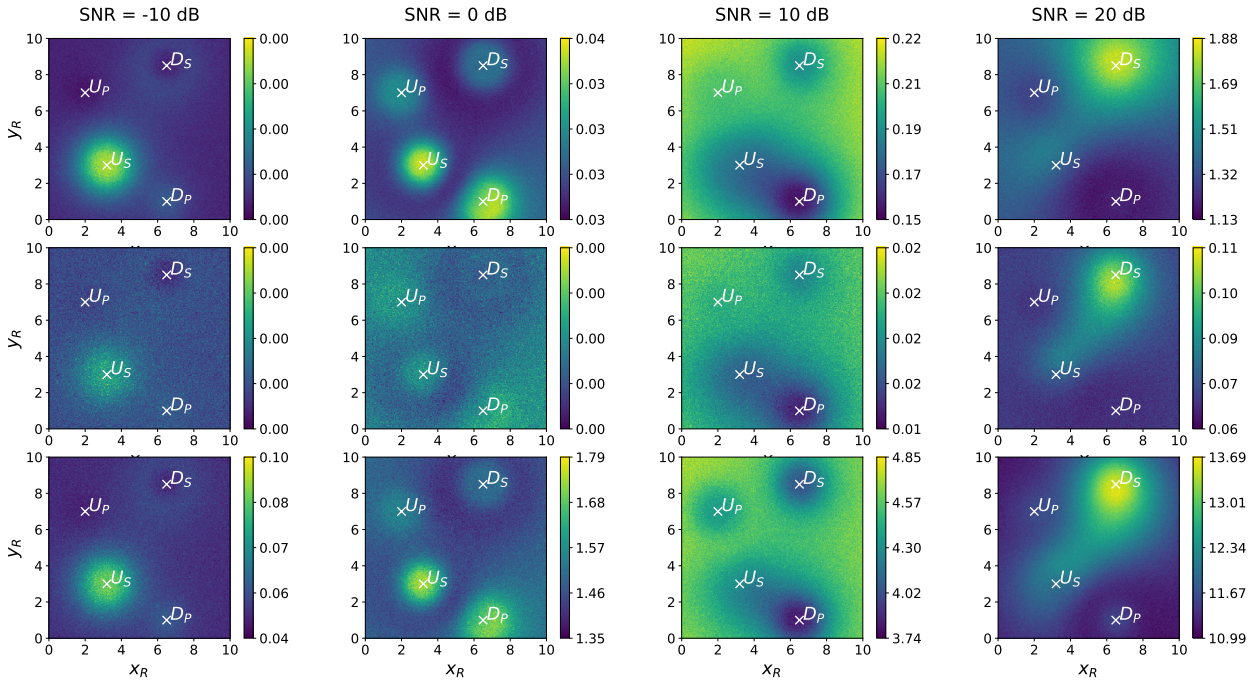

Figure 3.10: Impact of the relay position for CF relaying (third scenario). Top plots: average total power (W); middle: average secondary rate (bpcu); bottom: average primary rate degradation (%).

We end this Chapter by providing a summary and introduce briefly the objectives of the next Chapter.

3.5 Summary

In the previous chapter, perfect CSI was the underlying working assumption; the primary objective of this chapter is to relax this assumption. This Chapter starts by introducing the channel estimation models assumed regarding the channel gains related to the primary network. Secondly, we introduce a novel self-supervised DNN-based solution to address the power allocation problem for both CF and DF relaying under imperfect CSI. The novelty lies in our robust training technique used to tune the parameters of our DNN architecture introduced in Chapter 2. This robust training is based on a new dataset containing pairs of perfect and imperfect channel estimations. The perfect channels are exploited in the loss function, whereas the imperfect ones are used as inputs to the self-supervised DNN. This training technique makes our approach a self-supervised one, and renders our power allocation solution robust against imperfect CSI.

We then evaluate the performance of our proposed robust self-supervised DNN method against imperfect CSI for both CF and DF relaying. To accomplish this, we conduct simulations and compare our method with the closed-form solution for CF and exhaustive search for DF. First, we demonstrate the impact of the hyperparameter λ which denotes the unit price in bits/Watt of the primary QoS violation on the secondary rate by computing the relative gap between the secondary rate obtained through the self-supervised DNN under CF relaying and that obtained via exhaustive search. Additionally, we present the average secondary rate obtained via our self-supervised DNN approach under CF relaying as a function of the hyperparameter λ. Furthermore, we assess the performance of our self-supervised DNN approach by considering both the outage and the primary degradation metrics. Through our investigation, we identify the best value of λ that maximizes the secondary throughput while satisfying the QoS of the primary network for CF relaying. Our approach demonstrates a close secondary rate to that obtained through exhaustive search. This remarkable performance is achieved even in scenarios where channel estimation is not highly accurate.

In summary, our findings demonstrate that employing a self-supervised DNN with robust training against imperfect CSI enables us to achieve noteworthy enhancements. Specifically, we observe an improvement in outage performance that remains below 5% while simultaneously reducing the average degradation by 0 to 40%. However, it is important to note that the utilization of self-supervised DNN-based solutions does result in a reduction in the secondary rate. It is worth emphasizing that these results are obtained within the context of cognitive radio, where the primary communication takes precedence.

We notice that CF relaying presents superior performance when the relay is located close to the secondary destination. Conversely, DF relaying yield better results when the relay is in close proximity of the secondary user.

In the next Chapter, we delve deeper into the application of DNNs for relaying scheme selection. We explore the potential of DNNs by proposing a generalized DNN-based solution to tackle the power allocation problem under study. This novel DNN-based approach aims to provide an effective solution that can adapt to various scenarios, and generalize across different values of system parameters.

Chapter 4

Relaying scheme selection and generalized DNN solutions

4.1 Introduction

In this Chapter, we delve further into the exploration of our resource optimization problem by investigating the selection of an appropriate relaying scheme for our communication system. Our focus lies on the evaluation of two different approaches to choose between CF and DF relaying schemes. This choice plays an important role in the overall performance and efficiency of our communication system. This analysis is followed by a sequence of numerical simulation experiments to assess the effectiveness of the proposed methods.

Furthermore, we introduce our generalized self-supervised DNN solution, which enables generalization over system parameters. Firstly, we propose two self-supervised DNNs capable of generalizing over the maximum allowed primary rate degradation and the power budgets (at the relay and secondary transmitter). Secondly, we propose a self-supervised DNN to jointly generalize over all the aforementioned system parameters.

At last, we evaluate the performance of these self-supervised DNNs through numerous experiments to validate the efficacy of our methods by using metrics such as outage, primary rate degradation, and secondary rate under different channel estimation SNRs. The outcomes of this Chapter will be submitted in the journal paper [127].

In the next Section, we present the relaying scheme selection methods used in this study.

4.2 Relaying scheme selection

It is generally known that none of the two relaying schemes performs best for all network parameters and configurations. In this section, we investigate the problem of selecting the relaying scheme and we propose two different approaches to choose among CF and DF. In our cognitive radio setting, we focus the relay scheme selection on protecting the primary network, which of course may lead to a cost in terms of secondary instantaneous rate.

4.2.1 First relaying scheme selection

Usually, relaying scheme selection consists in choosing the relaying scheme achieving the largest SNR [10,88]. Such a criterion is well-suited for many communication models but not for cognitive radio networks where one should protect the primary transmission.

To simplify the presentation, let us denote by R_S^{CF}, R_S^{DF} the secondary rate achieved by CF and DF respectively. We further let Δ_ℓ^{CF} and Δ_ℓ^{DF} denote the degradation of the primary rate caused by the opportunistic transmission under CF and DF.

Algorithm 1 Relaying scheme selection baseline algorithm

Require: R_S^{CF}, R_S^{DF}, Δ_ℓ^{CF}, Δ_ℓ^{DF}, τ

if Δ_ℓ^{CF}, $\Delta_\ell^{DF} \leq \tau$ or $\Delta_\ell^{CF} = \Delta_\ell^{DF}$ **then** *// If the two relaying schemes meet the primary QoS // constraint then we select the one providing the larg- // -est opportunistic rate.*

  if $R_S^{DF} > R_S^{CF}$ **then**

    return DF

  else

    return CF

  end if

else

  if $\Delta_\ell^{DF} < \Delta_\ell^{CF}$ **then** *// Otherwise, we select the relaying scheme that causes the least // damage to the primary transmission.*

    return DF

  else

    return CF

  end if

end if

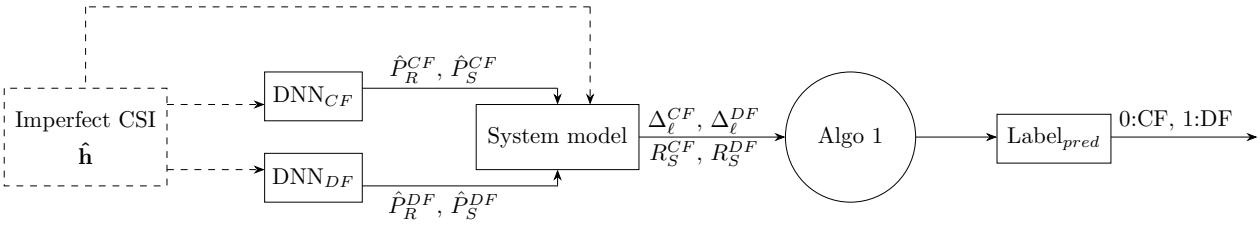

Figure 4.1: Diagram illustrating the operation of the proposed Algorithm 1 when used as baseline.

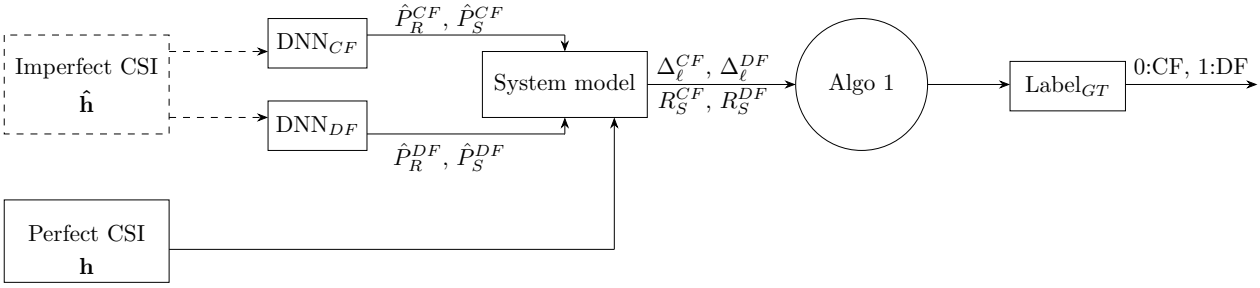

Figure 4.2: Diagram illustrating the ground truth generation process using Algorithm 1 for training the proposed Extra-DNN.

In order to choose between CF and DF, we propose the following scheme. First we compare the two degradations of the primary rate Δ_ℓ^{CF} and Δ_ℓ^{DF}. If both relaying scheme meet the QoS constraint and are somewhat equivalent in terms of primary degradation, i.e. they both meet the primary QoS constraints such that $\Delta_\ell^{CF}, \Delta_\ell^{DF} \leq \tau$, then we choose the relaying scheme yielding the largest secondary rate. If only one of the relaying scheme meets the QoS constraint, then we choose this scheme. At last, if neither relaying scheme meets the QoS constraint, we then choose the one inflicting the least primary rate degradation. Hence, we put more emphasis on meeting the primary QoS constraint, at the cost of the secondary rate. This relaying scheme selection principle is summarized in Algorithm 1.

We will exploit this first relaying scheme selection both as a baseline, as illustrated in Figure 4.1, where the block System model represents the mathematical equations allowing us to compute $R_S^{CF}, R_S^{DF}, \Delta_\ell^{CF}, \Delta_\ell^{DF}$ as detailed in Section 2.2.1. Additionally, we will also use it to build ground-truth data for our second relaying scheme selection method (Figure 4.2), described in the next subsection, which exploits the two self-supervised DNNs designed for CF and DF as well as an additional supervised one to decide between CF and DF (Figure 4.3).

To build the new data used for our second relaying scheme selection method, we make use of the perfect CSI to compute the instantaneous rates and the primary degradation but

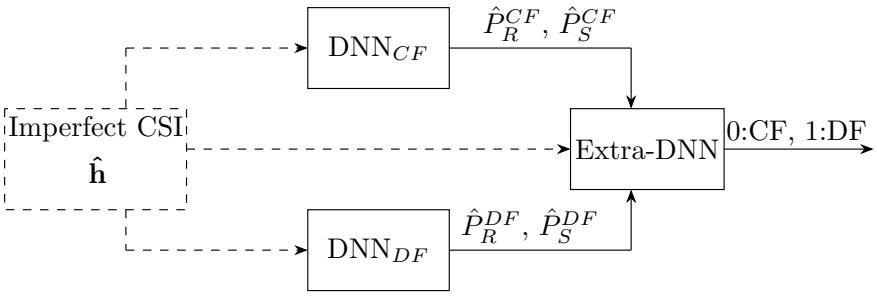

Figure 4.3: Diagram illustrating the operation of the Extra-DNN in the test phase based on imperfect CSI and on the outputs of DNN$_{CF}$ and DNN$_{DF}$.

given the predicted powers obtained with imperfect CSI as the self-supervised DNN inputs (Figure 4.2). Indeed, we assume that for training purposes, we have access to high-quality or perfect CSI estimations similarly to the training of the self-supervised DNNs predicting the power allocations in Section 3.3.

More precisely, for the ℓ-th entry of our new dataset, we first compute the estimated powers $\widehat{P_R}, \widehat{P_S}$ under CF and DF obtained as outputs of the self-supervised DNNs with the imperfect channel estimations as inputs. Once the estimated powers are obtained, we compute the instantaneous rates and the primary rate degradations, under both CF and DF, by using the true channel gains (perfect estimation). Finally, we use the first relaying scheme selection method above to select between CF and DF for all CSI samples in our dataset (Figure 4.2). As such, the ℓ-th entry of our dataset contains: the perfect and imperfect channel gains estimations, the associated optimal powers obtained via the self-supervised DNN described in Section 3.3 as well as the corresponding selected relaying scheme.

Note that while we can exploit perfect CSI to build a dataset for training purposes, perfect CSI cannot be used to select the relaying scheme in the running phase. Indeed, making use of this knowledge would imply first to transmit with DF and then CF, then to compute the true rates at the receiver and feedback them to the transmitter, and finally to select the best relaying scheme for the next transmission, which is not realistic.

When Algorithm 1 is used as baseline to compare the performance of our two proposed methods, the rates and the primary QoS degradation are computed using the predicted powers of CF and DF with imperfect CSI as the self-supervised DNN inputs as well as imperfect CSI within the rate computations (Figure 4.1). Indeed, when predicting the optimal power allocations and also when selecting the relaying scheme, the secondary user has access only to an imperfect CSI (Figure 4.3).

4.2.2 Second relaying scheme selection

In this section, we introduce a novel supervised DNN-based relaying scheme selection, where a DNN takes as inputs the imperfect channel estimations as well as the corresponding optimal power allocations under both CF and DF, computed by our previously presented self-supervised DNN methods of Section 4.2.2, and outputs the best relaying scheme. Our intuition is that, whereas the previously presented approach only exploits two self-supervised DNNs specifically trained for either CF or DF, an additional supervised DNN could improve the relay scheme selection by learning some correlation between the imperfect channel gains and the best relaying scheme exploiting both imperfect CSI to predict the transmissions parameters and perfect CSI to select among CF and DF (the latter being available during its training).

We hence consider a binary classification problem, for which the binary cross-entropy, given below, is usually used as loss function [43, 44]:

$$\mathcal{L} = -\frac{1}{L} \sum_{i=1}^{L} y_i \log \hat{y}_i + (1 - y_i) \log(1 - \hat{y}_i), \tag{4.1}$$

where L is the number of available training data samples; $y_i \in \{0, 1\}$ corresponds to the ground truth or the best relaying scheme (such that 0 stands for CF and 1 for DF) obtained by the first selection method (Section 4.2.1), where the data rates and primary degradation are computed given the true channels and predicted powers based on the imperfect CSI; and $\hat{y}_i \in [0, 1]$ is the probability of selecting DF computed by the supervised DNN.

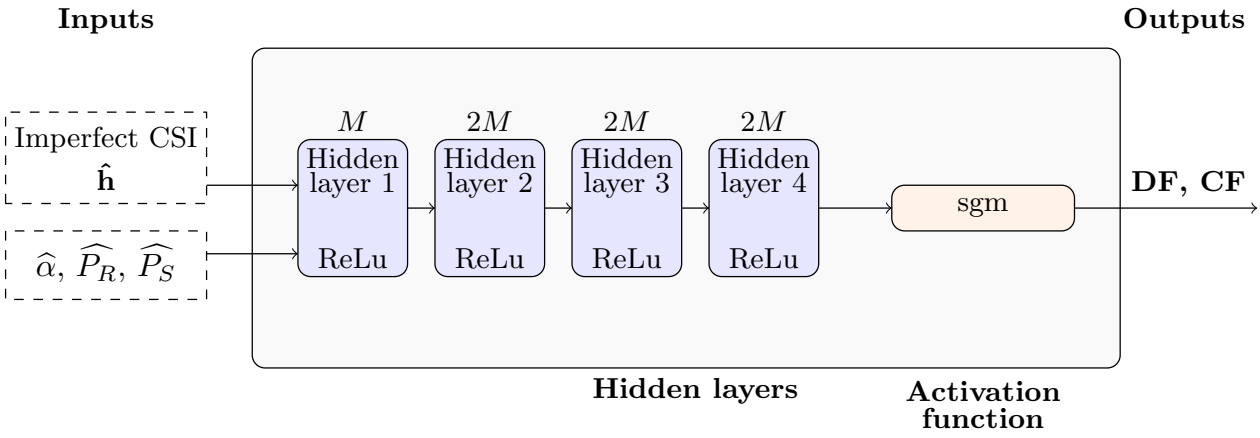

Figure 4.4: Proposed DNN architecture to choose among CF and DF with a fixed decision threshold at 0.5 (Extra-DNN).

The architecture of the considered supervised DNN for relaying selection, depicted in Figure 4.4, is similar to the previous self-supervised DNNs for solving the power allocation

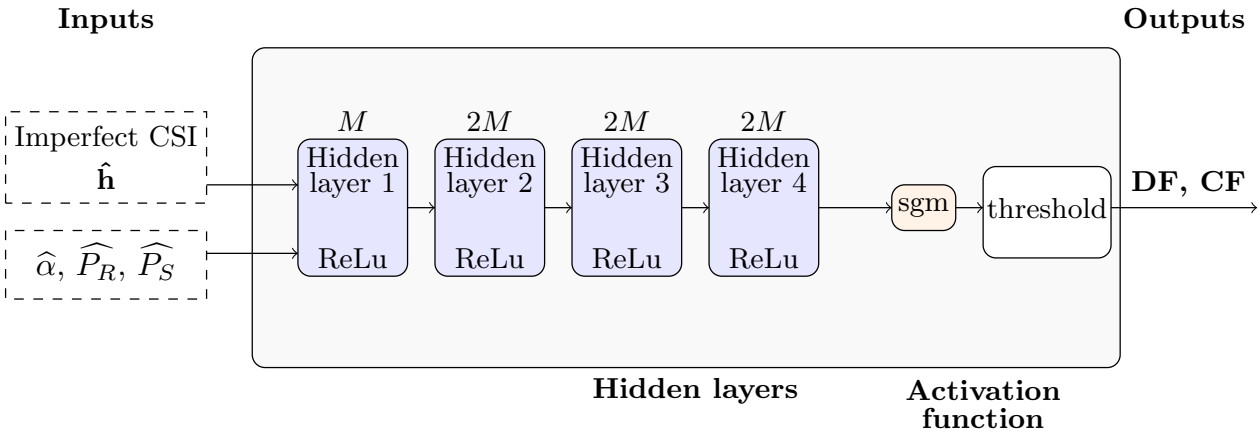

Figure 4.5: Proposed DNN architecture to choose among CF and DF with a finely tuned threshold (Extra-DNN-S).

problem. The decision to use the same DNN architecture for an entirely different problem can be justified due to the similarities in data characteristics. Both problems involve imperfect CSI as inputs, indicating a resemblance in the underlying data structure. Moreover, the fully connected architecture is justified because of its generality and given that there is no a priori structural or temporal information within the inputs to be exploited via more specialized architectures such as convolutional or recurrent network. Therefore, it is intuitive to conclude that changing the DNN architecture would not yield significant benefits, given the similarities in data and the DNN's proven effectiveness in related problems.

For the relaying scheme selection, we increase the number of neurons to $M = 256$ (instead of value $M = 128$ used for the power allocation prediction) as we empirically found that this value achieves good performance. Also, the final layer consists here in a sigmoid activation function outputting the probability $\hat{y}_i$ of selecting DF; the later is then compared to a threshold, set either to 0.5 or to a cognitive radio-tailored one allowing to minimize the average primary degradation when in outage Δ_{out}, to decide whether CF or DF should be selected (Figure 4.5).

The threshold is essential to take into account because its choice can significantly impact the performance of the supervised DNN model. This cognitive radio-tailored threshold is obtained by exhaustive search for each value of the channel estimation quality. In Table 4.1, we present the best obtained thresholds used for Extra DNN-S as a function of SNRs. If the predicted output value of the supervised DNN is below the threshold, the selected relaying scheme is CF; otherwise, the selected relaying scheme is DF.

Table 4.1: Best threshold as a function of the SNR

SNR (dB)	-10	-5	0	5	10	15	20
threshold	0.09	0.01	0.01	0.02	0.04	0.06	0.10

4.2.3 Numerical results

Before we present the experimental result of the our proposed relay selection scheme, we describe the dataset construction and the supervised DNN training (for the second method).

Dataset: The channel gains follow the same common fading and pathloss model as in Section 3.4 and are impaired by channel estimation errors, as in Section 3.3. The training set contains 10^7 samples of perfect and imperfect channel estimation $\mathbf{h}_\ell$ and $\widehat{\mathbf{h}}_\ell$, the associated optimal powers obtained via the self-supervised DNN described in Section 3.3 as well as the corresponding best relaying scheme obtained via the first selection method (where the data rates and primary degradation are computed with the true channels and power predicted with imperfect CSI).

The validation set is obtained as an excluded (20%) subset of the training set and our test set contains 2×10^6 samples of imperfect channel estimation with the corresponding optimal powers and the best relaying scheme as ground truth, enabling to assess the performance of our proposed approach.

To simplify the presentation of our numerical simulations, we will use the following terminology: "Two-DNN" refers to the baseline selection method where imperfect CSI is used both to predict the transmission parameters (i.e., power allocation policies and relay selection scheme) and to compute the rates and primary degradation used in our first selection scheme, as described in Algorithm 1. "Extra-DNN" refers to the second relaying scheme selection method, where the threshold is set to 0.5 (Figure 4.4), and "Extra-DNN-S" refers to the second relaying selection method with the cognitive-radio tailored threshold given in Table 4.1 to the cognitive radio network under study (Figure 4.5).

DNN training In the training phase, the optimal relaying scheme, computed via the Two-DNN method, where the rates and primary degradation are computed using the true channels but with powers predicted using the imperfect channels (Figure 4.2), is fed to our loss function in (4.1), whereas the imperfect channel estimations and the corresponding optimal powers under both CF and DF, obtained with the self-supervised DNN methods of Section 3.3

are given as the input of our additional supervised DNN. Note that the training process is restarted for each value of the considered SNR of the CSI estimator. Here, we adopt an early-stopping method for both CF and DF to avoid any overfitting effect, and the patience parameter is set to 10 epochs.

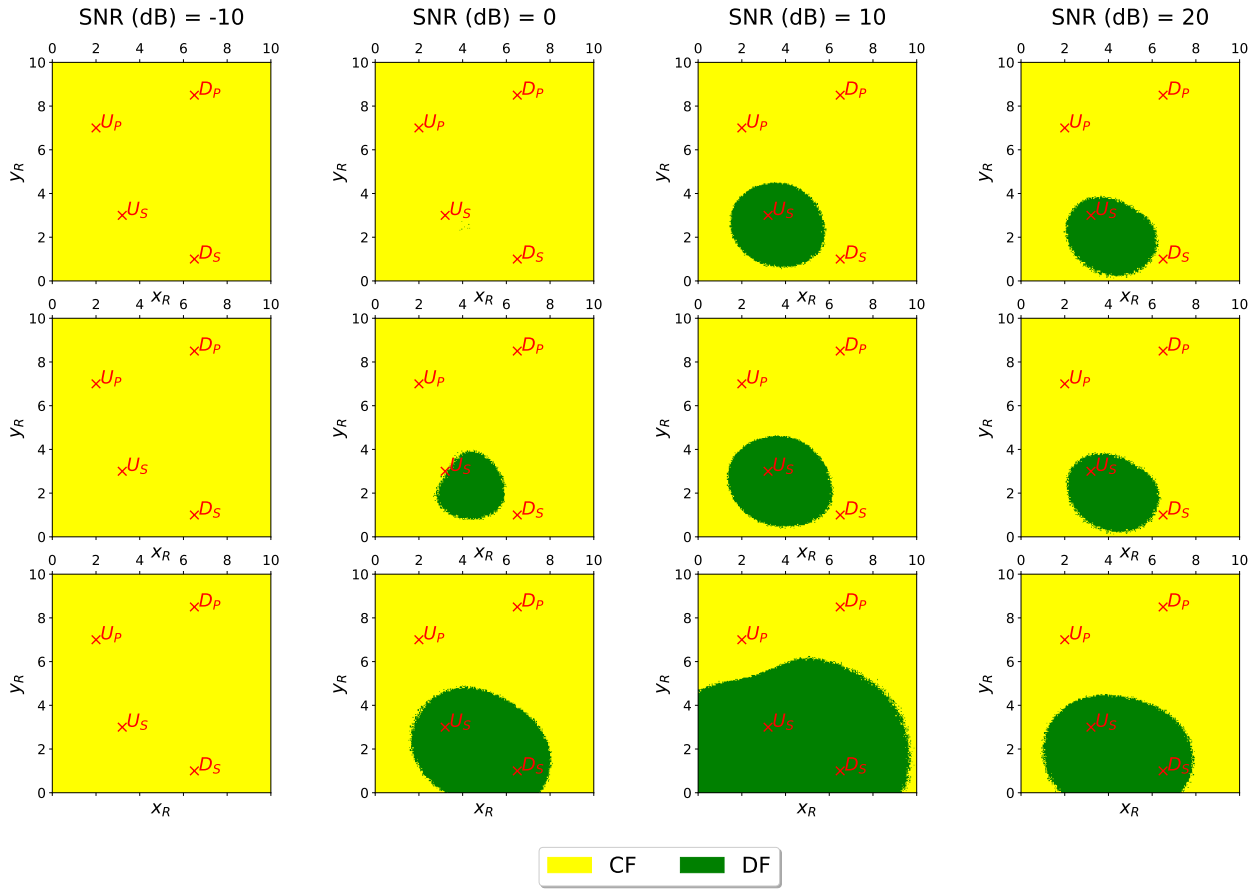

Figure 4.6: The selected relaying scheme between CF and DF. Top figures: Two DNN, middle: Extra DNN, bottom: Extra DNN-S.

Figure 4.6 shows the selected relaying scheme as a function of the relay position for the methods: Two-DNN, Extra-DNN and Extra-DNN-S, and assuming different levels of CSI estimation quality. Here, we assume that the position of the primary and secondary users and destinations are fixed, whereas the relay can be positioned anywhere. First, we can note that, regardless of the quality of the CSI estimation, CF is selected more often than DF under all approaches, which is to be expected since DF is limited by the fact that the relay needs to be able to decode the message from the secondary transmitter.
Furthermore, as also expected from a cooperative communications point of view, DF is more efficient when the relay is close to the secondary transmitter, which can be observed for a

CSI estimation quality between $0 - 20$ dB under the fixed-threshold Extra-DNN and the Two-DNN methods.

Remarkably, for the Extra-DNN-S method, the set of relay positions where DF outperforms CF also contains positions where the relay is close to the secondary destination, for which the instantaneous rate under DF is not expected to be large. The intuition is that our relay selection methods prioritizes the primary degradation over the instantaneous secondary rate. For these relay positions, CF achieves higher rates than DF by also consuming more transmit power, leading hence to larger primary degradation. We can observe that as the channel quality increases $(10 - 20)$ dB, the region in which DF relaying scheme is selected first expands (10 dB), but then contracts again when SNR $= 20$ dB. This phenomenon can be justified by the fact that, with an SNR of the channels estimation of 10 dB, the DNN chooses the relaying scheme that maximizes throughput and exhibits less sensitivity to imperfect CSI, favoring DF as can be confirmed from Figure 3.5 and Figure 3.8. Conversely, at higher SNR levels (20 dB), CF relaying displays lower sensitivity to imperfect CSI and outperforms DF in terms of throughput in more regions (Figure 3.5 and Figure 3.8), resulting in a preference for CF relaying in more regions.

Finally, under all approaches and irrespective from the position of the relay, CF is almost always chosen in very poor CSI estimation conditions -10 dB. DF seems indeed to be more sensitive to imperfect CSI, since the relay needs to correctly decode the secondary message; while it only quantizes the received signal under CF relaying.

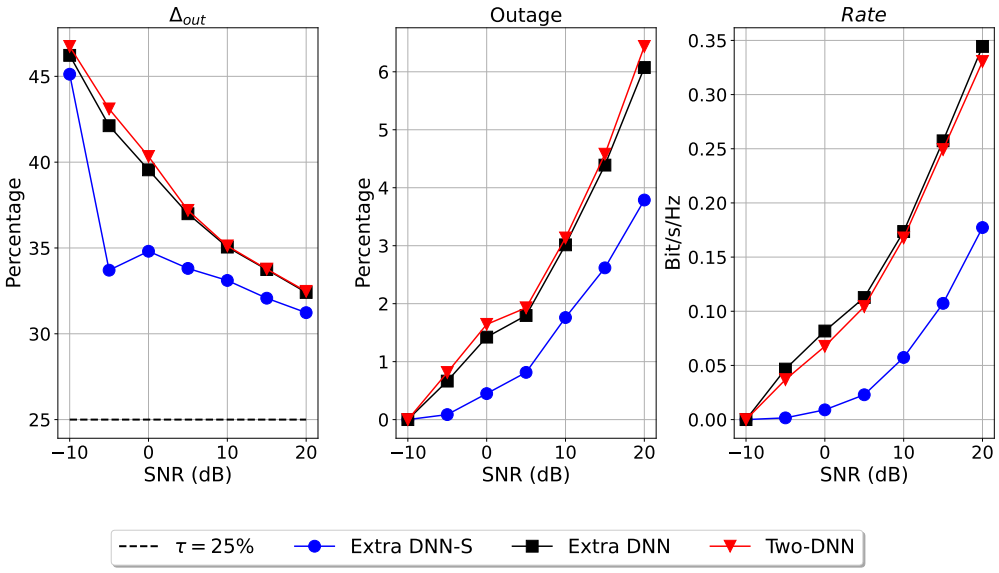

Figure 4.7: Average degradation when in outage, outage and secondary rate as functions of SNR over the test set.

In Figure 4.7, we compare the three methods: Two-DNN, Extra-DNN and Extra-DNN-S, in terms of primary rate degradation when in outage Δ_{out}, percentage of outage and secondary rate as functions of the CSI estimation SNR. First, we notice that Two-DNN and and Extra-DNN achieve more or less the same performance, meaning that there was little additional information to be learned between the channel gains and the best relaying scheme. This highlights the strength of our proposed self-supervised DNN-based power allocation policy for a fixed relaying scheme. This can also be explained by fact that each of the two relaying schemes (CF and DF) perform best for disjoint relay positions.

Second, tuning the threshold which minimizes the primary rate degradation when in outage, as performed for Extra-DNN-S, significantly increases the performance in terms of primary degradation: the number of outage is divided by a factor of almost 2 for all values of SNR $\in [-10, 20]$ dB, whereas the primary degradation when in outage is decreased by up to 8% especially under poor channel estimation conditions. Of course, the prioritized primary protection comes at the cost of secondary rate, which is decreased as shown in Figure 4.7.

At last, using an additional supervised DNN enables us to generalize over which criterion the relaying scheme should be selected. Indeed, here, the relay scheme selection was decided based on the minimization of the primary rate degradation when in outage. One could consider any tradeoff weighting between the secondary rate and primary protection instead, which is not feasible under the two DNN-based method.

4.3 Generalized DNN solution

So far the maximum allowed primary rate degradation τ, as well as the power budget within the secondary network $\overline{P_R}$ and $\overline{P_S}$ were fixed. We propose here to generalize our self-supervised DNN approach in terms of the system parameters: τ, $\overline{P_R}$, and $\overline{P_S}$ assuming that they lie within specified ranges.

4.3.1 Proposed generalized DNN solution

Although the system parameters are no longer fixed, the loss function to be minimized by the self-supervised DNN remains essentially the same as in Section 3.3. The main difference with the case of fixed parameters is that the values of τ, $\overline{P_R}$, $\overline{P_S}$ have to be provided as inputs of both the self-supervised DNN and the loss function. First, we start by generalizing over either τ or the power budgets separately. Then, we explore the capabilities of a self-supervised DNN to generalize over all these network parameters jointly. Figure 4.8 and Figure 4.9 present the

architecture of our new self-supervised DNNs that are capable to generalize our approach over the system parameters: τ, and the power budgets $\overline{P_R}, \overline{P_S}$ respectively.

The architecture of the self-supervised DNN able to generalize over τ, denoted as DNN$_\tau$, remains the same as in the previous Chapter, with the changes outlined above (see Figure 4.8).

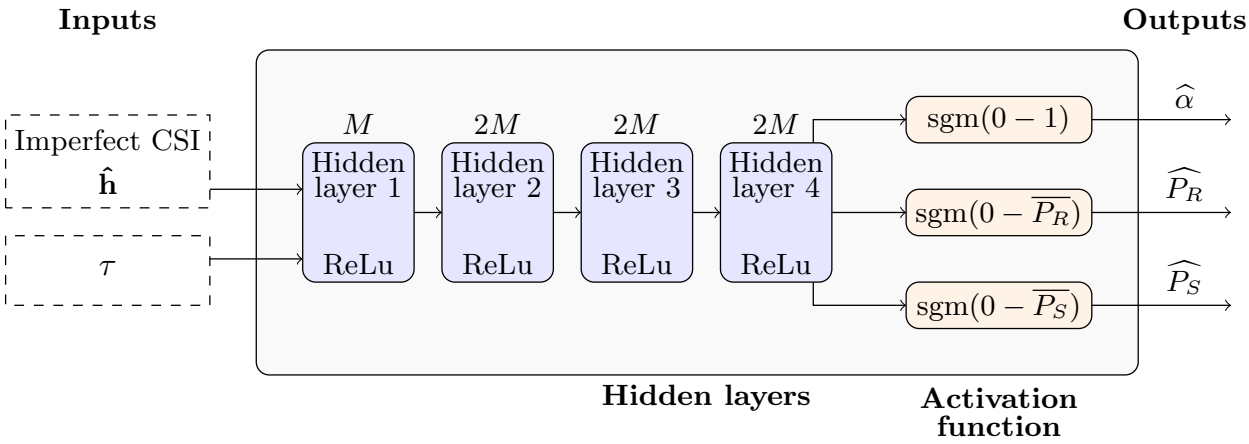

Figure 4.8: DNN$_\tau$: Proposed DNN-based generalization over the maximum allowed primary rate degradation.

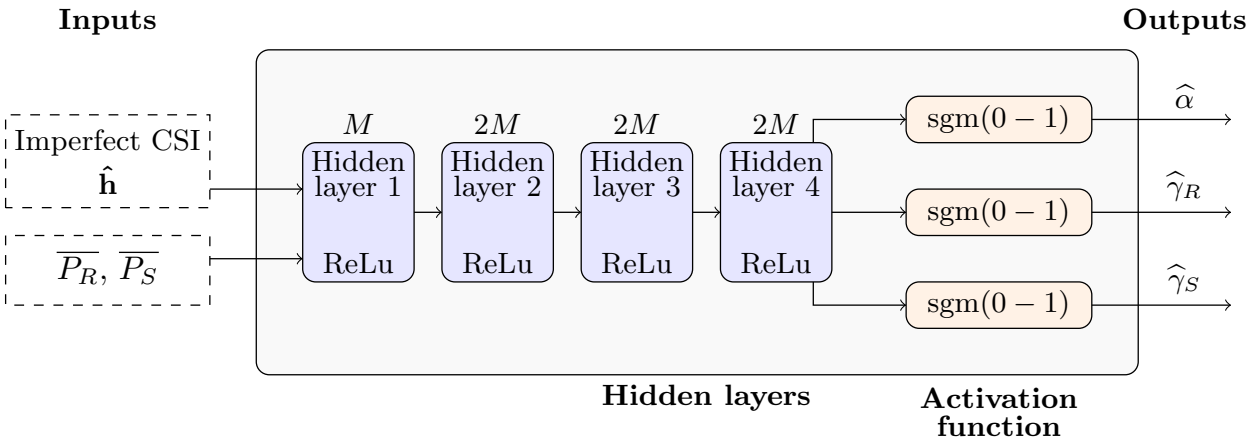

Figure 4.9: DNN$_P$: Proposed DNN-based generalization over the power budget.

On the contrary, when generalizing over the power budgets $\overline{P_S}$ and $\overline{P_R}$, which is denoted as DNN$_P$, another architectural change is required aside from the inputs: the new DNN$_P$ has to output the fractions $\widehat{\gamma}_R \in [0,1]$ and $\widehat{\gamma}_S \in [0,1]$ of the relay and secondary power to be consumed, instead of directly the estimated powers $\widehat{P_R}$ and $\widehat{P_S}$ computed as $\widehat{P_i} = \overline{P_i}\ \widehat{\gamma}_i, i \in \{R, S\}$, as illustrated in Figure 4.9. This a direct consequence of the fact that the maximum

power budgets are no longer fixed but input changing parameters. The remaining inner self-supervised DNN architecture, i.e., the number of layers and the number of neurons par layer, remains the same as in the previous Chapter.

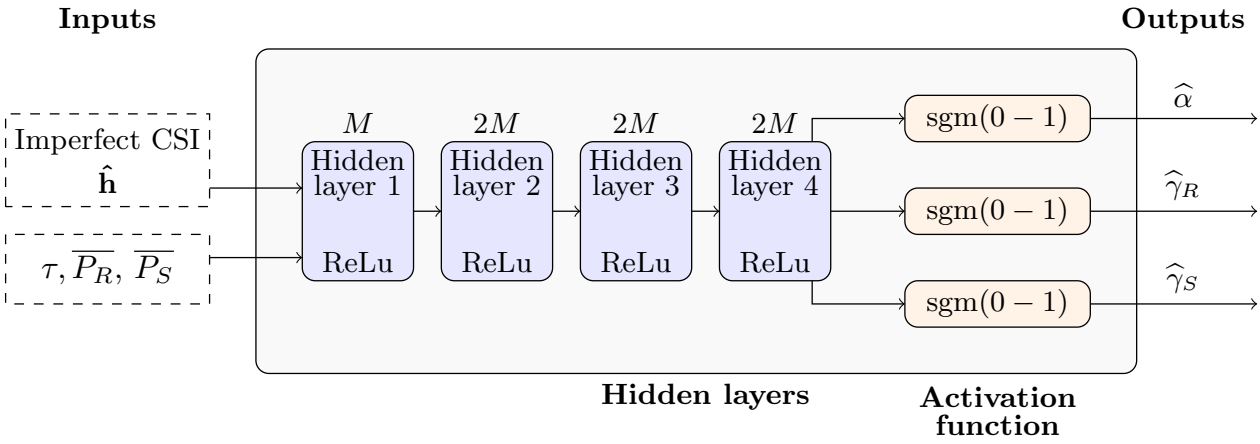

Figure 4.10: DNN†: Proposed DNN-based generalization over both the maximum allowed primary rate degradation and the power budgets.

Finally, in order to address the joint generalization over the power budgets and τ, we propose a new self-supervised DNN architecture in Figure 4.10. This architecture represents the most generic DNN†, which blends the two aforementioned self-supervised DNNs able to generalize either over τ or the power budgets.

4.3.2 Computational cost analysis

In this subsection, we compare the three approaches (DNN$_{\tau}$, DNN$_{P}$, and DNN†) in terms of number of trainable parameters and FLOPs (Floating Point Operations). For the test phase, the three DNNs differences in computational cost are minimal because they all share a very similar architecture and only differ in the first layer of the DNN. Therefore, during the test phase, we only compare the memory cost.

For the training phase, the trainable parameters refer to the learnable parameters: weights and biases, within a neural network model that are updated during the training process. These parameters are the variables that the model learns from the training data to make predictions or perform specific tasks. It is important to note that the number of trainable parameters is not the same for the DNN$_{\tau}$, DNN$_{P}$, and DNN†, because for DNN$_{\tau}$ we have 2 inputs, namely $\widehat{h}$ and τ, and for DNN$_{P}$ we have 3 inputs, namely $\widehat{h}$, $\overline{P_R}$ and $\overline{P_S}$, and for DNN† we have 4 inputs, namely $\widehat{h}$, τ, $\overline{P_R}$ and $\overline{P_S}$.

FLOPs specifically refer to the number of floating-point operations, which include addition, subtraction, multiplication, and division operations on floating-point numbers. The number of FLOPs is commonly used to measure the computational complexity or cost of a model. The higher the number of FLOPs a model requires, the more computationally intensive it is.

In Table 4.2 and Table 4.3, we present the total number of FLOPs and trainable parameters for CF and DF relaying using three different DNNs.

Table 4.2: FLOPs and Parameters as functions of DNNs for CF Relaying

DNNs	**DNN**$_\tau$	**DNN**$_P$	**DNN**†
FLOPs	331, 908	332, 162	332, 418
Parameters	166, 402	166, 530	166, 658

Table 4.3: FLOPs and Parameters as functions of DNNs for DF Relaying

DNNs	**DNN**$_\tau$	**DNN**$_P$	**DNN**†
FLOPs	332, 421	332, 675	332, 931
Parameters	166, 659	166, 787	166, 915

In the training phase, it is recommanded to use DNN† due to its efficiency, rather than DNN$_\tau$, and DNN$_P$. This choice is advantageous for several reasons. In Table 4.2, when comparing the number of trainable parameters and the number of FLOPs, we note that regardless of the used DNN architecture, whether it involves two or multiple inputs, it is primarily the first layer that costs slightly more per inputs. This is why, in terms of the number of FLOPs and number of parameters, we do not have a significant difference that would make one DNN excessively more complex or simpler than the other.

In the test phase, the memory cost is not the same for the three DNNs, because if we want to generalize over 10 values of τ and 10 values of power budgets exploiting both DNN$_\tau$ and DNN$_P$, we would need to train and store 100 DNNs, which is expensive in terms of both computation and storage. In contrast, for DNN†, we would need to train and store it only once, and it can generalize for any given values of τ and power budgets. Furthermore, we achieve almost the same communication performance (in terms of instantaneous rate, outage, etc.) with DNN†, than with DNN$_\tau$ and DNN$_P$ without increasing the size of the dataset.

4.3.3 Numerical results

Dataset: As in the previous sections, we assume that only imperfect CSI samples are available in the test set, whereas pairs of both perfect and imperfect CSI are available in the training and validation sets. In order to ease the presentation, we will separate the three datasets used for the self-supervised DNN able to generalize over τ, over the power budget and over all system parameters respectively.
i) The training set assessing the generalization over the primary degradation τ is composed of 10^6 samples of $\{\mathbf{h}_\ell, \widehat{\mathbf{h}}_\ell, \tau_\ell\}$, where each of the realization τ_ℓ is within the range $\tau_\ell \in [0.1, 0.5]$. The corresponding test set contains 2×10^5 samples of $\{\widehat{\mathbf{h}}_\ell, \tau_\ell\}$.
ii) The training set assessing the generalization over the power budget is composed of 2×10^6 samples of $\{\mathbf{h}_\ell, \widehat{\mathbf{h}}_\ell, \overline{P_{S,\ell}}, \overline{P_{R,\ell}}\}$, where each of the realization $\overline{P_{S,\ell}}, \overline{P_{R,\ell}}$ is within the range $\overline{P_{S,\ell}}, \overline{P_{R,\ell}} \in [1, 10] \times [1, 10]$, and that the powers are interdependent, such as $\overline{P_{S,\ell}} = \overline{P_{R,\ell}}$. The corresponding test set contains 4×10^5 samples of $\{\widehat{\mathbf{h}}_\ell, \overline{P_{S,\ell}}, \overline{P_{R,\ell}}\}$.
iii) The training set assessing the generalization over the three system parameters is composed of 2×10^6 samples of $\{\mathbf{h}_\ell, \widehat{\mathbf{h}}_\ell, \tau_\ell, \overline{P_{S,\ell}}, \overline{P_{R,\ell}}\}$, where each of the realization τ_ℓ is within the range $\tau_\ell \in [0.1, 0.5]$ and $\overline{P_{S,\ell}}, \overline{P_{R,\ell}}$ is within the range $\overline{P_{S,\ell}}, \overline{P_{R,\ell}} \in [1, 10] \times [1, 10]$, with $\overline{P_{S,\ell}} = \overline{P_{R,\ell}}$. The corresponding test set contains 4×10^5 samples of $\{\widehat{\mathbf{h}}_\ell, \tau_\ell, \overline{P_{S,\ell}}, \overline{P_{R,\ell}}\}$.
In all cases, the validation set is obtained as an excluded (20%) subset of the training set.

DNN training: As in the previous sections, the self-supervised DNNs are provided $\{\widehat{\mathbf{h}}_\ell, \tau_\ell\}$ or $\{\widehat{\mathbf{h}}_\ell, \overline{P_{S,\ell}}, \overline{P_{R,\ell}}, \}$, or $\{\widehat{\mathbf{h}}_\ell, \tau_\ell, \overline{P_{S,\ell}}, \overline{P_{R,\ell}}\}$ as inputs, whereas the perfect CSI $\mathbf{h}_\ell$ and the values of τ or $\overline{P_R}, \overline{P_S}$ are only fed to the loss function as $\{\mathbf{h}_\ell, \tau_\ell\}$ or $\{\mathbf{h}_\ell, \overline{P_{S,\ell}}, \overline{P_{R,\ell}}, \}$, or $\{\mathbf{h}_\ell, \tau_\ell, \overline{P_{S,\ell}}, \overline{P_{R,\ell}}\}$. The training process is restarted for each value of the considered channel estimation SNR, and the patience parameter is set to 10 epochs under both DF and CF to avoid any overfitting effects.

In the following, we present the performance obtained with CF and DF relaying.

First, we evaluate the self-supervised DNNs generalizing separately either over τ or over the power budgets $\overline{P_R} = \overline{P_S}$ under CF relaying. In Figure 4.11, we illustrate the outage, the average primary rate degradation (Δ_ℓ), the average and maximum primary rate degradation when in outage (Δ_{out} and $\Delta_{\max}$) as well as the mean plus and minus the standard deviation of the secondary rate for different qualities of channel estimator SNR $\in [-10, 20]$ dB, when the generalization is done over τ. The power budgets were set to $\overline{P_R} = \overline{P_S} = 10$ W. We can note that our proposed DNN$_\tau$ generalizes over different values of $\tau \in \{10, 20, 30, 40\}$% since the average primary degradation stays below

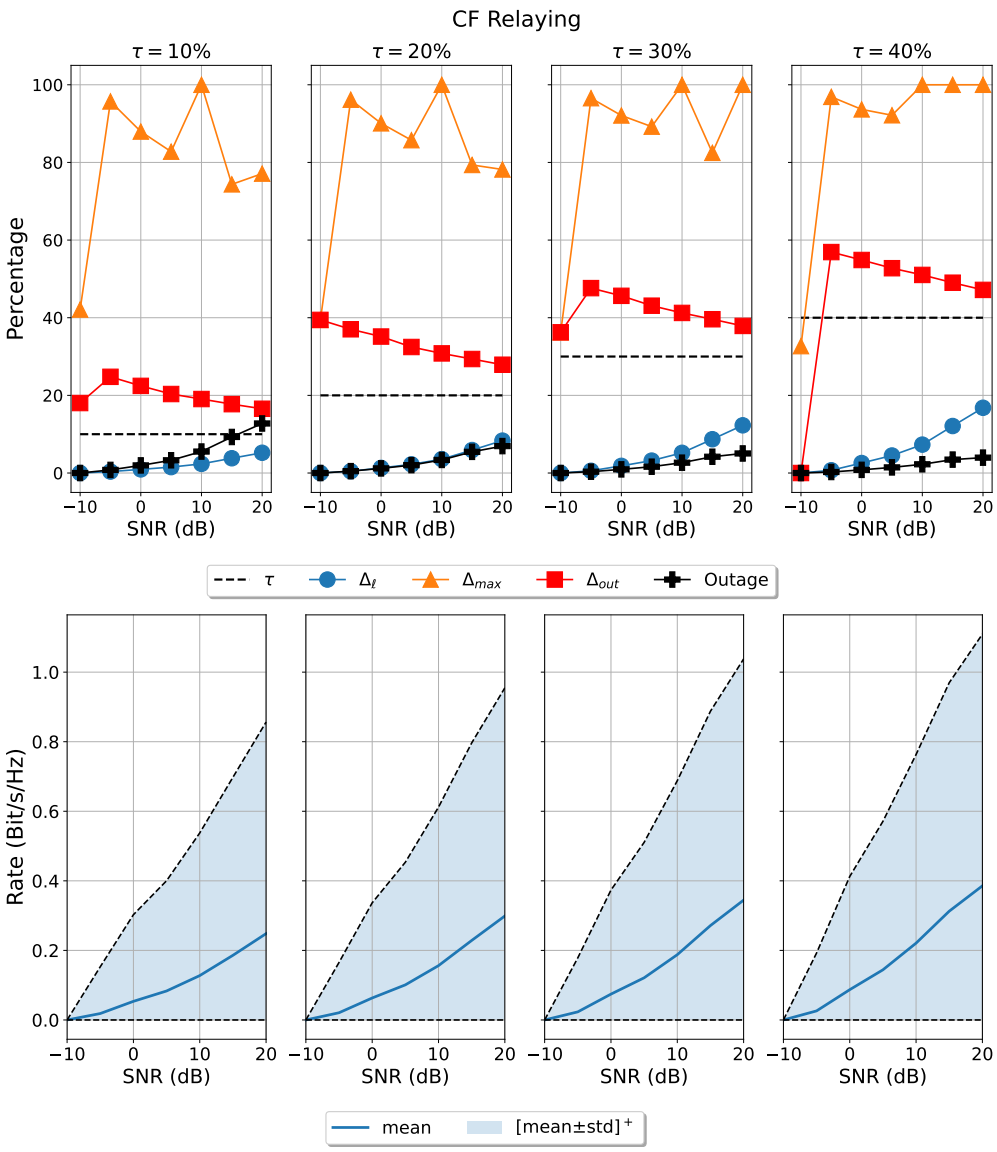

Figure 4.11: Generalization over the maximum allowed primary rate degradation τ, for fixed secondary power budget $\overline{P_R} = \overline{P_S} = 10$ W with DNN$_\tau$ and under CF relaying.

the threshold of τ, regardless of its value for a fixed secondary power budget. Furthermore, the percentage of outage and the secondary rate increase with the value of τ, as expected since the secondary network is allowed to transmit with higher levels of power. Nonetheless, even if the percentage of outage increases, the average primary rate degradation when in outage keeps close to the threshold of τ, especially for moderate to good channel estimations.

In Figure 4.12, we illustrate the same performance metrics as in Figure 4.11 for different qualities of channel estimator SNR $\in [-10, 20]$ dB and for the DNN$_P$ generalizing over the

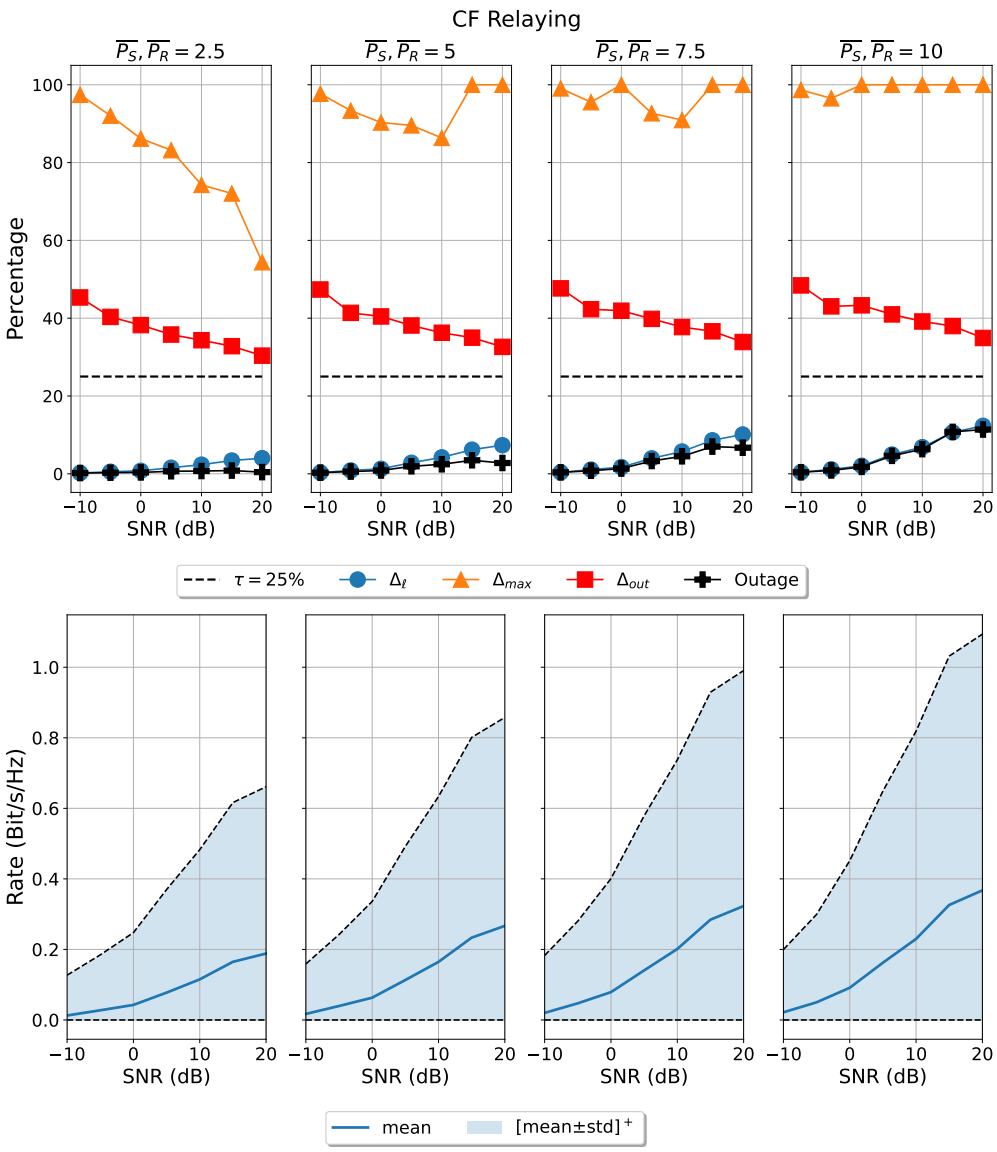

Figure 4.12: Generalization over the secondary power budgets, for fixed maximum allowed primary degradation $\tau = 0.25$ with DNN$_P$ and under CF relaying.

power budgets under CF relaying by fixing $\tau = 25\%$. Note that similar conclusions carry over for the generalization over the power budgets varying within $\overline{P_R} = \overline{P_S} \in \{2.5, 5, 7.5, 10\}$ W.

In the following, we investigate the performance obtained with our DNN† able to generalize jointly over both the secondary power budgets and the maximum allowed primary rate degradation τ under CF relaying.

In Figure 4.13, we present the same metrics as before, i.e., the outage, the average primary rate degradation (Δ_l), the average and maximum primary rate degradation when in outage

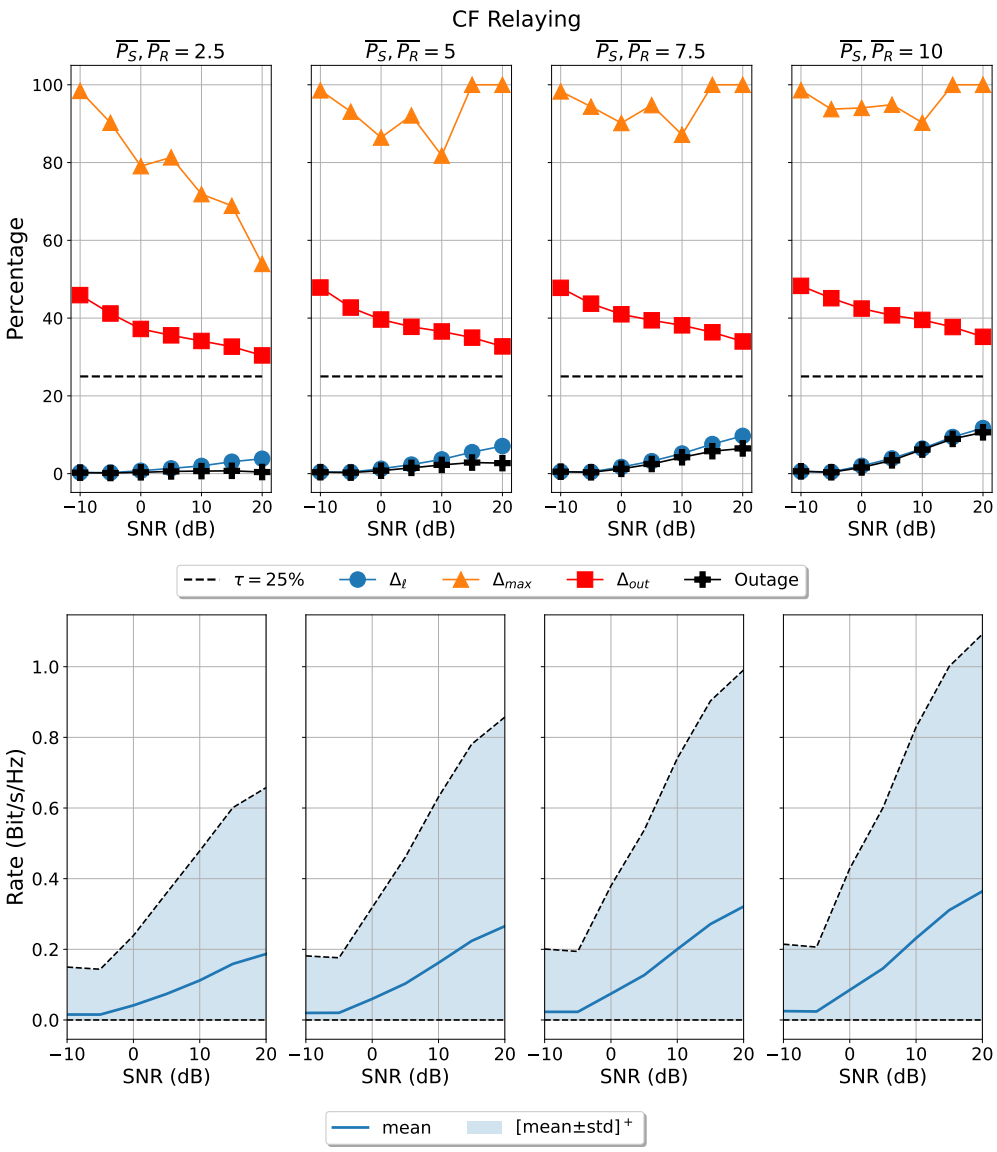

Figure 4.13: Joint generalization over the secondary power budget and the maximum allowed primary degradation with DNN† and under CF relaying: impact of secondary power budget when $\tau = 0.25$.

(Δ_{out} and $\Delta_{\max}$ respectively) as well as the mean of the secondary rate and the mean plus and minus the standard deviation of the secondary rate, for different qualities of channel estimator SNR $\in [-10, 20]$ dB with the DNN† and for CF relaying. These results were obtained for $\tau = 0.25$ and $\overline{P_R} = \overline{P_S} \in \{2.5, 5, 7.5, 10\}$ W. Our objective is to concentrate on a certain measure, either to test the DNN† ability to generalize on τ or to test its ability to generalize on power budgets. Therefore, in order to achieve this, we must either fix power budgets and vary τ, or vary power budgets while keeping τ fixed. Changing all parameters

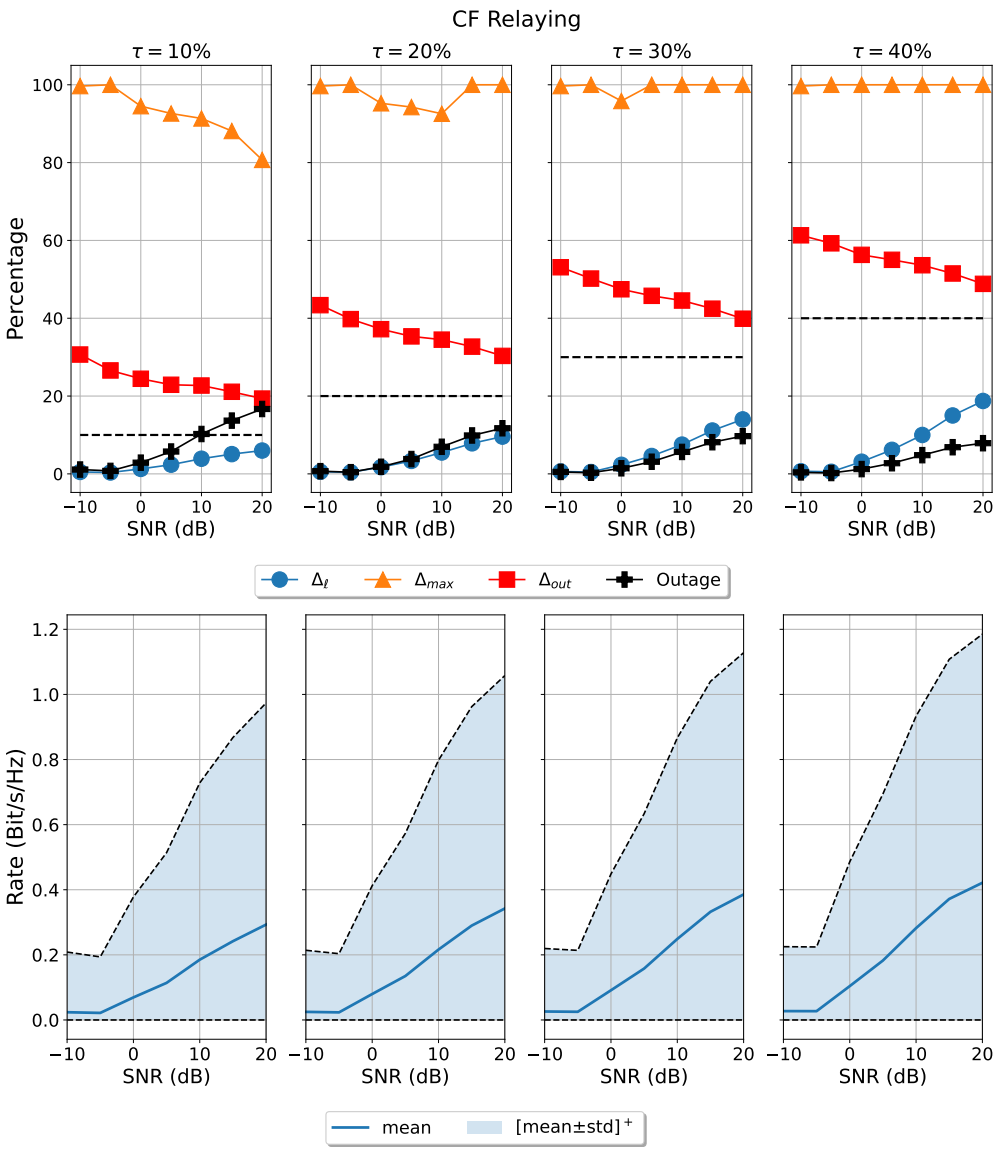

Figure 4.14: Joint generalization over the secondary power budgets and the maximum allowed primary degradation with DNN† and under CF relaying: impact of the maximum allowed primary degradation when $\overline{P_R} = \overline{P_S} = 10$ W.

simultaneously can make it challenging to interpret the results, as we cannot discern whether the DNN† is generalizing well on τ or the power budgets.

Note that, the performance obtained by the DNN$_P$ generalizing over the secondary power budget for a fixed value of τ, presented in Figure 4.12, and the one obtained by the DNN† jointly generalizing over all the system parameters when choosing the specific value of $\tau = 0.25$, given in Figure 4.13, are very close to each other, validating hence our more general proposed self-supervised DNN-based approach. Similar conclusions also hold when the sec-

ondary power budgets are $\overline{P_R} = \overline{P_S} = 10$ W and study the impact of $\tau \in \{0.1, 0.2, 0.3, 0.4\}$ on the performance obtained by the DNN† generalizing jointly over all system parameters in Figure 4.14 compared with Figure 4.11 for a DNN$_{\tau}$ generalizing only over τ.

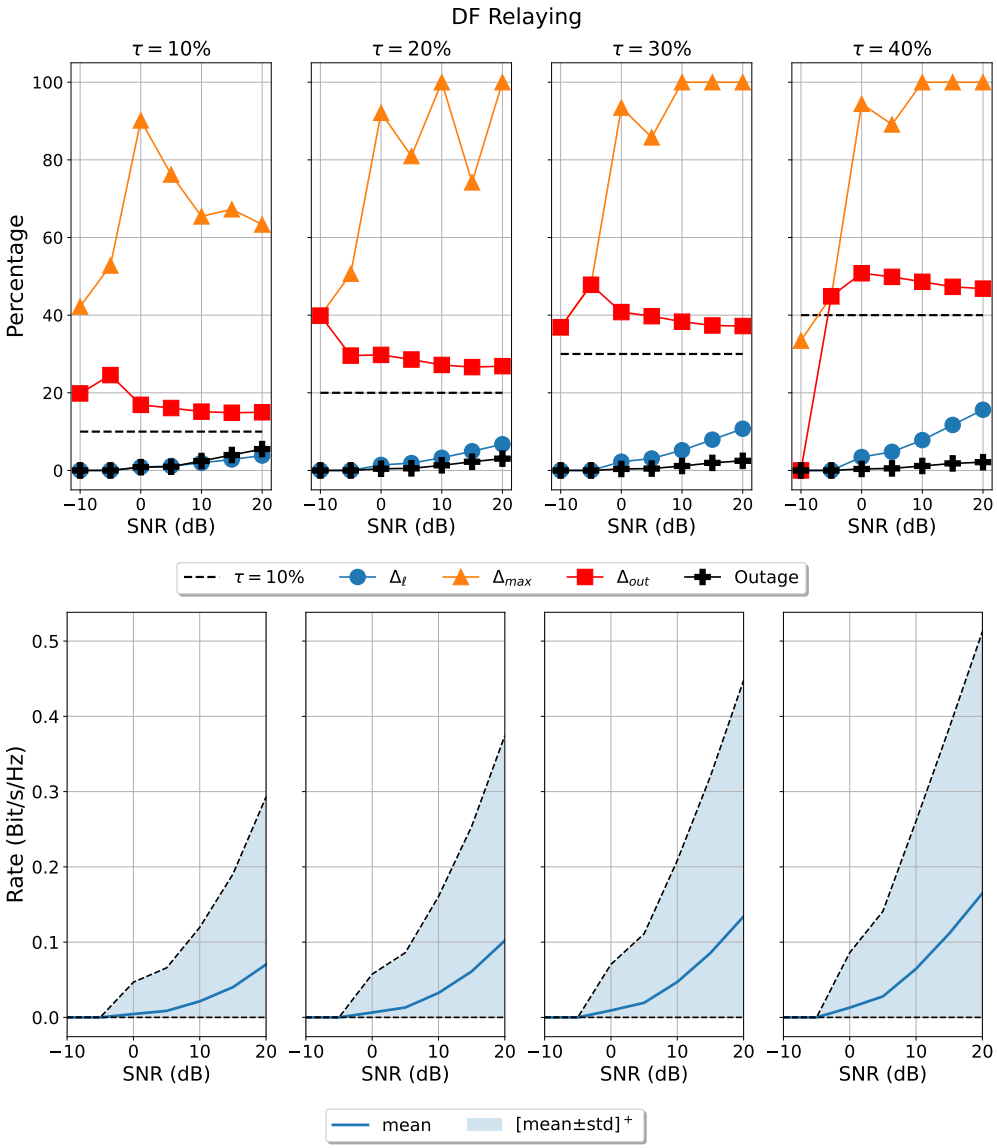

Figure 4.15: Generalization over the maximum allowed primary rate degradation τ, for fixed secondary power budget $\overline{P_R} = \overline{P_S} = 10$ W with DNN$_{\tau}$ and under DF relaying.

In order to compare our self-supervised DNN solution to our earlier results obtained for CF relaying, and have a better understanding of how well our self-supervised DNN solution performs, the simulations previously discussed and shown for CF in Figure 4.11 and Figure 4.12 are repeated for DF in Figure 4.15 and Figure 4.16, using the same performance metrics and different channel estimator qualities. We note that the suggested self-supervised

DNN can generalize whatever the given value of τ (Figure 4.15). It can also generalize whatever the given value of the power budgets (Figure 4.16), and also for all different qualities of channel estimator.

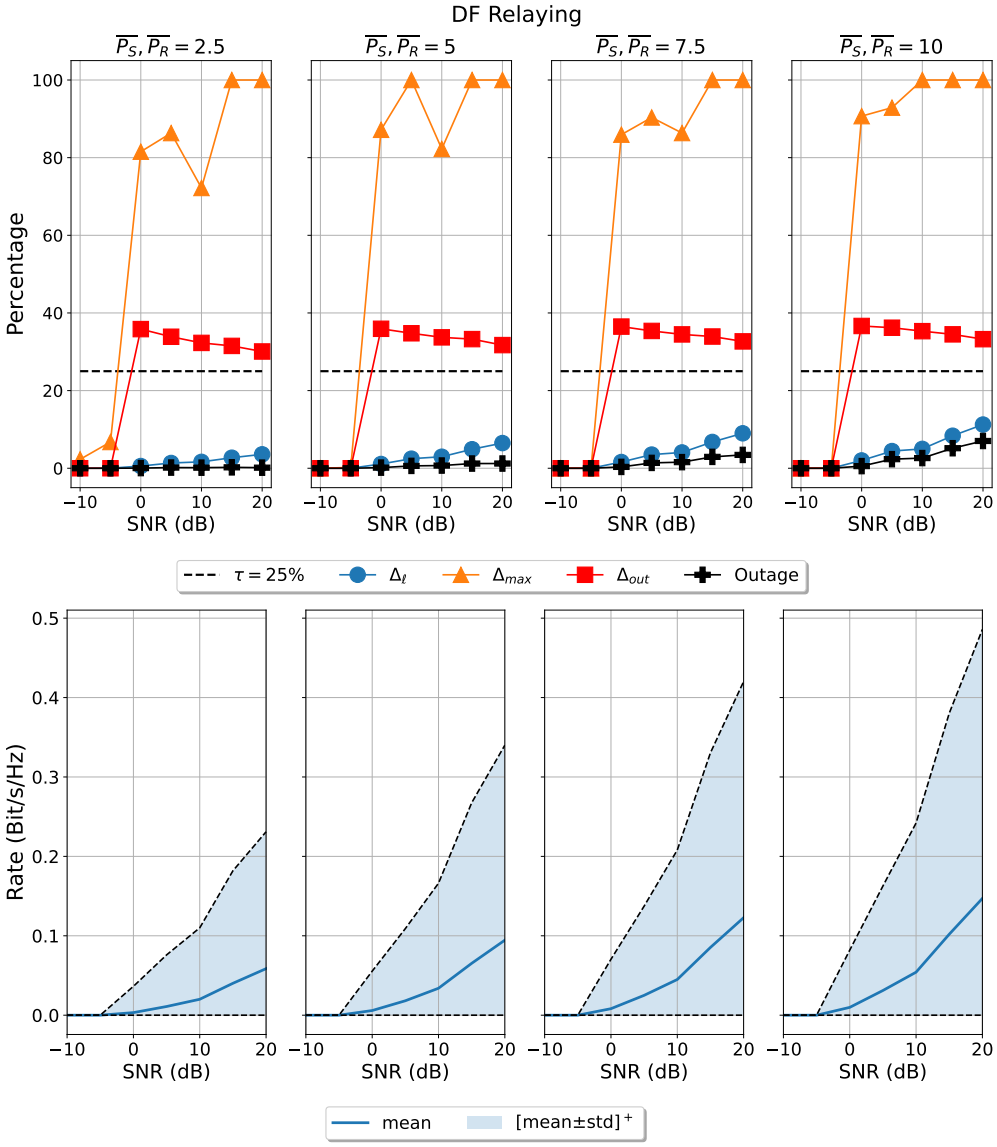

Figure 4.16: Generalization over the secondary power budgets, for fixed maximum allowed primary degradation $\tau = 0.25$ with DNN$_P$ and under DF relaying.

Figure 4.17 and Figure 4.18 present the results obtained from using DNN† generalizing jointly over all system parameters for DF relaying. These results demonstrate the generalization capabilities of the self-supervised DNN across various parameters, including the maximum allowed primary rate degradation and power budget. Furthermore, employing a single DNN† to address the generalization task yields similar outcomes compared to using

two separate self-supervised DNNs for individual parameter generalization. Moreover, this unified approach offers the advantage of reduced computation time, aligning with the findings from previous evaluations conducted for CF relaying.

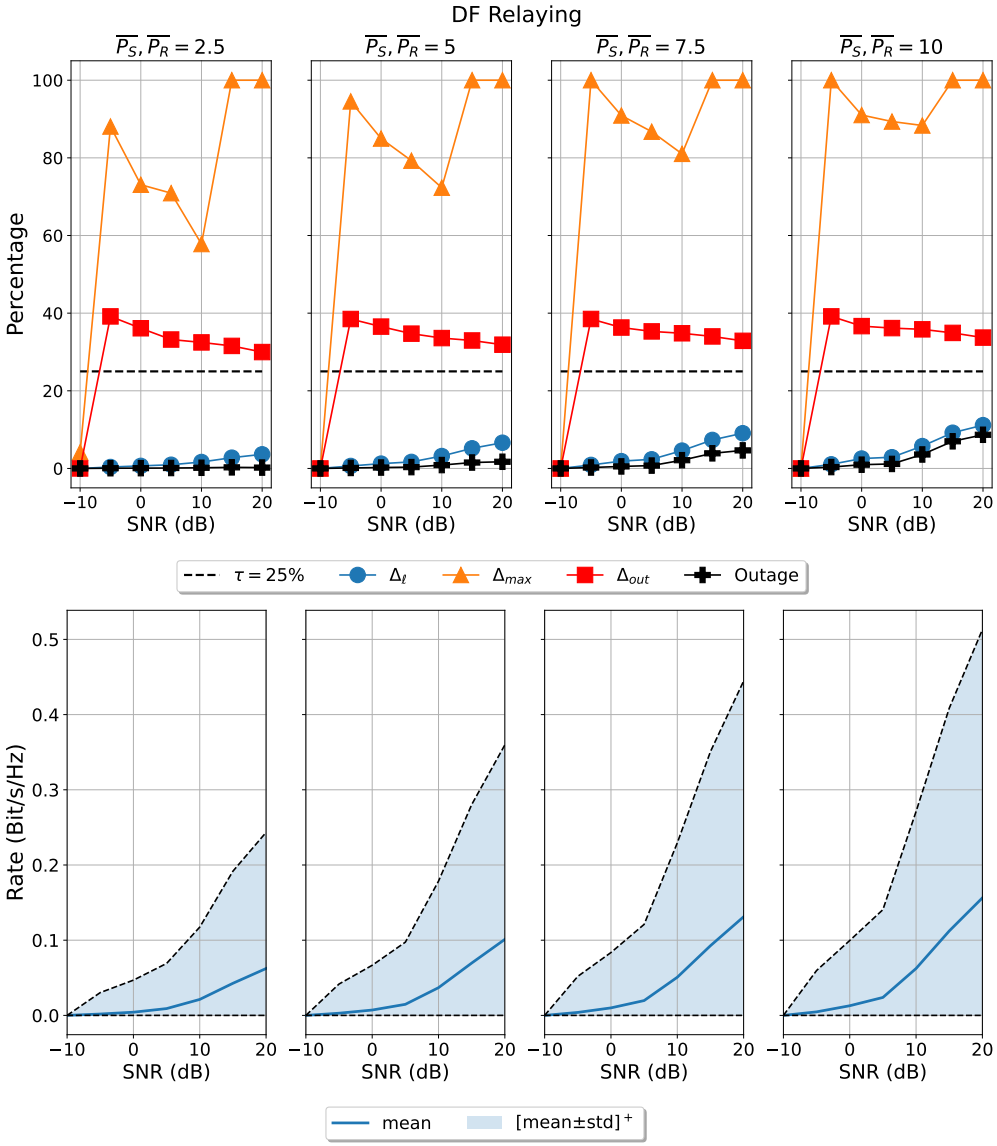

Figure 4.17: Joint generalization over the secondary power budget and the maximum allowed primary degradation with DNN† and under DF relaying: impact of secondary power budget when $\tau = 0.25$.

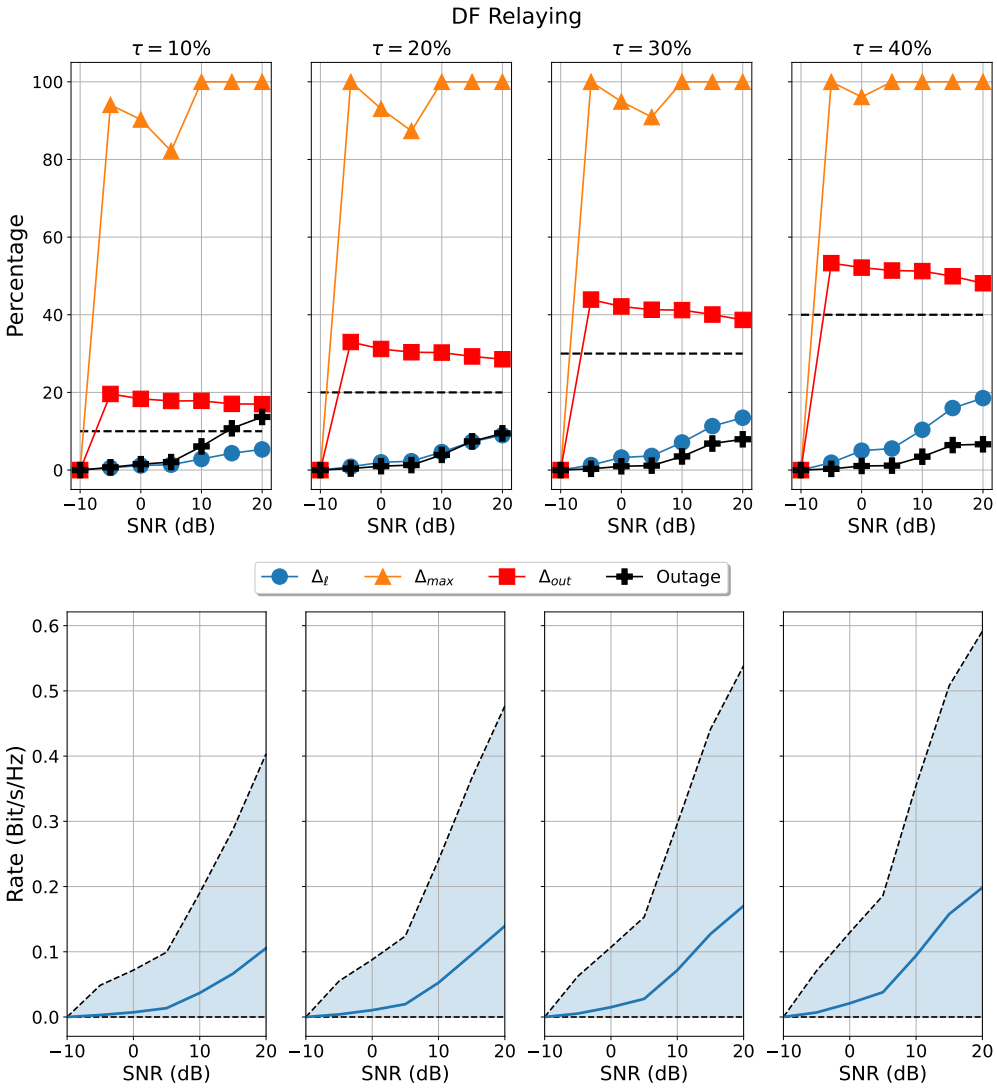

Figure 4.18: Joint generalization over the secondary power budgets and the maximum allowed primary degradation with DNN† and under DF relaying: impact of the maximum allowed primary degradation when $\overline{P_R} = \overline{P_S} = 10$ W.

To sum up, we have shown that our self-supervised DNN-based power allocation policy under imperfect CSI in Section 3.3 can generalize well over various system parameters for CF and DF relaying, by simply adding them as input features with little change in the architecture of the DNN and its training procedure (w.r.t. the custom loss function and datasets).

4.4 Summary

In this Chapter, we investigate the challenge of selecting the appropriate relaying scheme and propose two distinct approaches to choose between CF and DF relaying. We start by introducing the first method, which is based on the comparison of the primary rate degradation under the two relaying schemes. Then, we present the second method for selecting the relaying scheme, which is based on an supervised DNN, where this DNN is trained using optimal powers obtained via the self-supervised DNN described in the previous Chapter. We elaborate the architecture of this DNN and the novel loss function employed to determine the suitable relay choice between CF and DF. Additionally, we showcase numerical results that highlight the new proposed dataset used for DNN training, the DNN training process itself, and the evaluation of both approaches using diverse metrics such as primary rate degradation, and secondary rate metrics across various channel estimation SNRs.

Furthermore, our study in this Chapter provides a comprehensive investigation of a novel robust self-supervised DNN solution addressing power allocation challenges within cognitive relay networks under imperfect CSI. This solution is capable of generalizing over critical system parameters, such as the maximum allowed primary rate degradation τ and power budgets ($\overline{P_R}$, $\overline{P_S}$), thus proving to be also a flexible solution.

Our approach to the generalization involves two phases: initially, we generalize over the maximum allowed primary rate degradation or power budgets independently. Subsequently, we extend our self-supervised DNN solution to jointly generalize over all system parameters. The proposed self-supervised DNN solutions are validated through numerical results. The presented results illustrate the self-supervised DNN's efficacy in effectively generalizing over the specified parameters, ensuring excellent performance under diverse conditions.

Our study demonstrates that our proposed self-supervised DNN-based power allocation policy under imperfect CSI scenarios, showcases robust generalization capabilities. The architectural design, combined with well-suited training strategies, facilitates efficient adaptation to diverse system parameters, consequently contributing to enhanced power allocation solu-

tions in cognitive relay networks.

Chapter 5

Conclusions and Perspectives

5.1 Summary of the manuscript contributions

In this PhD thesis, we investigate the constrained and non-convex Shannon rate maximization problem of a relay-aided cognitive radio network. This network consists of a primary and a secondary user-destination pair and a secondary full-duplex relay performing CF and DF. The primary communication is protected by a QoS constraint in terms of tolerated Shannon rate degradation. The relaying operation leads to non-convex objective and primary QoS constraint. To address the power allocation problem, we propose to use deep learning techniques, and we show that our DNN-based solutions can be rendered robust against imperfect CSI with a modified training strategy. Then, we investigate DNN solutions for selecting the best relaying scheme for our communication system. Finally, we demonstrate that our deep learning solutions can generalize to the system parameters with a modification in the training strategy.

More precisely, the contributions of this PhD thesis are as follows.

- **Closed-form solution for CF relaying:** Despite that the power allocation problem under CF relaying is not a convex one, we derive a closed-form solution for it under perfect CSI based on the monotonicity of the objective function and the specific structure of the feasible set.

- **Unsupervised DNN-based power allocation for DF relaying:** We tackle the power allocation problem with perfect CSI and under DF relaying, where a closed-form solution is not achievable. Instead, we employ the unsupervised DNN-based approach that incorporates a cognitive radio tailored loss function. This approach relies solely on perfect CSI, provided at the input of the DNN and of the loss function, during both the

training and test phase. Our numerical results show that our unsupervised DNN-based solution is able to maximize the secondary rate while minimzing the number of outage.

- **Robust self-supervised DNN solution for imperfect CSI:** A novel self-supervised DNN-based solution is proposed to handle the power allocation problem under imperfect CSI. In the training phase of this self-supervised method, error-free channel estimations are provided to the loss function, and only channels gains impaired by estimation errors are provided at the input of the DNN. This approach demonstrated superior robustness compared to the bruteforce method. Moreover, our results show that the outage is much improved and stays below 5%, compared to the DNN trained with perfect CSI only, and our benchmark (i.e., brute force for DF, our closed-form solution for CF).

- **Combining self-supervised and supervised DNNs for relaying scheme selection:** We investigate the problem of selecting the best relaying scheme for our communication system. The first proposed method only exploits our robust DNN-based power allocation policies under CF and DF and compares the two obtained primary rate degradations: the relaying scheme exhibiting the smallest one is selected. We then propose to add an extra DNN to learn to select the best relaying scheme. This extra DNN solution exploits our robust DNN-based power allocation policies under CF and DF, and employs a second supervised DNN for relaying scheme selection. The performance of our communication system such as primary rate degradation, are improved by selecting the best relaying scheme.

- **Generalized self-supervised DNN-based solution:** We study a novel robust self-supervised DNN approach to solve power allocation problems in cognitive relay networks with imperfect CSI, with a generalization capability on system parameters. This solution provides a more adaptable solution because it can generalize over important system parameters such as power budgets and the maximum allowed primary rate degradation. We adopt a two-step approach to the generalization. First, we generalize over either the maximum primary rate degradation or the power budgets. Then, our self-supervised DNN solution is expanded so that it can jointly generalize across all system parameters.

Overall, the contributions of this work lie in the successful application of supervised, unsupervised and self-supervised deep learning techniques, particularly DNN-based methods, to optimize power allocation in cognitive relay-aided networks. These solutions proved to be

effective, adaptable, and robust even in the presence of imperfect CSI, making them valuable tools for resource allocation in future communication systems.

5.2 Perspectives

In this section, we will discuss some possible future research directions related to our work.

- In depth analysis of the secondary outage probability for imperfect CSI. Our study introduces a simplified methodology, differing from the approach of minimizing outage probability. The training dataset used in our study contains perfect CSI, and our proposed DNN is designed with the objective of maximizing instantaneous rates, a term similar to that used in the context of minimizing outage probability. It is expected that this new strategy will show promising results in terms of outage probability. Moving forward, our focus will delve deeper into the performance of our DNN specifically with respect to outage probability. This further examination aims to provide validation and a more thorough understanding of the effectiveness of our proposed DNN in addressing the challenges posed by imperfect CSI.

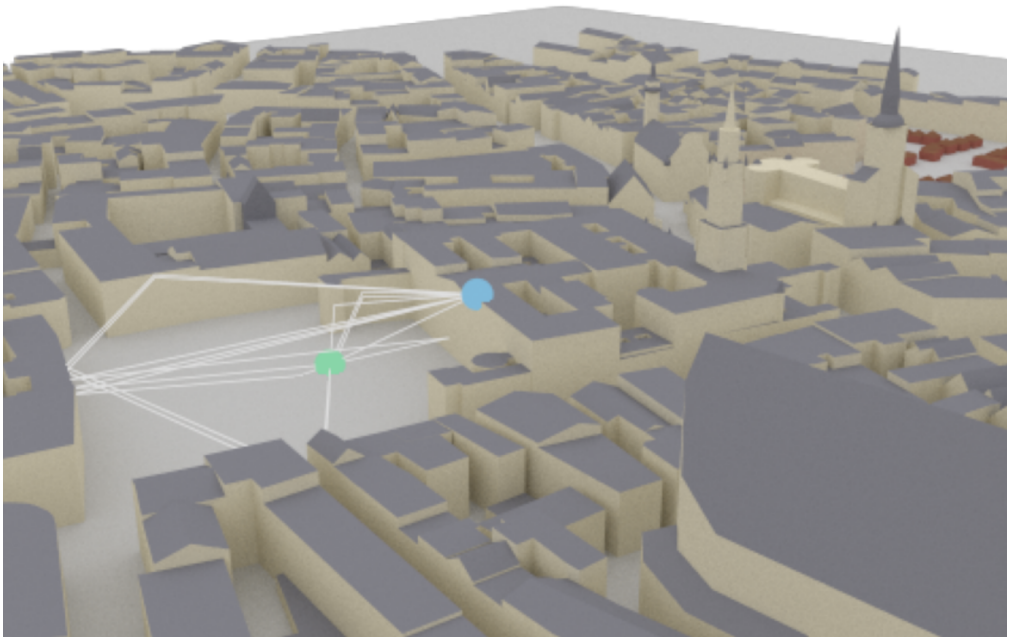

Figure 5.1: Primary Transmitter-Receiver scenario using Sionna: blue antenna for transmitter, green antenna for receiver.

- Investigating the efficacy of our proposed DNNs using realistic complex-gain chan-

nels obtained from Sionna [128]. Sionna is an open-source GPU-accelerated link-level simulator that utilizes Ray-tracing capabilities to simulate wireless 5G/6G networks, developed by NVIDIA. By employing these real-world channel conditions, we can evaluate the performance of our DNNs-based solutions in a practical and realistic setting. When applying our proposed DNN solution to solve the power allocation problem with complex wireless channels, a modification of the DNN architecture and a custom loss function is required when using complex channel gains. This work is already under study. We are currently designing a realistic setup, and the first numerical results are under investigation. Furthermore, given the complex channel gains in such realistic settings, for which the achievable Shannon rate regions have been derived in [129], we can explore another perspective: investigating the feasibility of a closed-form solution for the power allocation problem under complex channels and CF relaying.

- Considering more complex multi-user networks composed of an increased number of cellular, opportunistic users and helping relays. Then, moving towards distributed deep learning, where each of the users and relays computes locally it's own transmission's parameters (optimal relaying schemes and parameters as well as power allocation). For that, we can exploit tools from distributed deep learning (e.g., federated learning) to propose new resource allocation algorithms for cooperative multi-tier networks. These approaches can enhance the efficiency of resource allocation in complex network scenarios.

- Application of few-shot learning, which is indeed a promising approach when dealing with limited data scenarios, such as the case of channel gain estimation in Sionna. In our study, it was observed that channel gain computation and building a large dataset was time-consuming. However, few-shot learning can help alleviate these challenges by enabling a DNN to learn with only a small amount of data. Additionally, one application of few-shot learning is for classification problems. Since we have a relaying selection problem, which is essentially a classification problem that requires training with multiple data, we can apply few-shot learning techniques to select the best relaying scheme.

These future research directions can pave the way for innovative solutions and advancements in cooperative wireless networks, addressing the evolving demands of modern communication systems.

Bibliography

[1] Cisco annual internet report (2018-2023). https://www.cisco.com/c/en/us/solutions/collateral/executive-perspectives/annual-internet-report/white-paper-c11-741490.html.

[2] Chintha Tellambura and Sachitha Kusaladharma. *An Overview of Cognitive Radio Networks*, pages 1–17. John Wiley and Sons, Ltd, 2017.

[3] Neural networks kernel description. https://tikz.net/neural_networks/. Accessed: 2010-09-30.

[4] Walid Saad, Mehdi Bennis, and Mingzhe Chen. A vision of 6G wireless systems: Applications, trends, technologies, and open research problems. *IEEE Network*, 34(3):134–142, 2020.

[5] Emilio Calvanese Strinati, Sergio Barbarossa, Jose Luis Gonzalez-Jimenez, Dimitri Ktenas, Nicolas Cassiau, Luc Maret, and Cedric Dehos. 6G: The next frontier: From holographic messaging to artificial intelligence using subterahertz and visible light communication. *IEEE Veh. Technol. Mag.*, 14(3):42–50, 2019.

[6] Xiaohu You, Cheng-Xiang Wang, Jie Huang, Xiqi Gao, Zaichen Zhang, Mao Wang, Yongming Huang, Chuan Zhang, Yanxiang Jiang, Jiaheng Wang, et al. Towards 6G wireless communication networks: Vision, enabling technologies, and new paradigm shifts. *Science China Information Sciences*, 64:1–74, 2021.

[7] Samad Ali, Walid Saad, Nandana Rajatheva, Kapseok Chang, Daniel Steinbach, Benjamin Sliwa, Christian Wietfeld, Kai Mei, Hamid Shiri, Hans-Jürgen Zepernick, et al. 6G white paper on machine learning in wireless communication networks. *arXiv preprint arXiv:2004.13875*, 2020.

[8] Youness Arjoune and Naima Kaabouch. A comprehensive survey on spectrum sensing in cognitive radio networks: Recent advances, new challenges, and future research directions. *Sensors*, 19(1):126, 2019.

[9] Yuhan Su, Xiaozhen Lu, Yifeng Zhao, Lianfen Huang, and Xiaojiang Du. Cooperative communications with relay selection based on deep reinforcement learning in wireless sensor networks. *IEEE Sensors J.*, 19(20):9561–9569, 2019.

[10] Tran Trung Duy and Hyung Yun Kong. Performance analysis of mixed amplify-and-forward and decode-and-forward protocol in underlay cognitive networks. *China Communications*, 13(3):115–126, 2016.

[11] Dhoni Putra Setiawan and Hua-An Zhao. Performance analysis of hybrid af and df protocol for relay networks. In *2017 ICCREC*, pages 207–211. IEEE, 2017.

[12] Fatima Hussain, Syed Ali Hassan, Rasheed Hussain, and Ekram Hossain. Machine learning for resource management in cellular and IoT networks: Potentials, current solutions, and open challenges. *IEEE Commun. Surveys Tuts.*, 22(2):1251–1275, 2020.

[13] Amanda Ly and Yu-Dong Yao. A review of deep learning in 5G research: Channel coding, massive MIMO, multiple access, resource allocation, and network security. *IEEE Open Journal of the Communications Society*, 2:396–408, 2021.

[14] Tulsi Pawan Fowdur and Bhuvaneshwar Doorgakant. A review of machine learning techniques for enhanced energy efficient 5G and 6G communications. *Engineering Applications of Artificial Intelligence*, 122:106032, 2023.

[15] Anzar Mahmood, Nadeem Javaid, and Sohail Razzaq. A review of wireless communications for smart grid. *Renewable and Sustainable Energy Reviews*, 41:248–260, 2015.

[16] Yasin Kabalci. A survey on smart metering and smart grid communication. *Renewable and Sustainable Energy Reviews*, 57:302–318, 2016.

[17] Wan Siti Halimatul Munirah Wan Ahmad, Nurul Asyikin Mohamed Radzi, FS Samidi, Aiman Ismail, Fairuz Abdullah, Md Zaini Jamaludin, and MohdNasim Zakaria. 5G technology: Towards dynamic spectrum sharing using cognitive radio networks. *IEEE Access*, 8:14460–14488, 2020.

[18] Ian F Akyildiz, Won-Yeol Lee, Mehmet C Vuran, and Shantidev Mohanty. A survey on spectrum management in cognitive radio networks. *IEEE Commun. Mag.*, 46(4):40–48, 2008.

[19] Beibei Wang and KJ Ray Liu. Advances in cognitive radio networks: A survey. *IEEE J. Sel. Topics Signal Process.*, 5(1):5–23, 2010.

[20] Jianfeng Wang, Monisha Ghosh, and Kiran Challapali. Emerging cognitive radio applications: A survey. *IEEE Commun. Mag.*, 49(3):74–81, 2011.

[21] Abbass Nasser, Hussein Al Haj Hassan, Jad Abou Chaaya, Ali Mansour, and Koffi-Clément Yao. Spectrum sensing for cognitive radio: Recent advances and future challenge. *Sensors*, 21(7):2408, 2021.

[22] Amandeep Kaur and Krishan Kumar. A comprehensive survey on machine learning approaches for dynamic spectrum access in cognitive radio networks. *Journal of Experimental & Theoretical Artificial Intelligence*, 34(1):1–40, 2022.

[23] Joseph Mitola and Gerald Q Maguire. Cognitive radio: making software radios more personal. *IEEE personal communications*, 6(4):13–18, 1999.

[24] Ersan Kabalci and Yasin Kabalci. *From smart grid to internet of energy*. Academic Press, 2019.

[25] Sachitha Kusaladharma and Chintha Tellambura. Ocrns. *Wiley encyclopedia of electrical and electronics engineering*, pages 1–17, 1999.

[26] Andrea Goldsmith and Ivana Maric. Capacity of cognitive radio networks. In *Principles of Cognitive radio*, pages 41–101. Cambridge University Press, 2009.

[27] Fatemeh Shah Mohammadi. *Machine Learning-enabled Resource Allocation for Underlay Cognitive Radio Networks*. Rochester Institute of Technology, 2020.

[28] Juhi Garg, Priyanka Mehta, and Kapil Gupta. A review on cooperative communication protocols in wireless world. *International Journal of Wireless & Mobile Networks.*, 5(2):107, 2013.

[29] Xiaoming Chen, Hsiao-Hwa Chen, and Weixiao Meng. Cooperative communications for cognitive radio networks—from theory to applications. *IEEE Commun. Surveys Tuts.*, 16(3):1180–1192, 2014.

[30] Edward Cornelis Van der Meulen. *Transmission of information in a T-terminal discrete memoryless channel*. University of California, Berkeley, 1968.

[31] Elena-Veronica Belmega, Samson Lasaulce, and Merouane Debbah. Capacity of cooperative channels: Three terminals case study. In *Cooperative Wireless Communications*, pages 3–24. CRC Press, 2009.

[32] Andrew Sendonaris, Elza Erkip, and Behnaam Aazhang. User cooperation diversity. part i. system description. *IEEE Trans. Commun.*, 51(11):1927–1938, 2003.

[33] Praveen Kumar Malik, Deepinder Singh Wadhwa, and Jaspal Singh Khinda. A survey of device to device and cooperative communication for the future cellular networks. *International Journal of Wireless Information Networks*, 27(3):411–432, 2020.

[34] Muhammed Enes Bayrakdar. Cooperative communication based access technique for sensor networks. *Int. J. Electron.*, 107(2):212–225, 2020.

[35] Beatrice Paillassa, Benoît Escrig, Riadh Dhaou, Marie-Laure Boucheret, and Caroline Bes. Improving satellite services with cooperative communications. *Int. J. Satell. Commun.*, 29(6):479–500, 2011.

[36] Muhammad Shahmeer Omar, Syed Ahsan Raza Naqvi, Shahroze Humayun Kabir, and Syed Ali Hassan. An experimental evaluation of a cooperative communication-based smart metering data acquisition system. *IEEE Trans. Ind. Informat.*, 13(1):399–408, 2016.

[37] Miao Pan, Pan Li, and Yuguang Fang. Cooperative communication aware link scheduling for cognitive vehicular networks. *IEEE J. Sel. Areas Commun.*, 30(4):760–768, 2012.

[38] Thomas Cover and Abbas El Gamal. Capacity theorems for the relay channel. *IEEE Trans. Inf. Theory.*, 25(5):572–584, 1979.

[39] Samira Pouyanfar, Saad Sadiq, Yilin Yan, Haiman Tian, Yudong Tao, Maria Presa Reyes, Mei-Ling Shyu, Shu-Ching Chen, and Sundaraja S Iyengar. A survey on deep learning: Algorithms, techniques, and applications. *ACM Computing Surveys (CSUR)*, 51(5):1–36, 2018.

[40] Hongji Huang, Song Guo, Guan Gui, Zhen Yang, Jianhua Zhang, Hikmet Sari, and Fumiyuki Adachi. Deep learning for physical-layer 5G wireless techniques: Opportunities, challenges and solutions. *IEEE Wireless Commun.*, 27(1):214–222, 2019.

[41] Linglong Dai, Ruicheng Jiao, Fumiyuki Adachi, H Vincent Poor, and Lajos Hanzo. Deep learning for wireless communications: An emerging interdisciplinary paradigm. *IEEE Wireless Commun.*, 27(4):133–139, 2020.

[42] Adeeb Salh, Lukman Audah, Nor Shahida Mohd Shah, Abdulraqeb Alhammadi, Qazwan Abdullah, Yun Hee Kim, Samir Ahmed Al-Gailani, Shipun A Hamzah, Bashar Ali F Esmail, and Akram A Almohammedi. A survey on deep learning for ultra-reliable and low-latency communications challenges on 6G wireless systems. *IEEE Access*, 9:55098–55131, 2021.

[43] Trevor Hastie, Robert Tibshirani, Jerome H Friedman, and Jerome H Friedman. *The elements of statistical learning: data mining, inference, and prediction*, volume 2. Springer, 2009.

[44] Shai Shalev-Shwartz and Shai Ben-David. *Understanding machine learning: From theory to algorithms*. Cambridge university press, 2014.

[45] Samuli Laine, Tero Karras, Jaakko Lehtinen, and Timo Aila. High-quality self-supervised deep image denoising. *Advances in Neural Information Processing Systems*, 32, 2019.

[46] Alessio Zappone, Marco Di Renzo, and Mérouane Debbah. Wireless networks design in the era of deep learning: Model-based, AI-based, or both? *IEEE Trans. Commun.*, 67(10):7331–7376, 2019.

[47] Chaoyun Zhang, Paul Patras, and Hamed Haddadi. Deep learning in mobile and wireless networking: A survey. *IEEE Commun. Surveys Tuts.*, 21(3):2224–2287, 2019.

[48] Francois Chollet. *Deep learning with Python*. Simon and Schuster, 2021.

[49] Xiao Liu, Fanjin Zhang, Zhenyu Hou, Li Mian, Zhaoyu Wang, Jing Zhang, and Jie Tang. Self-supervised learning: Generative or contrastive. *IEEE Trans. Knowl. Data Eng.*, 35(1):857–876, 2021.

[50] Peyman Setoodeh and Simon Haykin. Robust transmit power control for cognitive radio. *Proceedings of the IEEE*, 97(5):915–939, 2009.

[51] Wei-Kuang Lai, You-Chiun Wang, He-Cian Lin, and Jian-Wen Li. Efficient resource allocation and power control for LTE-A D2D communication with pure D2D model. *IEEE Trans. Veh. Technol.*, 69(3):3202–3216, 2020.

[52] Trinh Van Chien, Thuong Nguyen Canh, Emil Björnson, and Erik G Larsson. Power control in cellular massive MIMO with varying user activity: A deep learning solution. *IEEE Trans. Wireless Commun.*, 19(9):5732–5748, 2020.

[53] Yongjun Xu, Guan Gui, Haris Gacanin, and Fumiyuki Adachi. A survey on resource allocation for 5G heterogeneous networks: Current research, future trends, and challenges. *IEEE Commun. Surveys Tuts.*, 23(2):668–695, 2021.

[54] Yanxiang Jiang, Qiang Liu, Fuchun Zheng, Xiqi Gao, and Xiaohu You. Energy-efficient joint resource allocation and power control for D2D communications. *IEEE Trans. Veh. Technol.*, 65(8):6119–6127, 2015.

[55] Ali Majid Hasan Alibraheemi, Mhd Nour Hindia, Kaharudin Dimyati, Tengku Faiz Tengku Mohmed Noor Izam, Jamaiah Yahaya, Faizan Qamar, and Zuriani Hayati Abdullah. A survey of resource management in D2D communication for B5G networks. *IEEE Access*, 11:7892–7923, 2023.

[56] Le Liang, Hao Ye, Guanding Yu, and Geoffrey Ye Li. Deep-learning-based wireless resource allocation with application to vehicular networks. *Proceedings of the IEEE*, 108(2):341–356, 2019.

[57] Wali Ullah Khan, Tu N Nguyen, Furqan Jameel, Muhammad Ali Jamshed, Haris Pervaiz, Muhammad Awais Javed, and Riku Jäntti. Learning-based resource allocation for backscatter-aided vehicular networks. *IEEE Trans. Intell. Transp. Syst.*, 23(10):19676–19690, 2021.

[58] Xiang Li, Lingyun Lu, Wei Ni, Abbas Jamalipour, Dalin Zhang, and Haifeng Du. Federated multi-agent deep reinforcement learning for resource allocation of vehicle-to-vehicle communications. *IEEE Trans. Veh. Technol.*, 71(8):8810–8824, 2022.

[59] Woongsup Lee, Minhoe Kim, and Dong-Ho Cho. Deep power control: Transmit power control scheme based on convolutional neural network. *IEEE Commun. Lett.*, 22(6):1276–1279, 2018.

[60] Zhiqun Song, Xin Wang, Yutao Liu, and Zhongzhao Zhang. Joint spectrum resource allocation in NOMA-based cognitive radio network with swipt. *IEEE Access*, 7:89594–89603, 2019.

[61] Raouia Masmoudi, E Veronica Belmega, Inbar Fijalkow, and Noura Sellami. A closed-form solution to the power minimization problem over two orthogonal frequency bands under qos and cognitive radio interference constraints. In *2012 IEEE DSPAN*, pages 212–222. IEEE, 2012.

[62] Anne Savard and E Veronica Belmega. Optimal power allocation policies in multi-hop cognitive radio networks. In *2020 IEEE 31st Annual International Symposium on Personal, Indoor and Mobile Radio Communications*, pages 1–6. IEEE, 2020.

[63] Hajar El Hassani, Anne Savard, and E Veronica Belmega. A closed-form solution for energy-efficiency optimization in multi-user downlink NOMA. In *2020 IEEE 31st Annual International Symposium on Personal, Indoor and Mobile Radio Communications*, pages 1–5. IEEE, 2020.

[64] Hajar El Hassani, Anne Savard, E. Veronica Belmega, and Rodrigo C. De Lamare. Energy-efficient cooperative backscattering closed-form solution for NOMA. In *2021 IEEE GLOBECOM*, pages 1–6, 2021.

[65] Waleed Ejaz, Shree K Sharma, Salman Saadat, Muhammad Naeem, Alagan Anpalagan, and Naveed Ahmad Chughtai. A comprehensive survey on resource allocation for cran in 5G and beyond networks. *Journal of Network and Computer Applications*, 160:102638, 2020.

[66] Peng Wang, Ming Zhao, Limin Xiao, Shidong Zhou, and Jing Wang. Power allocation in ofdm-based cognitive radio systems. In *IEEE GLOBECOM 2007-IEEE Global Telecommunications Conference*, pages 4061–4065. IEEE, 2007.

[67] Wei Yu, Wonjong Rhee, Stephen Boyd, and John M Cioffi. Iterative water-filling for gaussian vector multiple-access channels. *IEEE Trans. Inf. Theory*, 50(1):145–152, 2004.

[68] Elena-Veronica Belmega, Samson Lasaulce, and Merouane Debbah. Power allocation games for MIMO multiple access channels with coordination. *IEEE Trans. Wireless Commun.*, 8(6):3182–3192, 2009.

[69] Gesualdo Scutari, Daniel P Palomar, and Sergio Barbarossa. The MIMO iterative waterfilling algorithm. *IEEE Trans. Signal Process.*, 57(5):1917–1935, 2009.

[70] Elena Veronica Belmega, Samson Lasaulce, Mérouane Debbah, and Are Hjørungnes. Learning distributed power allocation policies in MIMO channels. In *2010 18th European Signal Processing Conference*, pages 1449–1453. IEEE, 2010.

[71] Qilin Qi, Andrew Minturn, and Yaoqing Yang. An efficient water-filling algorithm for power allocation in ofdm-based cognitive radio systems. In *2012 ICSAI*, pages 2069–2073. IEEE, 2012.

[72] Søren Skovgaard Christensen, Rajiv Agarwal, Elisabeth De Carvalho, and John M Cioffi. Weighted sum-rate maximization using weighted MMSE for MIMO-BC beamforming design. *IEEE Trans. Wireless Commun.*, 7(12):4792–4799, 2008.

[73] Qingjiang Shi, Meisam Razaviyayn, Zhi-Quan Luo, and Chen He. An iteratively weighted mmse approach to distributed sum-utility maximization for a MIMO interfering broadcast channel. *IEEE Trans. Signal Process.*, 59(9):4331–4340, 2011.

[74] Gerard J Foschini and Zoran Miljanic. A simple distributed autonomous power control algorithm and its convergence. *IEEE Trans. Veh. Technol.*, 42(4):641–646, 1993.

[75] Panayotis Mertikopoulos and E Veronica Belmega. Transmit without regrets: Online optimization in MIMO-OFDM cognitive radio systems. *IEEE J. Sel. Areas Commun.*, 32(11):1987–1999, 2014.

[76] Panayotis Mertikopoulos and E Veronica Belmega. Learning to be green: Robust energy efficiency maximization in dynamic MIMO–OFDM systems. *IEEE J. Sel. Areas Commun.*, 34(4):743–757, 2016.

[77] Alexandre Marcastel, Elena Veronica Belmega, Panayotis Mertikopoulos, and Inbar Fijalkow. Online power optimization in feedback-limited, dynamic and unpredictable IoT networks. *IEEE Trans. Signal Process.*, 67(11):2987–3000, 2019.

[78] Irched Chafaa, E Veronica Belmega, and Mérouane Debbah. One-bit feedback exponential learning for beam alignment in mobile mmwave. *IEEE Access*, 8:194575–194589, 2020.

[79] Hajar El Hassani, Anne Savard, and E Veronica Belmega. Energy-efficient 1-bit feedback NOMA in wireless networks with no CSIT/CDIT. In *2021 IEEE Statistical Signal Processing Workshop (SSP)*, pages 106–110. IEEE, 2021.

[80] Stephen P Boyd and Lieven Vandenberghe. *Convex optimization*. Cambridge university press, 2004.

[81] Hengameh Takshi, Gülüstan Doğan, and Hüseyin Arslan. Joint optimization of device to device resource and power allocation based on genetic algorithm. *IEEE Access*, 6:21173–21183, 2018.

[82] Saeed Motiian, Mohammad Aghababaie, and Hamid Soltanian-Zadeh. Particle swarm optimization (PSO) of power allocation in cognitive radio systems with interference constraints. In *2011 4th IEEE International Conference on Broadband Network and Multimedia Technology*, pages 558–562. IEEE, 2011.

[83] Anne Savard and E. Veronica Belmega. Full-duplex relaying for opportunistic spectrum access under an overall power constraint. *IEEE Access*, 8:168262–168272, 2020.

[84] Le Thanh Tan, Lei Ying, and Daniel W Bliss. Power allocation for full-duplex relay selection in underlay cognitive radio networks: Coherent versus non-coherent scenarios. *arXiv preprint arXiv:1703.01527*, 2017.

[85] Liying Li, Xiangwei Zhou, Hongbing Xu, Geoffrey Ye Li, Dandan Wang, and Anthony Soong. Simplified relay selection and power allocation in cooperative cognitive radio systems. *IEEE Trans. Wireless Commun.*, 10(1):33–36, 2010.

[86] Yuwen Pan, Andrew Nix, and Mark Beach. Distributed resource allocation for ofdma-based relay networks. *IEEE Trans. Veh. Technol.*, 60(3):919–931, 2011.

[87] Ahmad Alsharoa, Hakim Ghazzai, and Mohamed-Slim Alouini. Efficient multiple antenna–relay selection algorithms for MIMO unidirectional–bidirectional cognitive relay networks. *Transactions on Emerging Telecommunications Technologies*, 27(2):170–183, 2016.

[88] Salama S Ikki and Mohamed H Ahmed. Performance analysis of adaptive decode-and-forward cooperative diversity networks with best-relay selection. *IEEE Trans. Commun.*, 58(1):68–72, 2010.

[89] Ahmed Abdelreheem, Osama A Omer, Hamada Esmaiel, and Usama S Mohamed. Deep learning-based relay selection in D2D millimeter wave communications. In *2019 ICCIS*, pages 1–5. IEEE, 2019.

[90] Yichen Wang, Pinyi Ren, and Feifei Gao. Power allocation for statistical qos provisioning in opportunistic multi-relay df cognitive networks. *IEEE Signal Processing Letters*, 20(1):43–46, 2012.

[91] Peng Lan, Fenggang Sun, Lizhen Chen, Peng Xue, and Jialin Hou. Power allocation and relay selection for cognitive relay networks with primary qos constraint. *IEEE Wireless Communications Letters*, 2(6):583–586, 2013.

[92] Woongsup Lee and Byung Chang Chung. Ensemble deep learning based resource allocation for multi-channel underlay cognitive radio system. *ICT Express*, 2022.

[93] Honghao Qiu and Yehong Liu. Novel heuristic algorithm for large-scale complex optimization. *Procedia Computer Science*, 80:744–751, 2016.

[94] Quoc-Viet Pham, Seyedali Mirjalili, Neeraj Kumar, Mamoun Alazab, and Won-Joo Hwang. Whale optimization algorithm with applications to resource allocation in wireless networks. *IEEE Trans. Veh. Technol.*, 69(4):4285–4297, 2020.

[95] Fei Liang, Cong Shen, Wei Yu, and Feng Wu. Power control for interference management via ensembling deep neural networks. In *IEEE ICCC*, pages 237–242, 2019.

[96] Woongsup Lee and Robert Schober. Deep learning-based resource allocation for device-to-device communication. *IEEE Trans. Wireless Commun.*, 21(7):5235–5250, 2022.

[97] Woongsup Lee and Kisong Lee. Robust transmit power control with imperfect CSI using a deep neural network. *IEEE Trans. Veh. Technol.*, 70(11):12266–12271, 2021.

[98] Abuzar BM Adam, Lei Lei, Symeon Chatzinotas, and Naveed Ur Rehman Junejo. Deep convolutional self-attention network for energy-efficient power control in NOMA networks. *IEEE Trans. Veh. Technol.*, 2022.

[99] Yu Zhao, Ignas G. Niemegeers, and Sonia M. Heemstra De Groot. Dynamic power allocation for cell-free massive MIMO: Deep reinforcement learning methods. *IEEE Access*, 9:102953–102965, 2021.

[100] Kisong Lee, Jung-Ryun Lee, and Hyun-Ho Choi. Learning-based joint optimization of transmit power and harvesting time in wireless-powered networks with co-channel interference. *IEEE Trans. Veh. Technol.*, 69(3):3500–3504, 2020.

[101] Zain Ali, Guftaar Ahmad Sardar Sidhu, Feifei Gao, Jing Jiang, and Xiaoyan Wang. Deep learning based power optimizing for NOMA based relay aided D2D transmissions. *IEEE Trans. on Cogn. Commun. Netw.*, 7(3):917–928, 2021.

[102] Woongsup Lee. Resource allocation for multi-channel underlay cognitive radio network based on deep neural network. *IEEE Commun. Lett.*, 22(9):1942–1945, 2018.

[103] Woongsup Lee and Kisong Lee. Deep learning-aided distributed transmit power control for underlay cognitive radio network. *IEEE Trans. Veh. Technol.*, 70(4):3990–3994, 2021.

[104] Min Lu, Bin Zhou, Zhiyong Bu, and Yu Zhao. A learning approach towards power control in full-duplex underlay cognitive radio networks. In *2022 IEEE WCNC*, pages 2017–2022, 2022.

[105] Fuhui Zhou, Xiongjian Zhang, Rose Qingyang Hu, Apostolos Papathanassiou, and Weixiao Meng. Resource allocation based on deep neural networks for cognitive radio networks. In *2018 IEEE ICCC*, pages 40–45. IEEE, 2018.

[106] Fatemeh Shah-Mohammadi and Andres Kwasinski. Deep reinforcement learning approach to qoe-driven resource allocation for spectrum underlay in cognitive radio networks. In *2018 IEEE ICC Workshops*, pages 1–6. IEEE, 2018.

[107] Xuekai Zong, Xiaomei Zhu, Aichun Zhu, and John Oliver Byrne. Optimization and transmit power control based on deep learning with inaccurate channel information in underlay cognitive radio network. In *Journal of Physics: Conference Series*, volume 1746, page 012090. IOP Publishing, 2021.

[108] Saud Aldossari and Kwang-Cheng Chen. Relay selection for 5G new radio via artificial neural networks. In *2019 22nd International Symposium on WPMC*, pages 1–5. IEEE, 2019.

[109] Toan-Van Nguyen, Thien Huynh-The, and Beongku An. A deep CNN-based Relay selection in eh Full-Duplex IoT networks with short-packet communications. In *IEEE ICC*, pages 1–6, 2021.

[110] Anne Savard and E Veronica Belmega. Optimal power allocation in a relay-aided cognitive network. In *12th EAI International Conference on Performance Evaluation Methodologies and Tools (ValueTools)*, pages 15–22, 2019.

[111] Anne Savard and E Veronica Belmega. Optimal power allocation policies in multi-hop cognitive radio networks. In *IEEE PIMRC*, pages 1–6, 2020.

[112] Yacine Benatia, Romain Negrel, Anne Savard, and E Veronica Belmega. Robustness to imperfect CSI of power allocation policies in cognitive relay networks. In *2022 IEEE 23rd SPAWC*, pages 1–5. IEEE, 2022.

[113] Yacine Benatia, Anne Savard, Romain Negrel, and Elena Veronica Belmega. Unsupervised deep learning to solve power allocation problems in cognitive relay networks. In *IEEE ICC Workshop*, 2022.

[114] Zhiguo Ding, Zheng Yang, Pingzhi Fan, and H Vincent Poor. On the performance of non-orthogonal multiple access in 5G systems with randomly deployed users. *IEEE Signal Process. Lett.*, 21(12):1501–1505, 2014.

[115] Haoran Sun, Xiangyi Chen, Qingjiang Shi, Mingyi Hong, Xiao Fu, and Nikos D Sidiropoulos. Learning to optimize: Training deep neural networks for wireless resource management. In *IEEE SPAWC*, pages 1–6, 2017.

[116] Fei Liang, Cong Shen, Wei Yu, and Feng Wu. Towards optimal power control via ensembling deep neural networks. *IEEE Trans. Commun.*, 68(3):1760–1776, 2019.

[117] Irched Chafaa, Romain Negrel, E Veronica Belmega, and Mérouane Debbah. Self-supervised deep learning for mmWave beam steering exploiting Sub-6 GHz channels. *IEEE Trans. Wireless Commun.*, 21(10):8803–8816, 2022.

[118] Diederik P Kingma and Jimmy Ba. Adam: A method for stochastic optimization. *arXiv preprint arXiv:1412.6980*, 2014.

[119] Chinmay S Vaze and Mahesh K Varanasi. The degree-of-freedom regions of MIMO broadcast, interference, and cognitive radio channels with no CSIT. *IEEE Trans. Inf. Theory*, 58(8):5354–5374, 2012.

[120] Hamad Yahya, Emad Alsusa, and Arafat Al-Dweik. Blind receiver design for downlink cognitive-radio NOMA networks. In *2021 IEEE ICC Workshops*, pages 1–6. IEEE, 2021.

[121] An He, Srikathyayani Srikanteswara, Kyung Kyoon Bae, Timothy R Newman, Jeffrey H Reed, William H Tranter, Masoud Sajadieh, and Marian Verhelst. Power consumption minimization for MIMO systems—a cognitive radio approach. *IEEE J. Sel. Areas Commun.*, 29(2):469–479, 2011.

[122] Majed Haddad, Aawatif Menouni Hayar, and Mérouane Debbah. Power allocation policies over multi-band/multi-user cognitive radio system. In *4th IEEE international multi-conference on systems, signals and devices*, pages 17–19, 2007.

[123] Valentina Rizzello and Wolfgang Utschick. Learning the CSI denoising and feedback without supervision. In *IEEE SPAWC*, pages 16–20, 2021.

[124] Mohit Sewak, Sanjay K Sahay, and Hemant Rathore. An overview of deep learning architecture of deep neural networks and autoencoders. *Journal of Computational and Theoretical Nanoscience*, 17(1):182–188, 2020.

[125] Vladimiros Sterzentsenko, Leonidas Saroglou, Anargyros Chatzitofis, Spyridon Thermos, Nikolaos Zioulis, Alexandros Doumanoglou, Dimitrios Zarpalas, and Petros Daras. Self-supervised deep depth denoising. In *Proceedings of the IEEE/CVF International Conference on Computer Vision*, pages 1242–1251, 2019.

[126] B. I. Justusson. *Median Filtering: Statistical Properties*, pages 161–196. Springer Berlin Heidelberg, Berlin, Heidelberg, 1981.

[127] Yacine Benatia, Anne Savard, Romain Negrel, and E. Belmega Veronica. Robust DNNs for power allocation problems in cognitive relay networks. *In preparation for submission to IEEE Transactions on Machine Learning in Communications and Networking*, 2023.

[128] Jakob Hoydis, Sebastian Cammerer, Fayçal Ait Aoudia, Avinash Vem, Nikolaus Binder, Guillermo Marcus, and Alexander Keller. Sionna: An open-source library for next-generation physical layer research. *arXiv preprint arXiv:2203.11854*, 2022.

[129] Anne Savard and E. Veronica Belmega. Achievable rate regions for cooperative cognitive radio networks with complex channels and circular normal additive noises. In *XXVIIIème Colloque Francophone de Traitement du Signal et des Images, GRETSI 2022*.

[130] Tao Jiang, Jianhua Zhang, Pan Tang, Lei Tian, Yi Zheng, Jianwu Dou, Henrik Asplund, Leszek Raschkowski, Raffaele D'Errico, and Tommi Jämsä. 3GPP standardized

5G channel model for IoT scenarios: A survey. *IEEE Internet of Things Journal*, 8(11):8799–8815, 2021.

[131] Ji Bian, Cheng-Xiang Wang, Xiqi Gao, Xiaohu You, and Minggao Zhang. A general 3D non-stationary wireless channel model for 5G and beyond. *IEEE Trans. Wireless Commun.*, 20(5):3211–3224, 2021.

[132] Enrico Del Re, Gherardo Gorni, Luca Ronga, and Rosalba Suffritti. A power allocation strategy using game theory in cognitive radio networks. In *2009 International Conference on Game Theory for Networks*, pages 117–123. IEEE, 2009.

[133] Self-supervised learning: The dark matter of intelligence. https://ai.meta.com/blog/self-supervised-learning-the-dark-matter-of-intelligence/.

Appendix A

Proof of Theorem 1

PROOF In **[H1]**–**[H4]**, the search for the optimal solution is reduced to the candidate points meeting the QoS constraint with equality. Hence, by setting $P_R^* = x, P_S^* = \frac{A - g_{RP}\ x}{g_{SP}}$, the original problem (**OCF**) is reduced to ($\mathbf{OCF_x}$).

Proposition 1 *By studying the different cases in Fig. 2.2, the values of x_ℓ and x_u defining the feasible set of* ($\mathbf{OCF_x}$) *are*

$$[x_\ell;\ x_u] = \begin{cases} \left[0;\ \frac{A}{g_{RP}}\right], & \text{if } \textbf{\textit{[H1]}} \text{ is met,} \\ \left[\frac{A - g_{SP}\overline{P_S}}{g_{RP}};\ \frac{A}{g_{RP}}\right], & \text{if } \textbf{\textit{[H2]}} \text{ is met,} \\ \left[0;\ \overline{P_R}\right], & \text{if } \textbf{\textit{[H3]}} \text{ is met,} \\ \left[\frac{A - g_{SP}\overline{P_S}}{g_{RP}};\ \overline{P_R}\right], & \text{if } \textbf{\textit{[H4]}} \text{ is met.} \end{cases}$$

Now, the derivation of the closed-form solution x^* to the reduced problem ($\mathbf{OCF_x}$) amounts simply to the analysis of the first order derivative of the objective, denoted by $f'(x)$, and the critical points, which are the solutions to $f'(x) = 0$. The latter reduces to a second-order equation, whose roots are given by $\frac{-C_1C_5 \pm \sqrt{\Delta'}}{C_1C_4}$, where $\Delta' = C_1^2C_5^2 - C_1C_4(C_2C_5 - C_3C_4)$ represents the corresponding reduced discriminant. Ultimately, the analytical expression of x^* depends on the sign of the dominant coefficient C_1C_4 (of $f'(x) = 0$), the sign of Δ', and on the relative position of the critical points (when they exist) w.r.t. the feasible set $[x_\ell;\ x_u]$ given in Proposition 1. The next Theorem, although tedious presents the optimal relay power solving the optimization problem given in (2.4).

Theorem 2 *When the relay employs CF over the cooperative cognitive radio network, the optimal relay power allocation under cases **[H1]** to **[H4]** is given as follows in closed form:*
If $\Delta' > 0$ and $C_1C_4 \neq 0$, then the optimal value of $P_R^* = x$ is given in the Table A.1.
If $\Delta' \leq 0$, then the optimal value P_R^* is $P_R^* = x_u$ if $C_1C_4 > 0$; $P_R^* = x_l$ if $C_1C_4 < 0$.

	$x_m \geq x_u$ $x_M \geq x_u$	$x_m \in [x_l; x_u]$ $x_M > x_u$	$x_m \in [x_l; x_u]$ $x_M \in [x_l; x_u]$	$x_m < x_l$ $x_M \leq x_u$	$x_m < x_l$ $x_M \in [x_l, x_u]$	$x_m < x_l$ $x_M < x_l$
$C_1C_4 > 0$	x_u	x_1	$\arg\max\{f(x_1); f(x_u)\}$	x_l	$\arg\max\{f(x_l); f(x_u)\}$	x_u
$C_1C_4 < 0$	x_l	$\arg\max\{f(x_l); f(x_u)\}$	$\arg\max\{f(x_l); f(x_1)\}$	x_u	x_1	x_l

Table A.1: Optimal relay allocation under cases **[H1]** to **[H4]** when $\Delta' > 0$.

If $C_1C_4 = 0$, the optimal relay power is given as
1) if $C_1C_5 > 0$,
i) if $x_u \leq x_0$, then $P_R^* = x_l$
ii) if $x_l \leq x_0 < x_u$, then $P_R^* = \arg\max\{f(x_l), (x_u)\}$
iii) if $x_0 < x_l$, then $P_R^* = x_u$.
2) if $C_1C_5 < 0$,
i) if $x_u \leq x_0$, then $P_R^* = x_u$
ii) if $x_l \leq x_0 < x_u$, then $P_R^* = x_0$
iii) if $x_0 < x_l$, then $P_R^* = x_l$.
3) if $C_1C_5 = 0$, $P_R^* = x_u$ if $C_2C_5 - C_3C_4 \geq 0$; $P_R^* = x_l$ otherwise. In all these cases, the optimal secondary power is given as $P_S^* = \frac{A - g_{RP}P_R^*}{g_{SP}}$.
*Under **[H5]**, the optimal power allocation policy is given as $P_R^* = \overline{P_R}$, $P_S^* = \overline{P_S}$.*